~~THE STRUCTURE AND FUNCTION OF SPINACH PHOTOSYSTEM - I~~

Biochemical and spectroscopic study of the structure and function of higher plant PS1

A thesis submitted by Matthew C. Berry for the degree of Doctor of Philosophy

Department of Biology, Darwin Building, University College London, March 1995

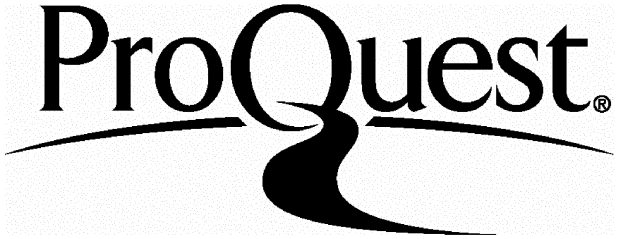

ABSTRACT

This thesis reports structural and functional studies of the photosystem I reaction centre of higher plants. The main techniques used were reaction centre preparation by detergent fractionation and modification by chaotrope treatment, optical and pulsed electron spin polarised kinetic spectroscopies at room and at cryogenic temperatures; continuous wave and time - resolved (ns time scale) pulsed electron spin resonance spectroscopies, and electron spin envelope echo modulation spectroscopy.

The kinetic behaviour of spinach PSI particles was examined where the iron - sulphur clusters were chemically prereduced at room temperature and at 4 K. A flash - induced electron spin polarised signal was observed in the out - of - phase detection channel using a short microwave pulse sequence, which decayed with a rate constant of 23 μs. Using microwave pulses of longer duration a spin polarised signal was observed in the in - phase channel decaying with the same rate constant as the former and spectrally identical to the spin polarised signal attributed to the $P700^{+}A_1^{-}$ radical pair. It is concluded that at 4 K forward electron transfer from A_1 is inhibited and that the observed spin polarised signal decays by a charge recombination and that the phasing of this signal depends on the characteristics of the pulse sequence used in detection.

At room temperature the flash - induced out - of - phase spin polarised signal was found to decay with a rate constant of 130 ns +/_ 50 ns and its decay was accompanied by the rise of a second spin polarised signal attributed to the radical pair, $P700^{+}FeS^{-}$ which in turn decays with a rate constant of 2 μs. When the iron - sulphur clusters, $Fe\text{-}S_{AB}$, were extracted the room temperature kinetic behaviour of the PSI core particles was largely unaltered relative to intact particles. When the iron - sulphur cluster, $Fe\text{-}S_X$, was extracted as

well, the decay of the out - of - phase signal was slowed down to give a rate constant of 1.3 μs and the in - phase signal was abolished. This demonstrates that in intact PSI particles at room temperature electron transfer takes place from $A_1$to the next acceptor and establishes unambiguously that this acceptor is the iron - sulphur cluster, Fe-S_X and means that the "200 ns" kinetic widely reported in the literature can be attributed to the reaction $A_1^{\cdot-}$ FeS_X---->$A_1FeS_X^{\cdot-}$. The same measurements were also carried out on PSI reaction centres prepared from the cyanobacterium, *Synechocystis*, and very similar kinetic behaviour was observed, implying that there is structural and mechanistic conservation between the two species.

The spatial arrangement of the redox components of spinach PSI relative to the iron - sulphur cluster, FeS_X, was studied using pulsed saturation recovery experiments. The strength of the magnetic interaction between the reduced non-metal radicals and the iron sulphur cluster, Fe-S_X, was quantified by measuring the intrinsic and enhanced spin lattice relaxation rates for each radical species. From these measurements we propose a model of PSI which resembles the 6 Å crystal structure and the photovoltage model, i.e. a branched arrangement of acceptors. Using a mathematical model we estimated the distances separating the electron acceptors of PSI.

Acknowledgements

I would like to thank Professor M.C.W. Evans for his patient supervision and encouragement over the three years. The spectroscopic work presented in this thesis is collaborative and in this regard I am greatly indebted to the practical and theoretical expertise of Dr. P. Bratt, Dr. P. Moenne - Loccos, Dr.P. Heathco te. I would also like to express my gratitude to Dr. J. Nugent and Dr. S. Rigby for their invaluable advice.

This work was funded by SERC.

CONTENTS **Page Number**

List of Figures and Tables

Chapter 1

Figures:

Chapter 2

Figures:

1.0 INTRODUCTION

1.1 General Introduction

Photosynthesis is the process whereby light energy is utilised for chemical means. The process is light dependent and involves the oxidation of an inorganic or organic molecule, acting as an electron donor. The overall reaction may be represented by the simple equation given below:

$$2H_2A + LIGHT \text{ ----------> } A_2 + 4e^- + 4H^+$$

In oxygenic photosynthesis the electron donor is water which is oxidised to oxygen. In anoxygenic photosynthesis the donor is an inorganic molecule other than water, eg H_2S which is oxidised without the production of oxygen. Photosynthetic organisms use the electrons to reduce fixed carbon dioxide for the generation of amino acids and sugars. Such organisms may be prokaryotes or eukaryotes, marine or terrestrial, they can all grow autotrophically though some are capable of feeding heterotrophically and occur in a wide range of environments.

The reactions of photosynthesis occur in pigment protein complexes which have a broadly similar design and bind electron carriers which are chemically similar in both eukaryotes and prokaryotes. For convenience sake photosynthesis can be broken down into

the **dark reaction** and the **light reaction**. The first of these refers to the processes that fix carbon dioxide and produce organic molecules required by the organism for its normal functioning and growth. The energy needed for this is supplied by the light reaction, an electron transport reaction generating reduced cofactors and a proton gradient.

1.1.1 Historical Background

In the early eighteenth century it was proved that green plant photosynthesis involved carbon dioxide fixation into carbohydrates with the evolution of oxygen. Ingenhousz (1779) showed that photosynthesis needed the illumination of the chlorophyll - containing parts of plants. The work of de Saussure (1804) dealt with the stoichiometry of the overall process, resulting in the well-known photosynthetic equation:

$$6\ CO_2 + 6\ H_2O \text{ ----------> } C_6H_{12}O_6 + 6\ O_2$$

The next stage was to study the processes underlying this simplified equation. One approach taken by Blackman (1905) was to look at the effect on rates of photosynthesis of varying the terms of the above equation. Under conditions of excess light and rate-limiting concentrations of carbon dioxide, the photosynthetic rate was temperature dependent. This shows the dark reactions are normal, temperature dependent reactions. Under conditions of excess CO_2 and limited light the photosynthetic rate was independent of temperature. This

shows that the light reactions are insensitive to temperature changes, a feature typical of photochemical processes.

Emerson and Arnold (1932) demonstrated using the alga *Chlorella* that the dark and light reactions can be separated in time. The cells were exposed to a 3ms pulse of light, followed by periods of darkness of varying lengths. During the dark period CO_2 was fixed, using energy generated by photochemical processes occurring during the light pulse. For the efficient utilisation of light energy it was found that a dark period considerably longer than the light pulse was needed. From these results it was deduced that the system carrying out the photochemistry was regenerated during this "longer" dark period. It is now known the light and dark reactions are not only separated in time but also in space in the chloroplast of higher plants.

Localisation of photosynthetic activity to the chloroplast was first achieved by Engelmann (1894). His work also proved the chloroplast to be the site of oxygen evolution. This was extended by Hill (1937). His experiments used isolated chloroplasts which produced oxygen under illumination only if a suitable electron acceptor was added to the system. The acceptor was a ferric salt which was reduced to the ferrous form in the course of the reaction. The donor oxidised to produce oxygen gas was identified as water by Ruben *et al* (1941) using ^{18}O-labelling experiments. The reaction by which water oxidation is coupled to the reduction of a ferric salt acceptor resulting in the production of oxygen gas, when isolated chloroplasts are illuminated became known as the Hill reaction. Hill could not show that CO_2 can serve as the terminal electron acceptor. It was Arnon *et al* (1954) who demonstrated chloroplasts are also the site of CO_2 fixation, using $^{14}CO_2$.

It was Hill along with Bendall(1960) who put forward the so-called Z-scheme which was the first time a thermodynamic framework was placed around the electron transfer

reactions of photosynthesis and incorporated new information concerning the cytochrome b_6f complex and ferredoxin as electron carriers (figure 1.1).

1.1.2 The Photosynthetic Unit

This is a term applied to the complex of pigments and other molecules involved in the harvesting, transfer of light energy and the use of this to drive the charge separation processes of the light and dark reactions. The chlorophyll molecules responsible for the transfer of light energy (excitation energy) to the reaction centre are known as *light-harvesting* or *antennae chlorophylls.* There are about 250-300 such chlorophylls per plant reaction centre (in cyanobacteria there are about 100 chlorophylls per reaction centre and 2000 in green bacteria). The photosynthetic unit is currently defined as the average number of chlorophyll molecules per reaction centre.

Figure 1.1 The Z - scheme showing the electron pathway from the primary electron donor, water, to $NADP^+$ in photosynthesis. The process is light dependent. The schematic also indicates the relationship between the two photosystems, PSI and PSII. Plastoquinol (QH_2) formed by PSII, serves as electron donor to the cytochrome b_6f complex, which reduces plastocyanin (PC), which acts as the electron donor to PSI. PSI reduces the iron sulphur protein ferredoxin (Fd), which in turn reduces $NADP^+$, forming NADPH. The proton gradient across the thylakoid membrane is formed when electrons pass through b_6f complex and is further enhanced by the fact that water oxidation and $NADP^+$reduction occur on opposite sides of the thylakoid membrane. P680 - primary donor of PSII, a chlorophyll dimer. P700 - primary donor of PSI . Z - tyrosine residue mediating electron flow between the manganese cluster (Mn), and P680. Ph - phaeophytin, the primary electron acceptor of PSII. Q_A and Q_B are plastoquinone binding proteins. A_0 and A_1 are electron acceptors in PSI. Fp is the flavoprotein, ferredoxin - dependent - $NADP^+$ reductase.

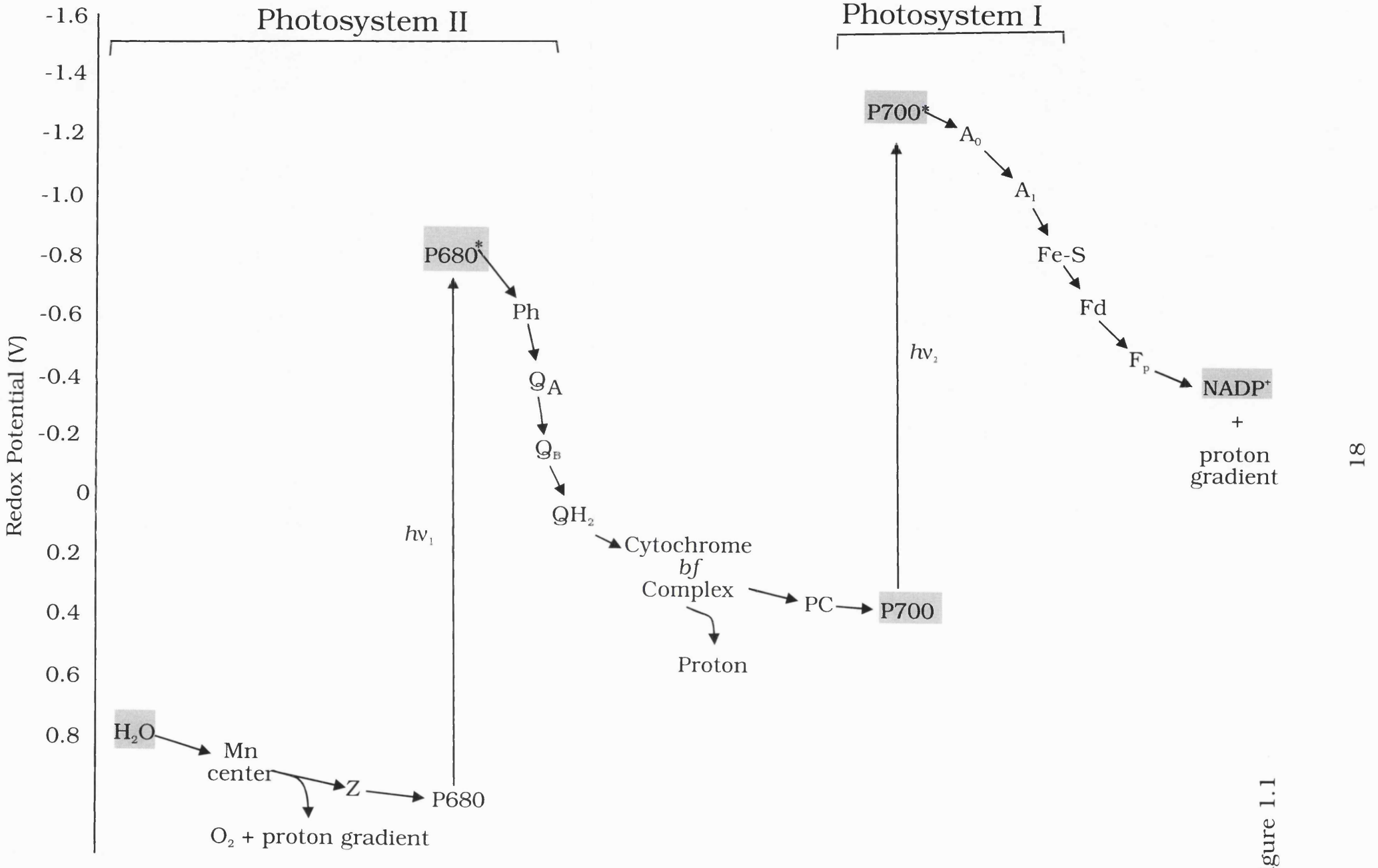
Photosystem II
Photosystem I
Redox Potential (V)
-1.6
-1.4
-1.2
-1.0
-0.8
-0.6
-0.4
-0.2
0
0.2
0.4
0.6
0.8
H_2O
Mn center
Z
P680
O_2 + proton gradient
$h\nu_1$
P680*
Ph
Q_A
Q_B
QH_2
Cytochrome *bf* Complex
Proton
PC
P700
$h\nu_2$
P700*
A_0
A_1
Fe-S
Fd
F_p
$NADP^+$
+
proton gradient

Figure 1.1

A quantum of light absorbed by any one of them will be transferred to the reaction centre, where it will result in a charge separation. The existence of a photosynthetic unit is supported by the experiments of various workers :

Emerson and Arnold, using *Chlorella* suspensions showed a maximum of $1O_2$ molecule is produced per light flash per 2500 chlorophylls, which means one quantum of light is absorbed by one chlorophyll molecule out of about 300. This inference follows on from an earlier observation indicating that about 8 quanta of light must be absorbed by chlorophylls in order to reduce 1 CO_2 molecule and release 1 O_2 molecule.

Gaffron and Wohl showed a large difference to exist between the theoretical rates of CO_2 reduction and O_2 evolution (calculated assuming the presence of a single chlorophyll molecule) and the actual rates measured in plant material. This led them to infer the presence of many other chlorophyll molecules whose function is to channel light energy to a single reaction centre.

The technique of difference spectroscopy has led to the discovery of the P700 special pair (a chlorophyll a dimer) of photosystem I (Kok *et al*) and also implicated cytochrome (Duysens *et al*) in the photochemistry. In algae and higher plants there is one light reacting cytochrome and one P700 dimer per 600 chlorophyll molecules.

The idea of a photosynthetic unit is rather outdated and the experimental work mentioned above which gave rise to it is at least forty years old, however it can still be crudely defined as a protein pigment complex consisting of about 600 chlorophyll molecules, and the redox components required to use harvested light energy to evolve oxygen and reduce NADP.

There are two types of photosystem. The first incorporates chlorophylls, phaeophytins (both kinds of tetrapyrrole pigment) and quinones as acceptors. It includes the photosystem

2 (PS II) of higher plants and the reaction centre found in purple bacteria. The other incorporates chlorophylls (or bacteriochlorophylls), quinones and iron-sulphur centres as acceptors. It includes the photosystem 1 (PSI) of higher plants and the reaction centre of green sulphur bacteria. The first type is functionally associated with water oxidation/oxygen evolution, the second type with ferredoxin and NADP reduction.

1.1.3 Pigments utilised in photosynthesis

Twsett (1906) was one of the first to extract and chromatographically separate leaf pigments involved in photosynthesis. There are three main groups of photosynthetic pigments : chlorophylls, carotenoids and phycobil ins. The first two are soluble only in organic solvents, the third group are water soluble. Carotenoids and phycobil ins are termed accessory pigments because they transfer light energy to chlorophylls.

In higher plants there are two kinds of chlorophylls a and b, which differ chemically. The structure of chlorophyll was worked out by Fischer (1940) and first synthesised by Woodward and co-workers (1960). All chlorophylls consist of a tetrapyrrole ring surrounding a magnesium atom (the polar porphyrin nucleus) and a lipophilic phytol tail. Phaeophytins, a third variety of pigment found in reaction centres, lack a magnesium atom but are otherwise chemically identical to chlorophylls. The molecular formula for chlorophyll a is $C_{55}H_{72}N_4O_5Mg$, for chlorophyll b, $C_{55}H_{70}N_4O_6Mg$. Chlorophyll a has a methyl group at position 3 on the tetrapyrrole ring, where b has a carbonyl group. Chlorophyll a and b also display characteristic absorption spectra. The absorption maxima observed for the pigments are different for different solvents. In ether the absorption maximum for chlorophyll a is 660nm and for chlorophyll b, 643nm; in acetone 663nm for chlorophyll a, 645nm for chlorophyll b. Figure 1.2 gives the structural formula of bacteriochlorophyll a.

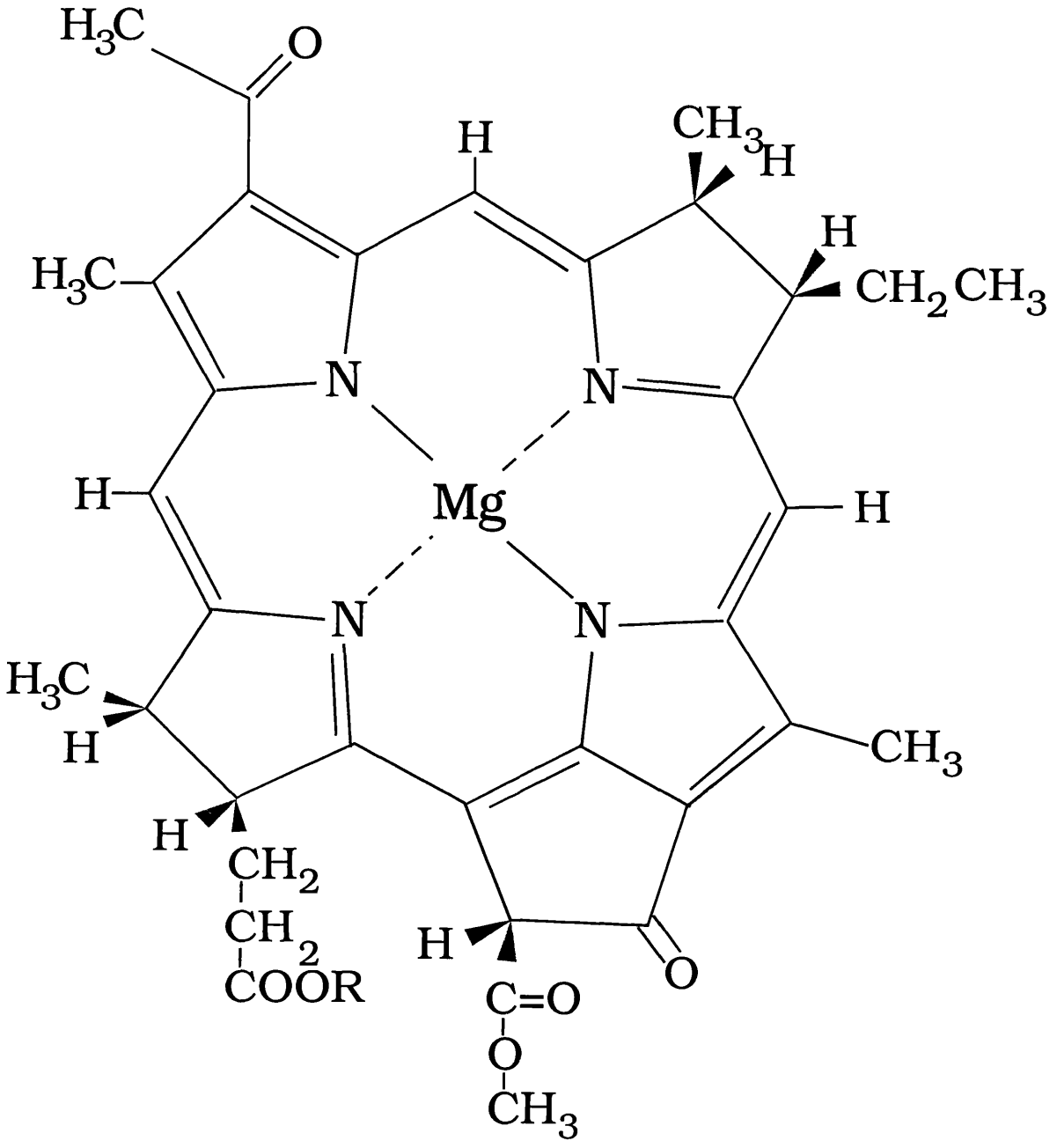

Figure 1.2 The structural formula of bacteriochlorophyll a. Chlorophyll a lacks the carbonyl group shown in the top left hand corner of this structure, having a C=C bond instead. R is a C_{20} hydrocarbon chain.

Carotenoids are pigments found in plants and purple bacteria. When dissolved in organic solvents they are yellow or orange in colour. Carotenoids are unsaturated organic compounds, containing alternating double and single C to C bonds. Broadly speaking there are two kinds - those which are hydrocarbons (the carotenes) and oxygenated hydrocarbons (the carotenols or xanthophylls) typically of 40 carbon atoms in length and composed of isoprene subunits. Their absorption spectra display three peaks, lying between 400 and 520nm. They are found in the lamellae of chloroplasts where they are closely associated with chlorophylls. Their functions are believed to include energy transfer to other pigments as already mentioned and also to protect against the photoinhibitory effects of high light intensity. The most important function carried out by carotenoids is the quenching of chlorophyll triplet and therefore prevention of singlet oxygen formation. Singlet oxygen is a highly reactive species which can cause damage to proteins.

Cyanobacteria and red marine algae additionally contain a class of pigments called *phycobil ins.* These are linear tetrapyrroles resembling chlorophyll a, which contains a cyclic tetrapyrrole ring, but lacking a phytol ring and central magnesium atom. They may be covalently bonded to polypeptides to form phycobil iproteins. There are three kinds of phycobil in - *phycoerythrins, phycocyanins* and *allophycocyanins.* Phycoerythrins give red algae their distinctive colour and absorb in the middle of visible range. It is the presence of these pigments at high levels that allows red algae to photosynthesise deep beneath the ocean surface. The greater the depth at which they occur, the higher their phycoerythrin:chlorophyll ratio. The blue phycocyanins and allophycocyanins are found in cyanobacteria (blue green algae) which occur terrestrially and close to the surface of lakes. As with carotenoids they are accessory pigments involved in energy transfer. Studies on *Porphyridium* species (red algae) using picosecond spectroscopy have established the following sequence of energy transfer: phycoerythrin ------>phycocyanin ------>allophycocyanin ------>chlorophyll a.

Photosynthetic bacteria, that is the *Rhodospirillineae* (Purple bacteria) and

Chlorobiineae (Green bacteria) contain bacteriochlorophylls and bacteriophaeophytins as well as chlorophylls), which are very much like their eukaryotic equivalents with only slight structural modifications.

1.1.4 Prokaryotic Photosynthetic Organisms

There are three groups of prokaryotic organism that can carry out phtosynthesis:

(a)*Rhodospirallales.*

(b)*Cyanobacteriales.*

(c)*Prochlorophyta.*

The organisms are grouped in this way according to pigment content and whether or not they evolve oxygen when they photosynthesise. They are all gram-negative bacteria apart from *Heliobacterium chlorum*.

(1)**Rhodospiralles..**

They are split into the purple bacteria (*Rhodospirillineae*) and the green bacteria (*Chlorobiineae*). Purple bacteria are sub-divided into the purple sulphur bacteria (*Chromatiaceae*) and purple non-sulphur bacteria (*Rhodospirillaceae*). Purple sulphur bacteria only grow under anaerobic conditions as autotrophs using hydrogen sulphide as an inorganic electron donor to reduce carbon dioxide in the Calvin cycle. Hydrogen sulphide is oxidised

in the process without oxygen formation, i.e. photosynthesis in these organisms is anoxygenic. The bulk of purple non-sulphur bacteria are aerobic heterotrophs requiring an organic compound such as acetate for a carbon source in their medium which they metabolise in the dark. In the light they can function as photoautotrophs using carbon dioxide as a carbon source. The purple non-sulphur bacteria have been more intensively studied than any other photosynthetic organism, this is partly due to their nutritional flexibility meaning they can be easily cultured in the laboratory and are amenable to genetic manipulation techniques., such as the production of mutants.

Green bacteria are sub-divided into the green sulphur bacteria (Chlorobiaceae) and the green non-sulphur bacteria (Chloroflexaceae). The green sulphur are obligate anaerobic photoautotrophs using hydrogen sulphide etc. as electron donors and possess a PS I-type reaction centre. The green non-sulphur bacteria are facultative aerobes which only photosynthesise under anaerobic conditions. They possess PS II- type reaction centres. The only representative of this group to be studied is *Chloroflexus auranticus*.

(2)**Cyanobacteriales**

They are predominantly aerobic photoautotrophs as is the case for higher plants and algae and like all photosynthetic eukaryotes they possess both types of reaction centre, PSI-type and PSII-type. Their light-harvesting apparatus includes phycobilins and chlorophyll a, giving the organisms a blue-green colour resulting in their alternative name of blue-green algae. Unlike eukaryotes they lack photosynthetic organelles as well defined as the chloroplasts of higher plants and their reaction centres do not have chlorophyll b. Some cyanobacteria are able to fix nitrogen gas and have no oxygen-evolving complex. e.g. *Anabaena* sp. which can form heterocysts.

(3)**Prochlorophyta**

The photosynthesis of organisms in this group is oxygenic. A representative species is *Prochloron didemni*, an endosymbiont associated with certain snail species. It has thylakoid membranes organised into a structure closely resembling the chloroplasts of eukaryotes, binding both PSI- and PSII-type reaction centres incorporating chlorophylls a and b, lacking the phycobilins encountered in cyanobacteria. *Proclorothrix* is a genus of free-living organisms belonging to this phylum.

1.1.5 Evolution of Photosynthesis.

There are a number of important similarities between the reaction centres of prokaryotic and eukaryotic photosynthetic organisms. Naturally this has led to the search for evolutionary relationships between the reaction centres through the comparison of sequence data. This has identified conserved residues and motifs involved in the binding of redox components. Detailed high resolution crystal structures are available for the reaction centres of the purple non-sulphur bacteria, *Rhodopseudomonas viridis* (Michel, 1982, Deisenhofer *et al*, 1984) and *Rhodobacter sphaeroides* R26 (Chang *et al*, 1986/91, Allen *et al* 1986). Because of the similarity of these systems to the PSII of eukaryotic algae and higher plants, the X-ray crystal structures have been used as the basis for homology modelling of the latter, e.g. Ruffle *et al* (1992), Styring *et al* (1990), excluding the donor sides which are very different in the two systems with the purple bacteria lacking a manganese cluster and oxygen evolving complex(OEC). Such work as this suggests future experiments, eg by identifying informative targets for mutagenesis and generally aids functional and structural studies of

PSII. X-ray crystallography studies are being carried out on PSI (Witt *et al*) and PSII (Feher *et al*). There follows a brief survey of the similarities and differences between the different reaction centres and their possible evolutionary importance.

Photosynthetic bacteria, algae and plants all have light harvesting apparatus. In all cases the amounts of light harvesting material is regulated in response to changing levels of light intensity. In most cases (the exception being chlorosomes) the light harvesting pigments are associated with polypeptides. The differences between the groups arise in the organisation and pigment composition of the light harvesting apparatus. In green sulphur bacteria for example these pigments are localised to particles called *chlorosomes*, which are in turn associated with the cell membrane. In the purple bacteria and photosynthetic eukaryotes the light harvesting and reaction centre complexes are intimately associated integral thylakoid membrane proteins. In cyanobacteria and red algae, *phycobilisomes* found in the outer surface of the photosynthetic membranes contain the water-soluble phycobilins. These structures contain in the region of 300-800 chromophores absorbing visible light over a range of wavelengths. The light quanta absorbed by the phycobilisomes are transferred to the reaction centre pigments with high efficiency.

The reaction centres of plants and bacteria show a similar pattern of organisation. In all reaction centres the first photochemical event of photosynthesis proper (i.e. excluding light harvesting processes) is the transfer of an electron from a donor molecule to an acceptor molecule. In purple bacteria and PSII of eukaryotes the primary donor is a dimer of bacteriochlorophyll and chlorophyll a (P680) respectively; the primary acceptor is a bacteriophaeophytin and phaeophytin respectively. Subsequently the acceptors are as follows - a primary quinone (menaquinone or ubiquinone in purple bacteria, plastoquinone in PSII); a secondary quinone (ubiquinone in purple bacteria, plastoquinone in PSII). In both bacteria and

plants these quinone acceptors are closely associated with non-haem iron atom. The relatively low energies of the reaction centre chlorophylls a and bacteriochlorophylls means that the loss of excitation energy through fluorescence is reduced. Quantum yields of electron transfer through the carriers of the reaction centre are high and the likelihood of back reactions is reduced by having a series of carriers arranged across the complex, of increasingly positive redox potentials and at increasing distances from the primary donor, leading to a stabilisation of charge separation.

There are significant amounts of amino acid sequence homology and similarity between the L and M subunits of *Rhodopseudomonas* species and the 32kDa D2 subunit (herbicide binding protein) of PSII. From such homology a shared ancestor has been inferred. There are other experimental observations which support this relationship - both reaction centres consist of polypeptides able to bind herbicides such as azidoatrazine (Pfister *et al* 1991); they both have similar quinone-iron cw EPR signals, with metal and radical magnetically coupled in both cases. There are also important differences between them however- as already mentioned the donor side of PSII (the manganese cluster, tyrosine radicals ie the components involved in water oxidation/oxygen evolution) is peculiar to it; the redox potential of P680 (a chlorophyll a dimer, the primary donor of PSII) is about 600-800mV more positive than the purple bacteria equivalent (P870). The histidine ligands believed to bind the chlorophyll molecules of the primary donors in each case are conserved in the L and M subunits of purple bacteria and the D1 and D2 subunits of PSII (Trebst *et al* 1986). This has led to the postulation that the PSII primary donor is a chlorophyll dimer orientated perpendicularly to the plane of the membrane as in the bacterial reaction centre, this has some spectroscopic support (van Kan *et al*, 1990). However there is also spectroscopic evidence which indicates the P680 has properties different to the purple

bacterial reaction centre and that it exhibits considerable monomeric character (Losche *et al*, 1988, van Mieghem *et al*, 1991). ENDOR(electron nuclear double resonance) studies indicate that the oxidised P680 is a dimer but that the bulk of the electron spin is localised on one of the chlorophyll molecules (5:1ratio), (Rigby *et al*, 1994). Mutational studies in cyanobacterial PSII have also shown a difference in the primary donor ligand usage between the two system types. When one of the histidines in D1 protein of the *Synechocystis* 6803 reaction centre thought to ligand P680 is changed to a residue that does not ligate magnesium no change in the chlorophyll content is observed. When the equivalent residue is mutated in the purple bacterium reaction centre the magnesium is not inserted, so the chlorophyll is pheophytinised. This suggests strongly the analogy between the purple bacteria reaction centre and PSII does not extend to the primary donor site. It does seem to hold for the primary acceptor site, with the equivalent histidine residues ligating bacteriophaeophytin in purple bacteria and phaeophytin in PSII. The work done so far on P680 infers a distorted dimer. Such distortion would help to explain P680's high redox potential, a property necessary for its water oxidising function.

Inspite of these and other observations indicating sequence/structural differences between PSII and purple bacterial reaction centres it is generally believed the former has evolved from the latter. There are also significant similarities between these reaction centres and that of the green non-sulphur bacterium *Chloroflexus auranticus* (Trebst *et al*, 1986, Barber *et al*, 1988, Michel and Deisenhofer, 1988, Rutherford *et al*, 1989). There are also differences between the latter and the purple bacteria. In *Chloroflexus* one of the accessory bacteriochlorophylls is replaced by a bacteriophaeophytin and the non-haem iron found between the primary and secondary quinones is replaced by a manganese (Blankenship *et al*, 1987).

It has been assumed that PSI and the reaction centre of the green sulphur bacteria are related based on similarities of redox component composition and organisation. Two structural genes from the green sulphur bacteria, *Chlorobium limicola*, have been identified / one which at the nucleotide level and amino acid level corresponds to the *psaA*, *psaB* (encoding the major polypeptides of PSI) and one to the *psaC* (encoding the peptide which binds the extrinsic iron sulphur centres, FeS_{AB}) genes (Buttner *et al* 1992a). However there is only about 15% identity between the psaA/B and the corresponding *Chlorobium* protein when whole sequences are compared, with the most striking conservation of the region including the two cysteines thought to bind the intrinsic iron sulphur centre, FeS_X. Spectroscopic analysis of *Chlorobium* reaction centres prepared anaerobically has revealed the presence of two 4Fe4S-type iron-sulphur clusters with spectra resembling those produced by Fe-S_{AB} clusters of PSI (Kjaer *et al*, 1994). From the fact only one *psaA*-type gene has been identified in *Chlorobium* it was inferred the reaction centre of this species is a homodimer and not a heterodimer as in higher plants (Buttner *et al*, 1992b). The homodimeric structure of the *Chlorobium* reaction centre is supported further by ENDOR studies on its primary donor, a chlorophyll dimer P840 (Rigby *et al*, 1994), which indicates the electron spin is equally distributed over the two halves of the dimer. The reaction centre of heliobacteria, on the basis of sequence homology, is also thought to be related to green-sulphur bacterial reaction centre and PSI. There is now optical spectroscopic evidence for an Fe-S_X-type iron-sulphur cluster obtained from heliobacterial reaction centres depleted of their Fe-S_{AB}-type clusters (Kleinherenbrink *et al*, 1994), which further support this postulated relationship.

If one ignores the iron sulphur centres FeS_{AB} there are obvious similarities between PSI and the purple bacterial reaction centre. In both there is a dimer of tetrapyrrole chromophores acting as the primary donor, with a tetrapyrrole monomer and quinones acting

as acceptors. The non-haem iron of purple bacteria can be seen as being analogous to the intrinsically bound iron sulphur centre, FeS_X (though the former is not redox active). Indeed from the low resolution X-ray crystal structure of PSI currently available Fe-S_X can be seen to occupy an equivalent position in the reaction centre core as the non-haem iron in the purple bacterial reaction centre and it has been proposed the latter is derived from the former. It is well known from the X-ray crystal structure that the purple bacterial reaction centre has two paths for electron transfer from the primary donor to a quinone acceptor but that *in vivo* only one of them is used. A similar C-2 symmetry exists in PSI (Heathcote *et al* 1993), there being two molecules of each electron carrier per reaction centre and with only one of the paths being active under physiological conditions.

Other efforts have been made to construct a phylogenetic tree depicting the relatedness of the three PSI-type reaction centres : of cyanobacteria and higher plants, green sulphur bacteria and heliobacteria through careful sequence alignment. Taking the complete amino acid sequences there is only about 20%homology between the three types. Limiting the comparisons to known conserved regions gave more accurate and informative alignments (Liebl *et al*, 1993). The heliobacterial sequence shows 40%and 48%identity with PsaA and PsaB, respectively, compared to 32%and 39%between the *Chlorobium* sequences and PsaA/PsaB sequences. From this it is inferred the green sulphur bacteria diverged from the ancestral reaction centre, followed by the heliobacteria which is thus more closely related to the PSI subunits. This study also showed both green sulphur and heliobacterial sequences share greater homology with PsaB than with PsaA. This can be interpreted to mean that PsaB derives directly from a homodimeric ancestral reaction centre which later underwent a duplication to produce PsaA.

1.1.6 Chloroplasts

Chloroplasts are the specialised organelles found in eukaryotic photosynthetic algae and higher plants which house the thylakoid membranes that are the sites of the photochemistry of photosynthesis. They have their own genome encoding many of the protein subunits required for photosynthetic function and also proteins responsible for the regulation of their expression and assembly. As has already been mentioned neither the purple and green bacteria or the cyanobacteria have their photosynthetic membranes organised as chloroplasts. In the former, the pigment-containing bodies can be isolated from disrupted bacterial cells by differential centrifugation. Under the electron microscope these bodies known as *chromatophores*, appear spherical and are 30-100nm across. Each one contains a number of photosynthetic units, e.g. a chromatophore from the purple non-sulphur bacterium, *Rhodobacter sphaeroides* contains about 40 reaction centre complexes, 500 light harvesting complexes, 1000 carotenoid molecules and 1000 ubiquinone molecules. Chromatophores are believed to originate from elaborate infolding of the cytoplasmic membrane. In cyanobacteria, which are also prokaryotes, the accessory pigments are located in *phycobilisomes*.

In eukaryotes that photosynthesise, the pigments required for the photochemistry are found in *chloroplasts* (figure 1.3) which are organelles in their own right. In the unicellular green alga *Chlamydomonas reinhardtii* the single chloroplast is seen under the microscope in cross section as a cup-shaped structure enclosing the nucleus. In higher plants chloroplasts occur in large numbers in all the green parts of the plant, though their abundance varies seasonally and according to species. They can be isolated from the leaves of higher plants in large amounts using standard methods. Under the electron microscope the higher plant

Figure 1.3 Schematic of section through chloroplast showing the stacked thylakoid membranes in which the pigment protein complexes of the photosystems I and II are embedded.

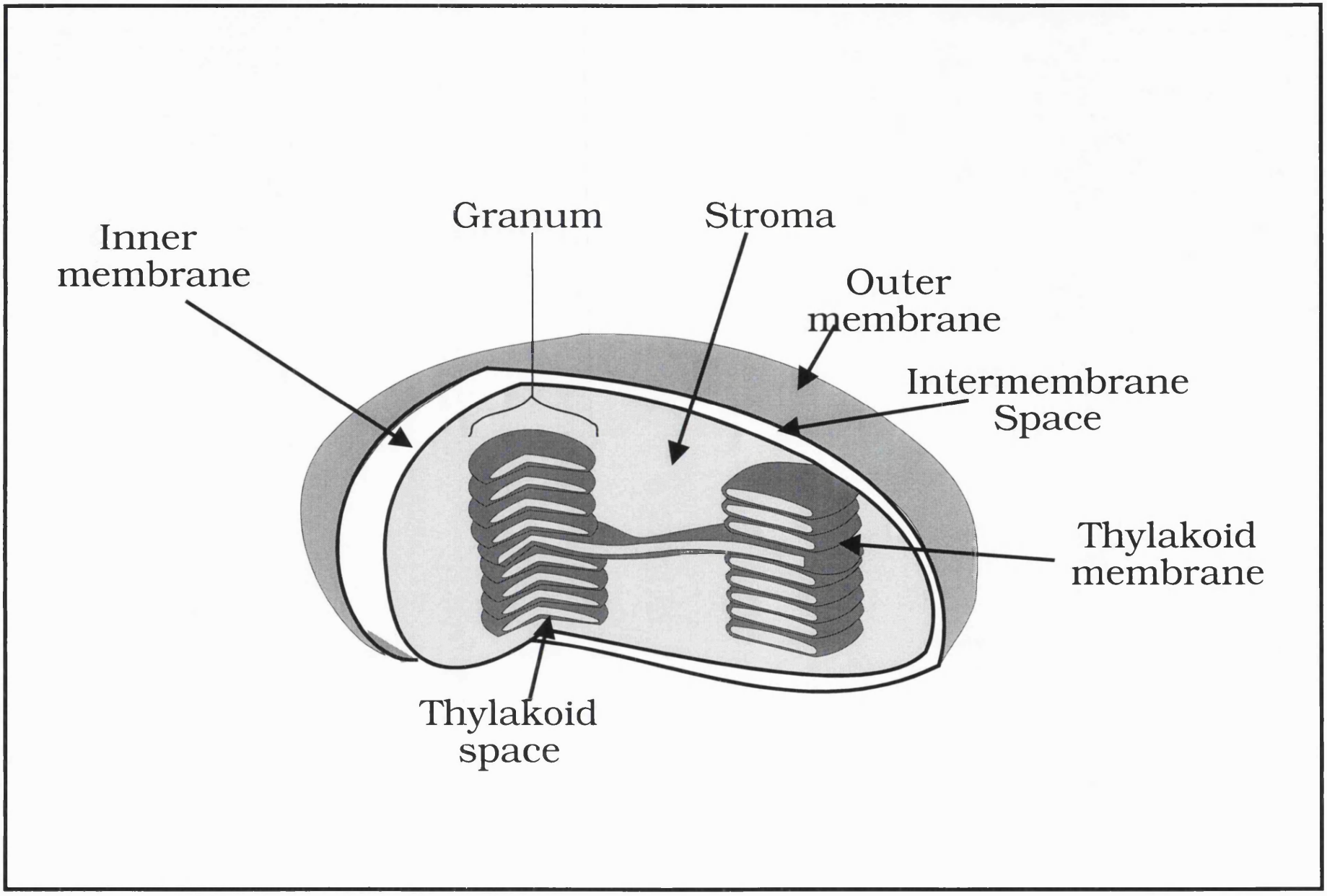
Granum
Stroma
Inner membrane
Outer membrane
Intermembrane Space
Thylakoid membrane
Thylakoid space

chloroplast is a saucer-shaped structure of 4-10μm across and about 1μm in thickness and has an outer double unit envelope separating its contents from that of the cytoplasm. In all plant species the chloroplast can undergo simple division.

Inside the chloroplast the photosynthetic membranes or *thylakoids* are arranged in stacks called *grana* which at lower resolutions appear as dense green areas within the chloroplast. The grana are embedded in a colourless matrix called the *stroma*(the chloroplast "cytoplasm"). The grana are interconnected by a system of loosely arranged membranes known as the stromal lamellae. Using electron microscopy it can be seen the thylakoids have embedded in them the protein-pigment complexes. There is a difference in the complex organisation between the stacked granal lamellae and the loosely packed stromal lamellae. This is because the granal membranes contain mainly PSII, and the stromal membranes contain mainly PSI.

It is possible to separate the pigment-containing thylakoid membranes from the stromal matrix and to analyse its protein/pigment content. The thylakoids are about half lipid and half protein. The proteins bind the redox components needed for electron transfer and also strengthen the membranes. Some of these membrane proteins bind the light harvesting chlorophylls a and b. The stroma contains the soluble enzymes involved in the Calvin cycle which reductively fixes CO_2 to produce sugars. Because the thylakoid lumen is separated from the rest of the chloroplast by a double unit membrane, its internal environment can be regulated independently to some extent and optimised for the photosynthetic reactions. As a result the stroma of the chloroplast has a different chemical composition and pH to that of the surrounding cytoplasm.

There is a popular hypothesis according to which the chloroplast is derived from an endosymbiotic prokaryote. This is based on the observations that the chloroplast is of very

similar dimensions to a photosynthetic bacterium or cyanobacterium and has its own nuclear material. The DNA of chloroplasts is a circular double stranded molecule containing enough genetic information for approximately 125 polypeptides, however it contains quite a lot of non - coding DNA and the characterisation of chloroplast genes and their products is by no means complete. Chloroplasts have all the machinery required for protein synthesis, including ribosomes in both the thylakoids and the stroma. These ribosomes resemble those of prokaryotes rather than those of eukaryotes, providing further support for the endosymbiotic hypothesis for the origin of chloroplasts. The primary structure of chloroplast DNA is significantly different to that of nuclear DNA.To begin with it contains a long inverted repeat sequence. Additionally chloroplast DNA is not complexed to histones as is nuclear DNA, another feature more characteristic of prokaryotes than of eukaryotes.

1.2 Redox Components of the Reaction Centres of Higher Plants.

General Features of Photosynthetic Reaction Centres

All reaction centres have a similar organisation and chemical composition because they carry out the same basic function i.e. the promotion of a stable charge separation with a cationic primary donor and negatively charged terminal acceptor spatially separated on opposing sides of a membrane. They are all integral membrane protein - pigment complexes. The most significant differences between reaction centres arise in relation to the additional functions that they carry out, such as water oxidation in the case of PS II.

There are two types of reaction centre : (1)Low potential - in which the electron passes from a chlorophyll dimer (or special pair) to a chlorophyll monomer, a quinone

acceptor and then onto three iron - sulphur clusters. The acceptors are bound by dimeric core comprising polypeptides with a molecular weight of 70 - 80 kDa. PSI, the reaction centres of green sulphur bacteria and heliobacteria are of this type. (2)High potential - here the sequence of acceptors is as follows : a chlorophyll dimer, a phaeophytin, and a quinone terminal acceptor. In this type of reaction centre the acceptors are bound by dimeric core consisting of monomeric polypeptides with a molecular weight of about 30 kDa. There follows brief accounts of the redox components and function of the reaction centres found in photosynthetic eukaryotes, PSI and PSII.

1.2.1 Photosystem II (PS II)

A schematic showing the proposed arrangement of the major components of PSII is shown in figure 1.4. PSII can be treated as an enzyme catalysing the photoinduced oxidation of water coupled to the reduction of the terminal acceptor, plastoquinone. Plastoquinone goes on to reduce plastocyanin through the b_6f complex, reduced plastocyanin being the electron donor to PSI. The passage of electrons through asymmetrically arranged photosystems I and II generates a proton gradient across the thylakoid membrane. This constitutes part of the proton - motive force (which has a pH gradient and a membrane potential component) and this drives ATP formation by the membrane - bound ATP synthase.

Our knowledge of PSII has been greatly increased by a number of developments in the last decade : the availability of improved preparations of purified PSII particles; the application of molecular genetics and above all the determination of a high resolution X - ray crystal structure of the reaction centre of purple non - sulphur bacteria which is closely related to PSII.

PSII consists of three functional domains: an antenna concerned with the harvesting

Figure 1.4 Schematic of photosystem II. This is a model based roughly on the solved X-ray crystal structure of the purple bacterial reaction centre, showing the major polypeptides and the various redox components thought to be involved in PSII photochemistry. D1 and D2 are the core polypeptides that provide ligands for the chlorin and quinone electron acceptors. α and β are the subunits of the b_{559} cytochrome.

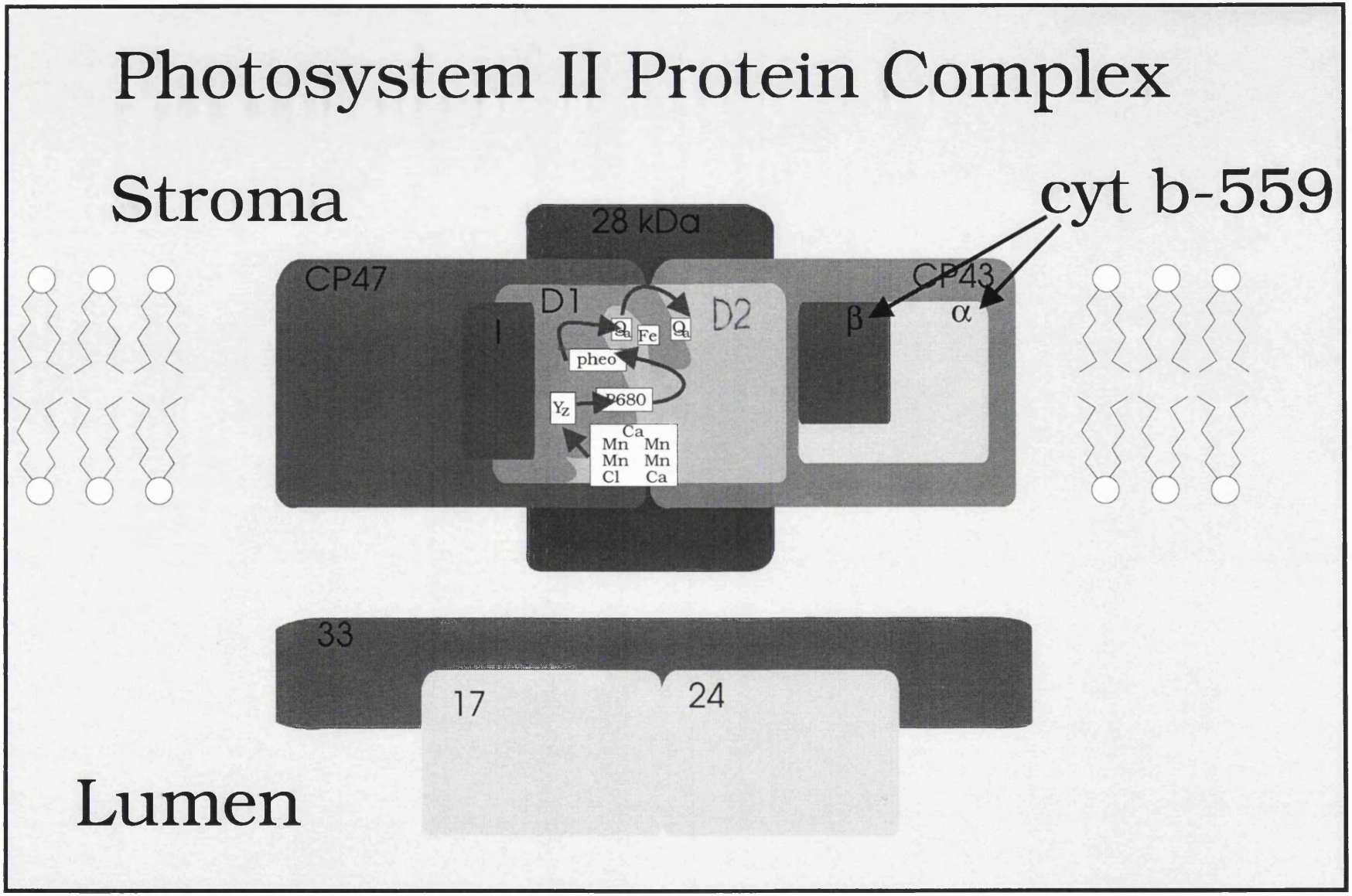
Photosystem II Protein Complex
Stroma
cyt b-559
28 kDa
CP47
D1
D2
CP43
I
β
α
Fe
pheo
P680
Ca
Mn Mn
Mn Mn
Cl Ca
33
17
24
Lumen

Figure 1.4

of light energy and its transfer to the reaction centre core; the reaction centre which contains the redox components involved in the photochemistry of charge separation and including the oxygen - evolving complex (OEC) which is concerned with water oxidation; the regulatory cap which is composed of polypeptides bound lumenally to the thylakoid membrane.The antenna is made up of proximal and distal antennae. The former encloses the reaction centre core and consists of two pigment - protein complexes, CP47 and CP43, which bind Chl a and β - carotene molecules, but not Chl b. The distal antenna consists of the light - harvesting complexes (LHCII) and binds Chl a, Chl b and xanthophylls. A 6 Å electron diffraction structure of LHCII (Kuhlbrandt and Wang, 1991) is available and from this it is clear that the complex is a trimer with each monomeric subunit binding 15 chlorophylls and some carotenoids. The LHCII can dissociate itself from PSII and associate itself more closely with PSI, so it plays a part in energy distribution by mediating between the two photosystems. The process is regulated by the phosphorylation and dephosphorylation of certain amino acid residues.

The regulatory cap is made up of three hydrophilic extrinsically bound proteins, EP33, EP24 and EP17. EP33 separates the OEC from the contents of the lumen. Cross - linking studies have shown that it is in contact with the reaction centre heterodimer. It is thought to have a role in water oxidation as its removal by Tris - washing results in reduced oxygen - evolving activity. It is sometimes referred to as the manganese - stabilising polypeptide because it is thought to be involved in the stable assembly of the manganese cluster and might even provide ligands to the manganese atoms.

The PSII core is the minimal functional unit. It is capable of carrying out the photoinducible charge separation reactions but is unable to evolve oxygen. The PSII core can be routinely isolated and has the following composition : 4 to 6 Chl a molecules, 2

phaeophytins, 2 β - carotenes, 1 D_1D_2 heterodimer, 1 CP47, 1 CP43, 1 or 2 cytochrome b_{559} and 1 110 kDa I polypeptide per P680. The core preparation contains no quinone (Q_A) and no OEC. PSII preparations that evolve oxygen also contain Q_A and a closely associated non - haem iron atom.

Kinetic studies have been carried out on the PSII reaction centre preparations using optical absorption techniques. The primary charge separation reaction which produces the radical pair $P680^+Phe^{--}$ occurs in 3 ps. Charge recombination is prevented by the rapid transfer of the electron from $Pheo^{--}$ to Q_A in 200 to 500 ps and the rapid rereduction of $P680^+$by the redox active tyrosine residue Y_Z. Q_A^{--} is oxidised in 100 to 200 ps by a second quinone, Q_B to give the semiquinone radical. This semiquinone is reduced by a second Q_A to give Q_B^{2--}. By analogy with the purple sulphur bacteria it is assumed that Q_B^{2--} is doubly protonated to plastoquinol which is released from its binding and migrates to the b_6f complex. The vacant Q_B niche in the D_1 polypeptide is filled by another Q_B drawn from the cell's plastoquinone pool.

PSII contains a second redox active tyrosine residue, Y_D, in the D_2 polypeptide present. This tyrosine residue is known to interact with the the oxygen evolving complex in various S states. For example, in the dark the OEC adopts the S_1 state from S_0 by donating an electron to Y_D^+, or from S_2/ S_3 by accepting electrons from Y_D. Y_D has also been implicated in the light - activated assembly of the manganese cluster of the OEC.

Cytochrome b_{559} is a heterodimer consisting of a 9 kDa α sub-unit and a 4 kDa β-subunit which coordinate a haem prosthetic group. This cytochrome may play a role in reducing the likelihood of photoinhibition and / or proton pumping during cyclic electron transfer in PSII.

The most intensively studied aspect of PSII is that of water oxidation. The active site

for water oxidation is thought to be a tetrad of manganese atoms. This manganese cluster is thought to provide the means of storing the oxidising equivalents needed to oxidise water, as well as containing the substrate binding site and site of oxygen evolution. As the reaction centre is turned over by the absorption of successive light quanta, electrons are stripped from the OEC, leading to the accumulation of oxidising equivalents by a process known as the Kok cycle. According to this cycle the OEC goes through 5 distinct redox states, designated S_0 to S_4. It is known that oxygen gas is liberated at the S_3 to S_0 transition. The actual mechanism of water oxidation, the identity of the S - state that binds water, which S - state transitions involve manganese oxidation are the subjects of ongoing investigation. The structure of the manganese cluster has been studied using X-ray absorption fine structure (XAFS) spectroscopy and should soon be known through X - ray diffraction studies of PSII crystals. The chemistry of the Kok cycle is being studied using ESR, XAFS and X - ray absorption near edge structure (XANES) spectroscopy.

1.2.2 Photosystem I (PSI)

Thanks to improvements in preparations/biochemical manipulation, the continuing application of spectroscopic techniques and more recently site directed mutagenesis, the structural and functional elucidation of PSI continues apace though several difficult questions remain to be answered. A schematic diagram of higher plant PSI is shown in figure 1. 5.

The PSI reaction centre can be viewed as a complex integral membrane enzyme system, a light dependent plastocyanin:ferredoxin oxidoreductase to be exact. This reaction centre is found embedded in the thylakoid membranes of higher plants, green algae and the prokaryotic cyanobacteria. Essentially an electron donated by lumenally bound plastocyanin,

Figure 1.5 Model of PSI viewed in the plane of the membrane, showing the arrangement of the important polypeptides. The various redox components are arranged linearly between the two core polypeptides for the sake of clarity, the actual arrangement of the acceptors is not known with certainty. This schematic does not take into accoun that the redox chain is branched, there being two A_1s and two A_0s per P700.

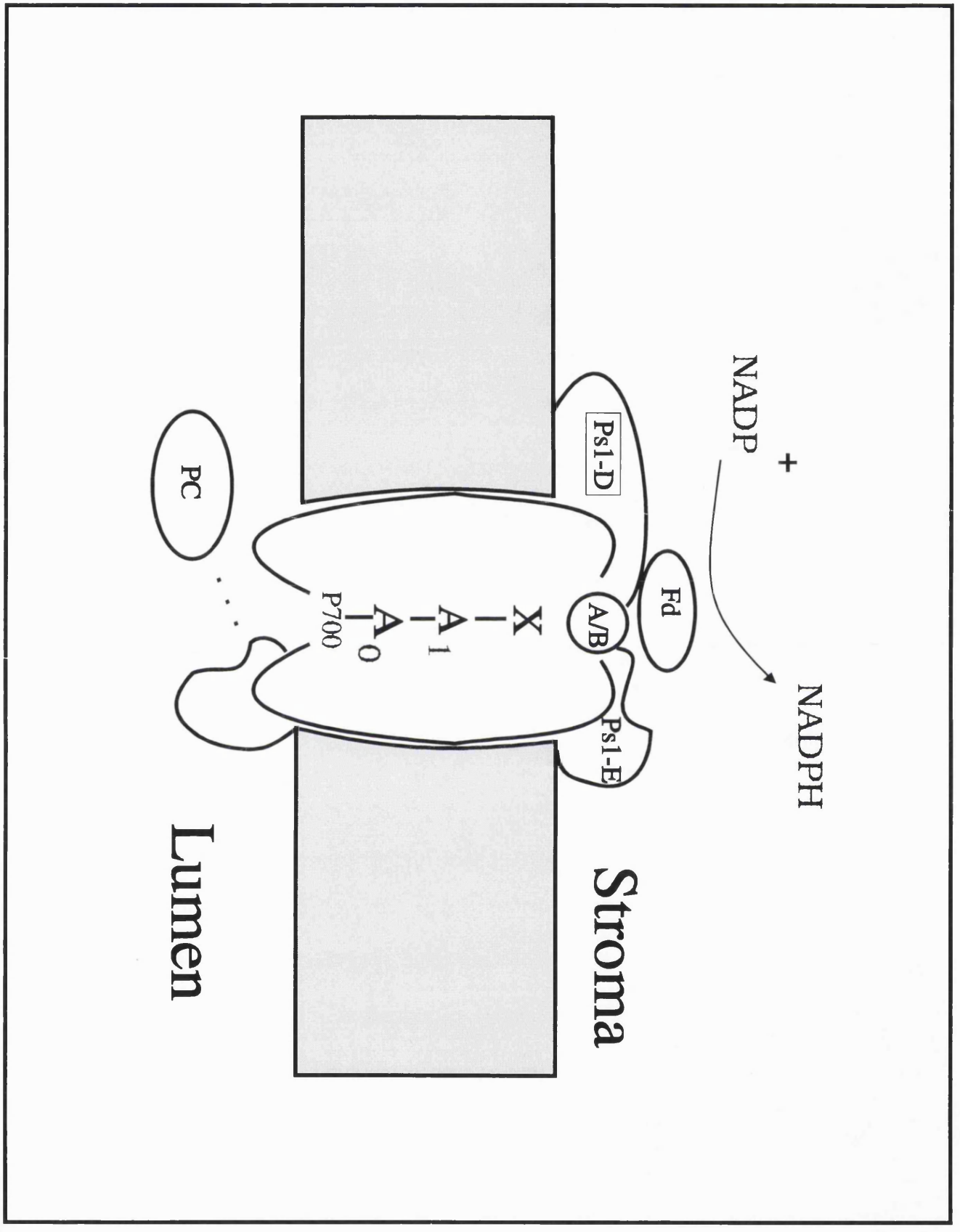

Figure 1.5

a soluble copper-containing protein is transferred across the thylakoid membrane via a series of redox components, whose chemical identity will be discussed below, to reduce ferredoxin, a stromally located soluble iron-sulphur protein. It is assumed the design of PSI, as with other reaction centres, has evolved to permit efficient electron transfer and high quantum yields i.e. charge separations per light quantum absorbed.

Although no PSI or analogous bacterial reaction centre crystal structure is available as yet there is a considerable body of experimental evidence to support the view that the major redox components involved in charge separation are bound by the polypeptides encoded by the following chloroplast genes : *psaA*, *psaB* and *psaC* . The psaA and psaB polypeptides form the heterodimeric core of the reaction centre. These polypeptides have molecular masses of about 82-83kDa and bind, apart from the various redox components connecting plastocyanin and ferredoxin, about 100 accessory chlorophyll molecules. This is different from PSII, in which the core polypeptides bind hardly any accessory chlorophylls, which are bound mainly in the light harvesting complexes. The terminal membrane - bound electron acceptors are two 4Fe-4S iron- sulphur centres designated Fe-S_{AB} which are bound by the 9kDa peptide, psaC which is in turn bound to the core polypeptides. Other extrinsic peptides are thought to stabilise the binding of psaC to the core. The PSI holocomplex also includes at least 10 other polypeptides, named PsaD to PsaO, some of which are nuclear and some of which are chloroplast encoded. In addition there are several light-harvesting chlorophyll proteins (LHCI) encoded by the *cab*-6A/6B, *cab*-7, *cab*-8, and *cab*-11/12 genes. The cyanobacterial PSI holocomplex is very similar to that of algae and higher plants in terms of polypeptide composition, with the important difference that the former completely lacks any LHCI proteins.

The PsaA and PsaB polypeptides are very hydrophobic molecules. Hydropathy plots

(which search for stretches of hydrophobic amino acid residues) predict up to 11 membrane-spanning α-helical regions for each subunit (Fish *et al*, 1986, Fish *et al*, 1985). The two subunits are about 45% identical and about 55% similar, i.e. taking into account the conservative amino acid substitutions. Alignment of the available higher plant sequences shows there is 95% identity between them. The sequences of the cyanobacterium, *Synechococcus* spp.PCC 7002, and the unicellular green algae, *Euglena gracilis* and *Chlamydomonas rheinhardtii* PsaA and PsaB proteins indicate a 95% similarity to the corresponding sequences of higher plants (Andersen *et al*, 1990). The most highly conserved region of the PsaB protein contains the proposed helices VIII - IX, two of the four cysteine residues thought to ligate the internally bound iron-sulphur centre acceptor, Fe-S_X(Golbeck and Cornelius,
1986) and the three leucines separated by a heptad of other residues thought to constitute a *leucine zipper* (Kōssel *et al*, 1990, Webber , 1990). This last feature, and Malkin
commonly associated with DNA-binding proteins, may here have a role in dimerisation and help explain the relative stability of PSI compared to PSII. From inspection of the sequences a case can be made for other putative leucine zipper motifs. However the discovery that the amino acid sequences of heliobacterium and *Chlorobium* (Liebl *et al*, 1993, Buttner *et al*, 1992, respectively) do not contain the zipper motif has cast doubt on the authenticity of the PSI leucine zippers. Modelling of this region (Nugent , unpublished) shows that there are and Berry
structural arguments against the existence of leucine zippers. Mutational studies of the conserved leucine residues in *Synechocystis PCC 6903* suggest strongly that the proposed leucine zippers are spurious (Smart *et al*, 1993). Helix IX contains three highly conserved histidine residues which have been put forward as candidate P700 / A_0 ligands.

The Redox Components

1.2.2 (a) P700- the Primary Donor

The structure of P700 has not been worked out beyond all doubt. It is possible to obtain ether - extracted PSI particles which have a chlorophyll:P700 ratio of 8 (Ikegami and Katoh *al*, 1989). Resonance Raman spectroscopy has been carried out on the P700 signal of such preparations (Moenne-Loccoz, P. *et al*, 1990). The spectrum so obtained can only be interpreted if P700 consists of two distinct chlorophyll molecules. This work also provides further structural information. In CP1 particles (i.e. PSI core containing P700 and functional A_0 only) P700 gives Raman bands at 1555 and 1612 cm^{-1} indicating that the central magnesium ion of each chlorophyll interacts with one external ligand. These results argue against a model in which the two chlorophyll molecules are bridged by water and supports a model in which the chlorophylls are hydrogen bonded to the surrounding protein. Further strong evidence for P700 being a dimer comes from "photochemical hole burning spectroscopy" (Ratajczak *et al*, 1988). P700, P870 (the purple bacterial special pair), and P960 have optical reorganisation energies an order of magnitude bigger than those observed for accessory (i.e. monomeric) chlorophyll. Optical absorption studies on P700 yield a spectrum with the area and bandwidth expected if the ratio of reduced to oxidised chlorophyll forms is 2:1 (Ikegami *et al*, 1988). This could be taken to mean P700 in the ground state i.e.unexcited) is a dimer and in oxidised P700 ($P700^+$) the unpaired electron is predominantly localised on one of the chlorophyll molecules giving it a highly monomeric character. If this is so it would go along way to explain a discrepancy between these and previous spectroscopic data. This suggested that the signals corresponding to the P700 cation and P700 triplet (a recombination signal described in more detail below) were best interpreted as belonging to a monomer. Linear dichroism studies on P700-enriched PSI preparations indicate

the unoxidised chlorophyll of $P700^+$ and a second chlorophyll absorbing at 686nm are orientated at 90^0 to the membrane normal (Brettel *et al*, 1987). The orientation of these redox active components obviously has important consequences for the rates of electron transfer. Orientation studies on the P700 triplet in magnetically ordered PSI membranes also supported a 90^0 orientation (Rutherford *et al*, 1990). ENDOR on P700 radical also favours its being a dimer albeit with most of the electron spin density localised on one chlorophyll of the pair in a ratio of 3:1 (O'Malley *et al*, 1984, Rigby *et al*, 1994). Analysis of electron spin echo envelope modulation (ESEEM) data has been carried out PSI reaction centre preparations (Davis *et al*, 1992) and supported a 3:1 electron spin distribution. This work is currently being extended in a way that will further clarify the electronic structure of P700 (Bratt *et al*, unpublished).

(b) The Primary Chlorin Acceptor (A_0)

A chlorin primary acceptor was predicted for PSI after it was discovered a phaeophytin served as the first acceptor to P680 in PSII and because it was thought such an arrangement would maximise electron transfer rates for the initial photochemical reactions. ESR spectroscopy provided good evidence that this was indeed the case. Signals accumulated in PSI samples either illuminated as they are frozen or illuminated at 200K in the presence of sodium dithionite, a reductant (conditions suggested by analogy with purple bacteria) were attributed initially to a monomeric chlorophyll anion and subsequently to a combination of the anion and another species, A_1 (Bonnerjea and Evans, 1982). Further support for the A_0 spectrum belonging to a chlorophyll anion has come from optical data. Picosecond optical kinetic measurements support the identification of A_0 as a chlorophyll. However these measurements are complicated by the presence within the sample of some 50 accessory chlorophylls per

P700 which transfer excitons at rates in the same time domain and give absorption spectra which are virtually the same as for A_0. Measurements have been made using ether-extracted PSI preparations which lack all functional acceptors after A_0 and have fewer accessory chlorophylls present (Mathis , 1988, Kim *et al*, 1989). Using such preparations A_0 was found to have a rise time of 14ps and a duration of 1ns. Adding vitamin K to the samples (i.e.effectively restoring A_1 which is known to be a molecule of phylloquinone, also known as vitamin K) shortens the duration of the A_0 signal to 150ps. From experiments using less harshly treated PSI preparations, a duration of 40ps was obtained (Wasielewski *et al*, 1987). The same measurements done on the reaction centre of Heliobacteria, believed to be closely related to PSI, strongly suggest the primary acceptor is a chlorophyll and in this system there is no interference from accessory chlorophylls because they absorb at a different wavelength to A_0 (Van den Meent *et al*, 1991). In Heliobacterial membrane fragments a rise time of <36 ps was estimated for the primary acceptor (Nuijs *et al*, 1985). In the absence of any acceptors after A_0 the electron of A_0^{--} back reacts with $P700^+$ and some of this charge recombination occupies the so-called triplet state. This P700 triplet decays to the ground state with a half-life of 3-5μs. The triplet signal is also associated with the back reaction between A_1^{--} and $P700^+$. More recently femtosecond transient absorption spectroscopy used with high intensity excitation under both oxidising and reducing conditions has been used to obtain a A_0/A_0^- difference spectrum (Hastings *et al*, 1994). From these observations it was estimated that A_0 was reduced in 28ps and reoxidised in 21ps. A photovoltage technique has been used to obtain a rate for electron transfer from A_0 to A_1 in a PSII minus *Synechocystis* mutant. Using this approach two phases were observed. A fast phase that gave a fluoresence decay time constant of 22ps which is thought to reflect the rate of primary charge pair formation; and a slower rising phase with a rate constant of 50+/_ 15 ps thought to correspond to the reaction,

and Setif.

A_0^{-}--->A_1(Hecks *et al*, 1994). The midpoint potential for the A_0/A_0^{-} pair has been indirectly estimated as --- 1.01V Vos *et al*, 1988). It must be emphasised the unambiguous identification of A_0 has not been achieved as yet.

(c) Quinone Secondary Acceptor (A_1)

Inconsistencies between the evidence supplied by different experimental approaches have hampered the positive identification of A_1. Most of the spectroscopic data is best interpreted as arising from phylloquinone. The redox potential of A_1 has been estimated at around - 800 to - 810mV (Breton , 1989, Vos *et al*,). The EPR signal of reduced and Ikegami and Van Gorkum A_1^{-} can be photoaccumulated by illuminating PSI preparations at pH 8.0 in the presence of sodium dithionite at 205K. In experiments done at more alkaline pHs and at 230 K the signal accumulated is a mixture of A_1^{-} and A_0^{-}. The A_1^{-} EPR signal occurs at g=2.0058 with a peak to peak linewidth of 0.95mT and is typical of the spectrum belonging to a semiquinone anion (Mansfield , 1988). There are two molecules of phylloquinone per reaction centre one of and Evans which can be doubly reduced by prolonged illumination and the other being more resistant to double reduction (Bottin , 1991, Heathcote *et al*, 1993). Such double reduction traps and Setif electrons in a high energy well with no forward or backward transfer possible. This phenomenon could provide clues to the photoinhibition seen in PSI under conditions of high light intensity and a highly reducing environment (Inoue *et al*, 1989). In the green algae *Euglena gracilis* and the cyanobacterium, *Anacystis nidulans*, phylloquinone is replaced by 5'-monohydroxyphylloquinone (Ziegler *et al*, 1989). An optical flash induced signal assigned to A_1 is also thought to arise from phylloquinone (Anderson , 1991), though as with some and M^{c}Intosh of the relevant EPR spectra, this spectrum is not straight forward and may contain contributions from other species.

By analogy with the purple bacteria it is assumed (but not proven) one phylloquinone is bound by PsaA and the other by PsaB. The two phylloquinones must be surrounded by chemically different environments as they require different treatments to remove them. One can be extracted by treatment with hexane and electron transfer is maintained, as judged by reduction of iron-sulphur centres Fe-S_{AB} , Ferredoxin and $NADP^+$(Biggins and Mathis ,1988, Malkin *et al*, 1986). From this result it appears that transfer to an external acceptor does not require the presence of both quinones and that the loosely bound quinone lies on the inactive path of PSI. However it is difficult to believe that this quinone would have been retained if it did not have some role in the photochemistry.

ESR kinetic measurements performed at 298K looking at electron transfer from A_1^{--} to the next acceptor yields a rate of 260ns (Bock *et al*, 1989). A rate of 200ns was obtained from time resolved EPR measurements on the spin polarised signal belonging to the $P700^+A_1^{--}$ (Thurnauer and Norris , 1980, Siekman *et al*, 1991). Optical determinations for the rate for this reaction have given different answers depending on the organism used etc., the observed rates ranging from 15ns (Mathis *et al*, 1988) to 200ns (Brettel *et al*, 1988). At low temperatures the electron on A_1^{--} recombines with oxidised P700 and the signal decays directly to the ground state with a half time of about 150μs (Setif *et al*, 1984). At room temperature in the presence of chemically or photochemically reduced iron sulphur centres Fe-S_{AB} and Fe-S_X, A_1^{--} back reacts with $P700^+$, showing biphasic kinetics, with a fast component decaying with a half-life of about 750 ns and a slower component decaying with a half life of a few μs. The back reacted electron populates the triplet state of P700. The triplet state then decays to the P700 ground state in a few microseconds. This work was done on PSI from *Synechocystis* sp.(Setif and Bottin, 1989).

Complete destruction of quinones in PSI by uv irradiation of preparations did not

produce any changes in the shape or linewidth of the EPR A_1 signal (Ziegler *et al*, 1987) or on the amount of $P700^+$ generated (Palace *et al*, 1987). It is possible this treatment did not inactivate the phylloquinone at all or at least not to completion, however some effect would be expected if phylloquinone was essential for forward electron transfer. However the uv irradiation experiments were repeated by another group resulting in the rereduction kinetics of $P700^+$ being slowed from the native 30ms to 220ms (Biggins *et al*, 1989) and the loss of $NADP^+$ photoreduction, while the photoreduction of iron-sulphur centres Fe-S_{AB} remained unimpaired at 7K.

Inconsistencies such as this have led to the suggestion that the A_1 EPR signal does not arise from the phylloquinone radical but a "reporter" species (Barry *et al*, 1988). This has been addressed to some extent in an experiment carried out under conditions that would double reduce phylloquinone to the quinol form leading to the disappearance of the A_1 radical signal. When the sample was treated so as to reoxidise the phylloquinone and illuminated briefly at 205K the A_1 was regenerated (Heathcote *et al*, 1993). As phylloquinone is the only possible electron carrier present in PSI that can plausibly be doubly reduced, this provides quite strong evidence that the A_1 EPR signal corresponds directly to phylloquinone.

Another source of confusion and inconsistency has been the use of deuteration experiments. A methionine auxotroph of the cyanobacterium *Anabaena* was grown on deuterated methionine containing medium to produce PSI preparations with phylloquinone deuterated at the 2-methyl group. The A_1 EPR signal photoaccumulated in deuterated PSI was not different to that of undeuterated PSI (Barry *et al*, 1988). This experiment has been repeated and the expected narrowing of the A_1spectrum observed in the deuterated case (Rigby, Heathcote and Evans, manuscript in preparation). In the previous experiment it is possible that the quinone was doubly reduced.

The similarity of the electron spin polarised ESR signal of PSI and that attributed to the spin polarised signal of iron-free purple bacterial reaction centres (which has a contribution from the semiquinone radical) supports the identification of A_1 as a quinone (Stehlik *et al*, 1989) Study of transient spin polarised signal in deuterated PSI preparations at times early after light excitation provides further support for a quinone secondary acceptor (Bock *et al*, 1989). The spin polarised signal was lost from PSI preparations that had been solvent extracted to remove the quinone and restored when the extracted PSI was reconstituted by addition of normal or deuterated vitamin K_1, with a concomitant restoration of forward transfer to the iron-sulphur centres, Fe-S_{AB}. The deuterated vitamin K_1 caused a narrowing of the linewidth of the A_1 EPR signal (Rustandi *et al*, 1990).

Another complication comes from the fact that at low temperatures the electron can pass from A_0^{--} direct to iron sulphur centres Fe-S_{AB} if both phylloquinones have been extracted or doubly reduced. Such a photoreduction of the iron sulphur centres has been observed at low temperature in higher plant PSI depleted of both phylloquinones though at a lower than normal quantum yield (Setif *et al*, 1987). Low temperature optical experiments on the extracted PSI yielded an amount of the laser induced P700/Fe-S_{AB} charge separation equal to 50%of that seen in intact PSI preparations. At room temperature optical measurements on laser-induced transients in the same extracted samples exhibit the 40ns back reaction of A_0^{--} with $P700^+$ in place of the 3μs back reaction of A_1^{--} with $P700^+$, and a small contribution from slow relaxing P700 triplet (Ikegami *et al*, 1987). There is evidence that the "by-pass" is less efficient in thermophilic cyanobacteria than in mesophilic cyanobacteria and higher plants (Ikegami *et al*, 1989).

Attempts have also been made to replace phylloquinone with 14 different benzo-, naphtho- and anthraquinones in extracted PSI and the back reaction kinetics were monitored

to assess the effectiveness of these compounds in restoring A_1 function. From this survey it emerged that a large number of tested quinones had redox potentials lying between those of A_0 and Fe-S_X and were able to functionally stand in for phylloquinone (Itoh *et al*, 1991, Iwaki and Itoh, , 1989). A similar survey in the hands of another group found a far narrower range of substituted quinones could substitute phylloquinone. There is an obvious objection which can be made to these reconstitution studies and this is the problem in telling whether the substituted quinones have penetrated the phylloquinone binding site or are only non specifically associated with the protein complex, acting as indiscriminate acceptors for P700 / A_0. Recently ENDOR analysis of PSI containing deuterated phylloquinone exhibits changes in its A_1 ENDOR spectrum compared to undeuterated. The presence of deuterated phylloquinone was confirmed using mass spectrometry and the results further pin down the identification of A_1 as phylloquinone (Rigby , manuscript in preparation).
Heathcote and Evan

(d) Iron--Sulphur Centre Fe---S_X

The first spectroscopic evidence for the existence of an intrinsically bound iron - sulphur centre, was supplied by the cw ESR measurements of Evans *et al*, 1975. These workers designated the centre as "X". Resonances were observed at g=1.76, g=1.86 at 9K. The spectrum could not be produced by chemical reduction alone, only by photochemical means, implying a highly negative redox potential. An assay detecting zero valence sulphur (a product of the oxidative denaturation of Fe-S clusters) provided the first evidence for the presence of an Fe-S cluster in the core protein of PSI (Golbeck , 1986, Hoj , 1986).
and Cornelius and Moller
The existence of a Fe--S centre bound by the PsaA and PsaB polypeptides was established

optically and by EPR measurements (Golbeck *et al*, 1986, Golbeck *et al*, 1987, Warden *et al*, 1986). The extrinsically bound iron-sulphur centres, Fe-S_{AB}, contained by the PsaC peptide, can be removed by treatments with chaotropes (urea, sodium iodide) leaving the intrinsically bound iron sulphur centre, which has been designated Fe--S_X (Golbeck *et al*, 1988, Parrett *et al*, 1990). This preparation can be used to do spectroscopy on the Fe--S centre, Fe--S_X without interference from other metal centres. Mōssbauer and X-ray absorption fine structure (XAFS) spectroscopy data on Fe--S_X indicate that it is a 4Fe-4S cluster (Evans *et al*, 1981, Petrouleas *et al*, 1989, M^{c}Dermott *et al*, 1989, respectively).

The redox potential of Fe-S_X is unusually negative for a 4Fe-4S cluster at --730mV and this probably relates to the fact that this iron sulphur cluster is bound between the two polypeptides which may result in this centre having a distorted geometry. The only other example of a characterised Fe-S cluster liganded by cysteines supplied by the two halves of a dimer is that found in the nitrogenase system and this also has an unusually negative redox potential. Fe-S_X gives an unusual EPR spectrum for an iron sulphur cluster. It has a $g_{average}$ value which is surprisingly low and resonances that are broad for an iron sulphur cluster, with major features at g=2.04, 1.86, and 1.78. The optical absorbance difference spectrum is more conventional with a typical broad iron-sulphur peak around 430nm, with a shoulder extending to 500nm.

Fe-S_X can be removed by oxidative denaturation which oxidises the sulphides to zero valency sulphur. This can be achieved by incubating PSI core with urea in the presence of potassium ferricyanide. It can be reconstituted by incubating the Fe-S_X-depleted core with $FeCl_3$, Na_2S and β-mercaptoethanol (Oh-oka *et al*, 1989). The preparation of a CPI particle (a PSI particle stripped of all extrinsic peptides by ionic detergents to leave the PsaA/PsaB heterodimer) containing a redox active Fe-S_X has not yet been achieved. This might be

because the treatment with ionic detergents destabilises the iron sulphur cluster or that it damages the A_1 site precluding electron transfer after the quinone acceptor.

The magnetic properties of the Fe-S_X have been interpreted as evidence for a 2Fe--2S cluster (Bertrand *et al*, 1988) but there is now a consensus that it is a 4Fe--4S cluster. There is a similar consensus for there being only one Fe--S_X cluster, making it the only intermediate component to break with the overall C-2 symmetry of PSI (e.g. Guigliarelli *et al*, 1989). Establishing that Fe-S_X is a 4Fe-4S cluster results in certain structural constraints , such centres most likely require 4 cysteine residues as ligands. The PsaA polypeptide contains 3 conserved cysteine residues and the PsaB polypeptide, 2. Therefore PsaB must provide at least 1 and more probably 2 out of the 4 ligands, making Fe--S_X an interpolypeptide cluster (Golbeck *et al*, 1986). 4 of the 5 conserved cysteines of PsaA and PsaB are found as part of a Cys-Pro motif on a proposed extra-membrane loop, which has been found to be characteristic of virtually all known 4Fe--4S clusters. The structural considerations favour the dimeric model of PSI. The dimeric model of PSI finds experimental support in the uniform ^{14}C - labelling work done on cyanobacteria (Wynn *et al*, 1989), the green alga, *Dunaliella salina* (Bruce and Malkin, 1988)[a], and higher plants (Bruce *et al*, 1988, Scheller *et al*, 1989). The size of the PSI reaction centre as determined by neutron scattering (Schafheutle *et al*, 1990), gel filtration (Rögner *et al*, 1990)[a], and electron microscopy of cyanobacterial PSI particles (Rögner *et al*, 1990)[a] agree with a dimeric structure for PSI. A heterodimeric structure is convincingly supported by mutagenesis studies in which the insertional inactivation of either of the structural genes encoding for the polypeptides PsaA or PsaB results in non assembly of the PSI reaction centre. It has now emerged cysteines are not the only possible ligands to low potential 4Fe-4S clusters, aspartate can serve the same purpose. Therefore the structure and ligand arrangement for Fe-S_X cannot be inferred and awaits direct experimental

demonstration. Mutagenesis studies targeting the proposed cysteine ligands are in progress (e.g. Smart *et al*, 1991). To date the participation of Fe--S_X in forward electron transfer has not been unambiguously determined. The general assumption is that the electron takes the following course through the thylakoid membrane : P700--->A_0--->A_1--->Fe-S_X--->FeS_{AB}. This arrangement is arrived at by arranging the redox components in order of increasingly positive redox potential. It is not at all inconceivable for the electron to take an alternative path through the membrane as long as the end result is an oxidised plastocyanin spatially well separated from reduced ferredoxin. It could be argued it would be more thermodynamically favourable for the electron to go from $A_1$to Fe-S_{AB}, bypassing Fe-S_X. It has already been mentioned the electron can by-pass A_1 at low temperatures in higher plant and some kinds of cyanobacterial PSI preparations. Never the less the linear arrangement shown above is the working model most widely adopted in the field. There is kinetic evidence to support it also. When Fe-S_{AB} are both chemically reduced a flash induced charge separation decays in 250μs, at room temperature, typical of a $P700^+$ Fe-S_X^- back reaction. When PsaC is removed by treatment with a chaotrope the flash induced charge separation decays in 1ms, indicative of a back reaction between $P700^+$Fe-S_X^- in the absence of repulsive Columbic effects exerted by the reduced Fe-S_{AB} centres. The situation is not clear cut. Some groups have argued the 250μs kinetic reflects the back reaction between $P700^+$and A_1^-, not Fe-S_X (Brettel *et al*, 1988, 1989). Low temperature kinetics measurements suggest it would be physically difficult to accommodate an acceptor between A_1 and Fe-S_{AB} (Crowder and Bearden, 1983). Also at low temperature, in the presence of reduced Fe-S_{AB} centres, about 90% of the back reaction is between $P700^+$and A_1^- (Setif *et al*, 1984). This last result may only reflect the inefficiency of forward electron transfer after A_1 at cryogenic temperatures, a suggestion reinforced by observations made in our group. Defining the exact role of FeS_X has been complicated by the

fact the spectra of the three iron-sulphur clusters cannot be distinguished optically so it is virtually impossible to tell if the electron is leaving A_1 and going to Fe-S_X or Fe-S_{AB}.

(e) Intrinsic Peptides of PSI

Associated with the PSI core are a number of small proteins which can be stripped from the PSI core by treatment with detergents but not by chaotrope or salt wash treatments, indicating they are intrinsic and not exposed at the complex surface. They include the following peptides: PsaI, PsaJ, PsaK, and PsaL. In prokaryotes there is PsaG, in eukaryotes PsaM and PsaN. None has been found to contain any redox active components and no definite function has been assigned to any of them. Their amino acid sequences are known and mutagenesis approaches have been applied to determine their function. It has also been possible to produce PSI core preparations deficient in some of the intrinsic peptides.

The PsaI and PsaJ proteins are chloroplast encoded and have molecular masses of 3.9kDa and 4.1kDa respectively in spinach, while both have masses of 4.1kDa (Ikeuchi *et al*, 1990, Steppuhn *et al*, 1989). The PsaJ protein has been identified in *Synechococcus vulcanus* (Koike *et al*, 1989), PsaI and PsaJ in *Anabaena* spp. ATCC 29413 (Ikeuchi *et al*, 1991). They are both rich in hydrophobic amino acid residues. From secondary structure prediction programs it is believed they span the thylakoid membrane as single α-helices. From analogy with small hydrophobic peptides in other systems it is inferred they are involved in stabilising proton-lipid interactions in the membrane.

The PsaK peptide is nuclear encoded in green algae and higher plants. In *Chlamydomonas rheinhardtii*, the processed peptide has a molecular mass of 8.4kDa (Franzen *et al*, 1989). As with I and J, PsaK is also very hydrophobic and predicted to consist of one membrane-spanning α-helix, unlike them its hydrophobic core is surrounded by basic and

acidic amino acid residues. The PsaG peptide is also nuclear encoded with a processed mass of 10.8kDa in spinach (Steppuhn *et al*, 1989) and 10.6kDa in *C.rheinhardtii* (Franzen *et al*, 1989). So far it appears to be absent from cyanobacteria. It is an acidic peptide with a transit sequence required for its import across the chloroplast envelope. It is located on the stromal side of the thylakoid membrane.

PsaL is nuclear encoded. The processed peptide is 14kDa in cyanobacteria (Li *et al*, 1991), 18kDa in barley (Okkels *et al*, 1991). Hydropathy plots predict 2 membrane-spanning α-helices. That it is hydrophobic is further supported by the fact chaotropes cannot extract it from either cyanobacterial (Li *et al*, 1991) and higher plant (Scheller *et al*, 1989)PSI complexes and that it partitions with the non-ionic detergent Triton X-114 (Zilber *et al*, 1990).

PsaM is a 3.5kDa peptide detected in certain cyanobacterial PSI preparations (Golbeck *et al*, 1991). A gene encoding a peptide homologous to PsaM has been isolated from the chloroplast genome of liverwort and the alga *C.paradoxa*, but not in any higher plants looked at so far. Its function is not known. PsaN is a 4.8kDa peptide detected in *Synechococcus vulcanus* (Koike *et al*, 1989) and *Anabaena* spp. ATCC 29413 but not as yet in other cyanobacteria or higher plants.

Extrinsic Peptides of PSI

The PSI complex includes a number of extrinsically located low molecular peptides that are generally hydrophil ic in nature and can be extracted with chaotropes or salt wash treatments. Some of these are bound to the stromal (i.e. the acceptor) side of the core complex and have an important function in forward electron transport, these are PsaC, PsaD, PsaE and in eukaryotes possibly PsaH. The first contains two 4Fe-4S clusters, Fe-S_{AB}, and has been

well characterised spectroscopically and biochemically though its function in electron transfer is still the subject of study. The others are thought to assist in the docking of terminal acceptors to the core, their exact structure and function in different organisms has not been settled.

(f)PsaC

This is a 9kDa highly acidic peptide encoded by the chloroplast in alga and higher plants. It contains a 4 cysteine-proline motif typical of 8Fe-8S proteins (Oh-oka *et al*, 1988). The amino acid sequence of the peptide is very highly conserved, with 90%identity among the cyanobacteria (with the exception of *Synechocystis* spp. PCC 6803) and about 95%identity among higher plants, with even higher degrees of similarity as many of the amino acid changes are conservative. There are very few significant differences in the primary structure between eukaryotes and prokaryotes and those do not lead to functional differences. The EPR spectrum of the Fe-S_{AB} clusters in eukaryotes and prokaryotes is the same apart from very slight g-value shifts (Mehari *et al*, 1991). The EPR spectrum of the Fe-S clusters in PsaC detached from the core is different to that in the PSI holocomplex. Its resonances are broader, the g-values are shifted downfield and it is much harder to distinguish between the Fe-S_A and Fe-S_B, the differences between the Fe-S spectra of the prokaryotic and eukaryotic PsaC are essentially lost. The midpoint potential of the two Fe-S clusters in isolated spinach PsaC have been determined by redox titration as -- 470mV and -- 560mV (Oh-oka *et al*, 1991). In the spinach PSI holocomplex the midpoint potentials were -- 530mV for Fe-S_A,--560mV for Fe-S_B (Evans and Heathcote, 1980). Redox titrations carried out on the isolated spinach PsaC gave a redox potential of 510 mV for both clusters (Hanley *et al*, 1992). It appears the redox and to some extent the magnetic properties of these clusters are influenced more by the environment supplied by PsaC than interaction with the core complex. Adding purified PsaC back to the

depleted core complexes of *Synechococcus* spp. PCC results in an almost complete restoration of the control-type spectra for the Fe-S_{AB} clusters, showing the resonance broadening arises because of separation from the core, disruption of some magnetic interaction rather than from damage induced by the organic solvent used to extract PsaC (Mehari *et al*, 1991, Oh-oka *et al*, 1988, Wynn *et al*, 1988). The extrinsic peptides PsaD and PsaE do not bind or bind negligibly to the PSI core in the absence of PsaC, When the core is reconstituted by addition of PsaC, these peptides rebind allowing speculation about the architecture on the stromal side of the PSI holocomplex. This observation implies that either that PsaD and PsaE are bound atop PsaC, or that the binding of PsaC to the core induces a conformational change allowing the binding of these peptides (Li *et al*, 1991).

The precise role of Fe-S_{AB} in forward electron transfer is still a subject of contention but by ordering the redox potentials in order of increasing electropositivity it would be predicted the path of the electron is : Fe-S_X --->Fe-S_B--->Fe-S_A . The reduced low temperature photoreduction of Fe-S_A observed after inactivation of Fe-S_B with diazonium compounds supports this arrangement (Malkin, 1984). Other experimental observations disagree with this finding. For example the removal of Fe-S_B with urea (Golbeck and Warden, 1982) or mercurous chloride (Sakurai *et al*, 1991) has a negligible effect on the room and low temperature kinetics of Fe-S_A photoreduction. This had led to the proposal of their being a branch point at Fe-S_X with the electron passing either to FeS_A or FeS_B. A mutagenesis approach has also been taken to study the function of Fe-S_{AB}. The production in *Synechococcus* sp. PCC 6301 of mutants with altered 3Fe-4S Fe-S_B cluster, which gives an ESR spectrum with modified g-values, has led to a tentative identification of the cysteine residues binding the Fe-S_A cluster and the Fe-S_B cluster (Zhao *et al*, 1992). This work further supports the proposal that the presence of Fe-S_B is not necessary for electron transfer to Fe-S_A, as the latter can be photoreduced in PSI

complexes containing the altered cluster. In *C. rheinhardtii* the disruption of the *psaC* gene results in non-assembly of PSI complexes, suggesting PsaC has a part in complex assembly in this organism and perhaps in higher plants. In the recently published, relatively low resolution crystal structure of the PSI reaction centre, one Fe-S cluster is more buried than the other cluster, meaning it will be physically closer to Fe-S_X and thus probably the next acceptor, physical separation in this instance being at least as important a factor as midpoint potentials in determining the path of the electron.

It would be useful from the point of view of piecing together the protein architecture of the stromal side of the PSI complex, if a three-dimensional structure of the PsaC peptide could be obtained using 2D-nuclear magnetic resonance (NMR) spectroscopy, to fit in with the NMR and crystallographic functional studies being carried out on other peptides associated with the PSI complex. While PsaC is a relatively small peptide and hydrophilic, the presence of metal clusters would greatly broaden spectral lines, so the high resolution needed for a three-dimensional solution structure could not be achieved at present.

(g) PsaD

This is a nuclear encoded basic peptide with a molecular weight of about 18kDa in eukaryotes and about 16kDa in cyanobacteria (Reilly *et al*, 1988). There is about 55%similarity between the higher plant and cyanobacterial amino acid sequences of PsaD. Among the higher plant sequences there is identity of about 85%, among cyanobacterial sequences of about 65%. From the observations that PsaD is accessible to proteases and cross-linking reagents it was concluded PsaD is exposed at the stromal side of the thylakoid membrane (Zanetti and Merati, 1987). The peptide's leader sequence, required in eukaryotes for import into the chloroplast and which is cleaved off in the mature peptide, is not hydrophobic

either. Reconstitution and chemical modification experiments have given strong hints as to the function of this peptide in PSI. Treatment of PSI with the zero-length cross-linker N-ethyl-3-3-(dimethylaminopropyl) carbodiimide (EDC), which supposedly only cross-links proteins interacting electrostatically, generated covalently bound ferredoxin-PsaD complexes. Such an interaction, required for binding of ferredoxin to the core, fits in with the fact that at physiological pHs, PsaD is a basic peptide and ferredoxin is acidic.

Secondly, using cyanobacterial PsaD overexpressed in *E.coli,* it was found that the presence of PsaD was necessary for the stable rebinding of PsaC to the core. The effect of PsaD addition was monitored by looking at the EPR spectrum of Fe-S_{AB} cluster compared with that in control PSI. In the absence of PsaD the PsaC does rebind to the apo-complex and forward electron transfer becomes possible with both Fe-S_A and Fe-S_B getting equally photoreduced (Li *et al*, 1991, Zhao *et al*, 1990). In the presence of added PsaD the electron is preferentially transferred to the Fe-S_A cluster at low temperature, the resultant Fe-S_{AB} EPR spectrum more closely resembled that of control particles, the resultant "holo"complex was more stable than that formed in the absence of PsaD. This suggests PsaD is needed for PsaC to bind in a specific orientation which would be important in determining which is the next acceptor after Fe-S_X. In this study it was found the addition of recombinant PsaE to the reaction mixtures produced no additional effect. The same sort of study was carried out on the spinach system, using PsaC, D and E isolated from spinach leaves. However it was found the PsaD and PsaE copurified and so it was a mixture of the two peptides that led to stable rebinding of PsaC and restoration of near-control levels of $NADP^+$ photoreduction (Hanley *et al*, 1992). In higher plant PSI at least it is not yet known whether either PsaD or PsaE alone will suffice to restore control-type binding and function.

At present there is no available three dimensional structure for PsaD. With a molecular

weight depending on the source that ranges from 16 to 18 kDa it is a little too large to do 2D NMR on, the molecule in solution would tumble relatively slowly resulting in line broadening and loss of resolution.

A mutagenic approach has also provided useful information. The *psaD* gene has been inactivated in *Synechocystis* spp. PCC 6803 (Chitnis *et al*, 1989). The mutants ability to grow on a sugar carbon-source in the presence of DCMU, an inhibitor of electron transfer, was largely unimpaired. However under conditions necessitating photoautotrophic nutrition its growth rate compared to wild type was considerably slowed down. As disruption of *psaD* did not result in non assembly of the PSI complex or total loss of photosynthetic function, it follows PsaD is not absolutely required for PSI photochemistry to occur, but is needed for it to occur at optimal rates. The PSI complexes prepared from this mutant also lacked PsaE. It may be PsaE was lost as a consequence of the purification protocol used, or because PsaD is additionally required for the stable docking of PsaE to the PSI core.

(h) PsaE

This is another nuclear encoded peptide occurring in green algae and higher plants. Its molecular weight varies from one organism to another, almost 10kDa in spinach, 8.1kDa in *C.reinhardtii* and 7.7--8.1kDa in cyanobacteria. Again there is a considerable amount of identity of amino acid sequence within these groups and similarity between them. ^{14}C-labelling experiments suggested there were two PsaE molecules per reaction centre. This is now known to be a misinterpretation arising from the fact that PsaE and PsaL comigrate

during SDS polyacrylamide gel electrophoresis (Zilber *et al*, 1990). In tobacco PsaE exists as two isoforms, one of 17.5kDa and one of 18.6kDa which might give this plant adaptive possibilities under stressful conditions (Obokata *et al*, 1990). PsaE can be cross-linked to PsaD and ferredoxin, indicating a stromal location for this peptide (Andersen *et al*, 1990, Oh-oka *et al*, 1989). It has been demonstrated in reconstitution studies, PsaE binding to extracted PSI core is simultaneous with that of PsaC and PsaD (Li *et al*, 1991). Mutagenic approaches to studying PsaE in maize have not yet borne fruit.

More recently PSI complexes have been isolated from a mutant *Synechocystis* sp. PCC 6803 in which the *psaE* has been insertionally inactivated. The isolated complexes were subjected to spectroscopic and biochemical analysis. The rate of direct photoreduction of ferredoxin was found to be very much reduced relative to the wild type complex. The wild type rate was restored when purified PsaE was added back (Rousseau *et al*, 1993). The same workers labelled wild type cyanobacterial PSI when membrane-integrated and found residues after the N-terminal sequence of PsaE were labelled with a fluorescent marker, concluding they were exposed at the stromal side of the membrane. Site-directed mutagenesis of these labelled residues indicated they are needed for the correct integration of PsaE into the PSI complex. This study implies PsaE, like PsaD, is required for optimisation of electron transfer processes.

There is also now available a three-dimensional solution structure for *Synechococcus* sp. PCC 7002 PsaE solved by 2-D NMR (Falzone *et al*, 1994). The main structural feature seen is a five stranded β-sheet with very little overall helicity. Conformational homology searches turned up a striking similarity between PsaE and Src homology 3 (SH3) domain, a eukaryotic membrane-bound protein believed to be involved in signal transduction. The dynamic interaction between PsaE and other PSI proteins comprising the holocomplex could

also be studied using NMR.

(i) PsaH

This protein is encoded in the nucleus (in eukaryotes) and is targeted to the stromal side of the thylakoid by a leader sequence. Its molecular weight varies from one organism to another : spinach and barley - 10.2 kDa (Steppuhn *et al*, 1989, Okkels *et al*, 1989 respectively), *C.reinhardtii* - 11 kDa. There is about 82% identity between higher plant sequences but only 40%between higher plant and *C.reinhardtii* sequences. It is hydrophilic and can be cross-linked with PsaD (Anderson *et al*, 1990). It does not partition with Triton X-114 (Staffan and Andersson, 1991). This stromally bound peptide is absent from cyanobacteria. The fact that *psaH* transcripts accumulate after a delay in bleached chloroplasts which have been illuminated, a characteristic shared by LHC components, has led some to postulate a role for this peptide in docking of light harvesting complex to the core.

(j) PsaF

To date this is the only known lumenally bound peptide of PSI. It is nuclear encoded in eukaryotes, having a transit peptide sequence directing it to the lumenal side of the thylakoid (Steppuhn *et al*, 1988). In spinach the processed peptide has a molecular weight of 17.3kDa and is highly charged (basic). PsaF also has two distinctly hydrophobic regions. This explains why PsaF partitions in Triton X-114. Conventional chaotropes cannot remove PsaF from *Synechococcus* PSI preparations (Li *et al*, 1991). Prolonged exposure to 0.2-1% Triton X100 does however extract this peptide and so it is absent from most, if not all Triton PSI particle preparations.

PsaF is thought to be involved in the docking of plastocyanin and cytochrome c_{553}, both donors to $P700^+$. PsaF has six hydrophilic regions, all rich in lysine residues. These positively charged patches are expected to interact electrostatically with the acidic plastocyanin molecule, possibly allowing it to dock in an orientation specific fashion that optimises forward electron transfer to $P700^+$. It has been shown that $P700^+$ rereduction rates are slowed in PSI complexes from which the psaF has been removed by extraction with Triton-X100 and restored to near-normal by addition of N-methylphenazonium-3-sulphonate, an artificial electron donor (Bengis and Nelson, 1977). Treating spinach PSI with EDC results in the formation of a 31kDa adduct of plastocyanin and PsaF (Wynn *et al*, 1988). One kinetic study demonstrated that fast $P700^+$rereduction rates were only achieved in the presence of PsaF (Hippler *et al*, 1989). However, a *Synechocystis* mutant lacking PsaF has been shown to grow photoautotrophically at wild-type rates (Chitnis *et al*, 1991).

In cyanobacteria the plastocyanins examined so far have proved to be less acidic than their higher plant equivalents (p*I*=5.6 against p*I*=4.0 for plants) and this may reflect a difference in the requirement for a PsaF- type peptide to mediate plastocyanin and PSI core interactions between the two types of organism. In addition cyanobacteria differ from photosynthetic eukaryotes in that they can use c-type cytochromes in place of plastocyanin as the immediate donor to $P700^+$. It has been argued that no subunit (PsaF or otherwise) is needed for electron donation to the core by cytochrome in *Synechococcus elongatus* (Hatanaka *et al*, 1993). A laser flash kinetic study has been carried out on cytochrome c_6 and plastocyanin electron donation in *Synechocystis* (Hervas *et al*, 1994). In this study it was observed that the cytochrome was the more efficient donor at physiological mild acid pH. For both donors there was shown to be a linear relationship between rate of electron transfer and protein concentration suggestive of a "one-hit/one step" interaction mechanism, rather than

one including a complex formation step (and thus participation of a PsaF-like peptide). Clearly for PsaF, perhaps more than for other peripheral proteins of PSI choice of organism for study is important and where parallels between cyanobacterial and algal/plant systems do not hold.

2.0 A Kinetic Study of Spinach Photosystem I Using Pulsed ESR Spectroscopy

Sub-Introduction

(a) Principles of Electron Spin Resonance (ESR) Spectroscopy

This is a technique which can be used to study the electronic structure and electron transfer processes involving chemical species that contain an unpaired electron (i.e. paramagnetic). Examples of such paramagnetic species include free radicals, transition metal complexes, odd-electron molecules, rare earth ions and triplet state species. An electron, having both spin and charge, can behave as a magnet. Paired electrons have their spins opposed so their net magnetic moment is equal to zero. An unpaired electron has a net magnetic moment able to interact with an externally applied magnetic field. When an external magnetic field is applied to a population of unpaired electrons the majority of them are aligned so that their magnetic moment is parallel to that of the applied field (and their spin antiparallel to it), a far smaller proportion with their magnetic moment antiparallel(and their spin parallel) to the external field. The second case is the less energetically favourable and an electron populating this higher energy state will rapidly return to the stabler lower energy state by a process of *relaxation.*

The proportion of unpaired electrons occupying the higher energy state can be boosted if the sample is irradiated with microwaves. In this case electrons flip back and forth between the states absorbing or emitting microwaves in the process. However the higher energy state will remain the least populated. It is this inequality along with absorptive/emissive phenomena that provides the basis of an ESR spectrum.

The principles of ESR spectroscopy may be explained in a slightly more rigorous form as follows. An electron has a *spin quantum number* of a half meaning it has two energy levels it can occupy and which differ in energy by a small degree when exposed to a strong magnetic field. The lower energy level is termed m=--1/2 and the higher one, m=+1/2, the difference being due to the electron's negative charge.

The difference in energy between the two levels can be expressed in the form of the following equation :

$$\Delta E = h\nu = \mu \beta_N H_0 \ / I \ = g \beta_N \ H_0$$

where h is Planck's constant (6.62 x 10^{-34} J s) , ν is the frequency of radiation (microwave), μ is the energy of the elecron's magnetic moment, H is the frequency of the applied magnetic field, β is the Bohr magneton with a value of 9.27408 x 10^{-24} J/T, I is the spin quantum number and g is the splitting factor. This value varies according to the electron's environment and is empirically derived. For a free electron g = 2.0023; for an unpaired electron in a molecule or ion g occurs within a few percent of this value , the biggest shift being encountered for the transition metals. X-band ESR spectrometers routinely use a magnetic field of 3400 G. If this figure is inserted in the equation above a value for ν of 9500 MHz is arrived at. Therefore the radiation frequency which will enable the observation of a resonance for a particular unpaired electron is in the microwave range. In ESR spectroscopy the microwave frequency is usually fixed and the magnetic field is scanned until the resonance is observed.

(b) Origin of an ESR Spectrum

Most molecules are ESR silent i.e. produce no spectrum in an ESR spectrophotometer. This is because they are *diamagnetic,* containing only paired electrons which when placed in an external magnetic field produce very small fields which act in opposition to the applied field. On the other hand paramagnetic species containing unpaired electrons produce stronger fields which have the effect of reinforcing the applied field. In a magnetic field an unpaired electron undergoes energy level splitting which can be observed through microwave absorption.

The splitting pattern for a particular sample is complicated through the interaction of the electron spin with the spin of nuclei. If an electron interacts with n equivalent nuclei, its resonance peak is split into $(2nI+1)$ peaks, where n is the number of equivalent nuclei and I is the spin quantum number of the nuclei. This is known as *hyperfine splitting*.

(c) Applications of ESR Spectroscopy in Photosynthesis

Photosynthesis involves electron transport reactions with redox components being oxidised and reduced, in the process radicals are generated which are paramagnetic. Therefore photosynthesis lends itself to being studied with ESR spectroscopy. At the most qualitative level it can be used to identify redox active chemical species within a given system. An ESR spectrum for a radical or metal yields information such as *linewidth* (the distance in Gauss or mT between the maxima and minima of signals), the lineshape, spectral structure and g - value which are 'chemical species dependent' and give insights into electronic structure. The spectrum is also sensitive to changes in the environment of the paramagnet induced for example by different biochemical treatments. Because transition metals(iron, manganese for example) also play an important part in the photochemistry of photosynthetic organisms, ESR

spectroscopy has been applied to better define their functions. The relaxation rates of transition metal complexes are very rapid and for this reason ESR spectroscopic measurements are often carried out at cryogenic temperatures (\<77K). Each ESR spectrum can be optimised by adjusting the parameters of temperature, microwave power, magnetic field frequency etc.

In continuous wave (cw) ESR the sample is continuously irradiated with microwaves of an unvarying frequency. In pulsed ESR microwaves are delivered to the sample in pulses. In the following work pulsed ESR is used to study the kinetics of forward electron transfer from A_1 in spinach PSI. A laser flash induces transient spin polarised signals whose decay is measured. Microwave pulses flip the signals into an orientation or *phase* in which they are detectable. Microwaves are emitted to produce an *echo* which is detected.

2.1 The Use of Pulsed ESR Spectroscopy to Measure Electron Transfer Kinetics.

The rates of electron transfer reactions may be measured using optical methods such as flash absorbance or by magnetic resonance techniques, e.g. cw or pulsed ESR spectroscopy as defined above. In the following sections a pulsed ESR kinetics study of PSI is presented.

The pulsed ESR spectrophotometer can measure the decay or rise of light - induced radicals with a ns resolution- in the case of the instrument used here the resolution limit is 8ns, a resolution of 1 ns is probably the greatest possible using ESR spectroscopy. The charge separation is induced using a laser flash with a wavelength of 532 nm. The spectrometer has two detection channels. A dark signal, from a chemically reduced or dark stable radical, is required for the phasing of the instrument. Phasing refers to the calibration of the detection

system and is achieved when the dark signal gives in one channel a wholly absorptive spectrum (i.e positively phased) and in the other a wholly emissive spectrum (i.e. 90^0 out of phase). Once the instrument has been phased the decay and / or rise of the light - induced radical can be measured against time to give a kinetic trace.

(a)Spin Polarised Resonance Signals of PSI

These are unusually high intensity ESR signals arising from interactions between paramagnetic species. The existence of spin polarised signals associated with PSI was first recognised by Blankenship *et al*, 1975 and Thurnauer *et al*, 1979. It is now probable that the spin polarised signal recognised in the first instance belonged to the $P700^+Fe\text{-}S^{--}$ radical pair and that in the second instance to the $P700^+A_1^{--}$ radical pair. These signals were unambiguously correlated with PSI because of the fact the signals were significantly attenuated if P700 was oxidised prior to signal induction; and also because extraction of the quinone, A_1 resulted in the disappearance of the spin polarised signal (Rustandi *et al*, 1990). This signal is also lost when PSI is illuminated at a highly reducing redox potential, conditions under which $A_1$is doubly reduced to the quinol form (Snyder *et al*, 1991). It was first observed by Thurnauer and Norris (1980) that the $P700^+A_1^{--}$ spin polarised signal displayed an echo phase shift phenomenon. The effect can be summarised as follows : after the execution of the flash/pulse sequence required for the induction and detection of the signals, a g=2.0053 absorptive and a g=2.0023 emissive signal were observed in the detection channel termed Y; unexpectedly the g=2.0023 was also observed in the detection channel termed X as absorption. This shift effect was found by us to depend on the intensity of the microwave pulses used to probe the sample and not to be time - dependent as Thurnauer and

Norris found. Both the g=2.0023 signals in the X and Y channels gave electron spin echo envelope modulation patterns expected for a nitrogen-containing species such as a chlorophyll molecule. Thurnauer and Norris interpreted the effect as follows : during the microwave pulse one of the components of the radical pair (assumed to be A_1^{--}) becomes diamagnetic through oxidation, leading to a loss of interaction between the components of the radical pair which would allow a change in the Lamor frequency of $P700^+$, which could in turn lead to the observed echo shift. This interpretation is not compatible with our own observations however. Very recently a theoretical description accounting for the origin of the spin polarised signal and echo shift was attempted by Tang *et al*, 1994 however experiments in which the interval between laser flash and spin echo were increased indicated that this model is incorrect (Bratt and Evans, unpublished). It is possible that time-resolved ESR work done on the radical pair in bacterial reaction centres (Bittl *et al*, 1994) may shed light on how the spin polarised signals arise but for the moment their origin is unknown. However this does not affect their worth as markers of electron transport. There is a difference in nomenclature between our work and that of Thurnauer and Norris, what they refer to as the X- and Y-channels we term the out - of - phase and in - phase channels respectively.

(b)The Kinetics of PSI Electron Transfer in PSI

With time-resolved cw ESR two consecutive electron spin polarised signals were observed (Bock *et al*, 1989, Stehlik *et al*, 1991). The first ESP signal exhibited an absorption/emission pattern and like the signal described above using pulsed EPR has been attributed to the $P700^+A_1^{--}$ radical pair (Blankenship *et al*, 1975, Gast, 1982, Furrer and

Thurnauer, 1983, Hore *et al*, 1987). The second ESP signal covers the same spectral region as the $P700^{+}$, was mainly emissive in character and has been attributed to the $P700^{+}Fe\text{-}S^{-}$. These observations were made on PSI prepared from cyanobacteria. From the decay and rise times of the ESP signals, it was inferred that forward electron transfer from A_1 took place in 260 ns (Bock *et al*, 1989). Such transient signals have also been studied with time-resolved optical spectroscopy. From this work the rate of A_1^{-} reoxidation was determined as 250 ns (Brettel *et al*, 1988). A similar study was undertaken on spinach PSI Triton particles. The kinetic observed for electron transfer beyond A_1 was biphasic, consisting of a 'fast' component with a half life ($t_{1/2}$) of 25 ns and a 'slow' component with $t_{1/2}$ of 150 ns (Mathis and Setif, 1988; Setif and Brettel, 1993). The discrepancy in kinetic profiles for what should be the same reaction is not thought to involve a genuine species - specific phenomenon. The faster spinach component is thought to arise from Triton induced damage to the reaction centre.

A reoxidation rate of 200 - 250 ns for A_1^{-} has generally been settled on. There is also wide agreement that the next acceptor after A_1 is an Fe-S cluster. The exact identity of this cluster was not known with certainty because of various complications. Chemical pre-reduction of $Fe\text{-}S_A$ and $Fe\text{-}S_B$ clusters strongly inhibits electron transfer after A_1 presumably due to repulsive Columbic effects, so this method cannot be used to differentiate between the three possible electron pathways : A_1 ----> $Fe\text{-}S_A$, A_1 ---> $Fe\text{-}S_B$, A_1 ---> $Fe\text{-}S_X$. Nor can optical absorbance techniques be applied to determine the identity of $Fe\text{-}S_?$, because the molar extinction coefficients of the three clusters are too small and they all give the same absorbance spectrum. Resonance spectroscopy can distinguish between them but at the cryogenic temperatures needed to observe the spectra of fast relaxing species such as paramagnetic Fe-S clusters, forward electron transfer after A_1 even in intact PSI particles

containing oxidised iron - sulphur clusters, has been found to be highly inefficient(Malkin *et al*, 1984) with low yields of reduced iron - sulphur clusters being produced by single turnover flashes. In chemically prereduced PSI examined at 4 K using resonance spectroscopy the predominant kinetic observed is a 120 μs decay and not the 200 ns kinetic associated with forward electron transfer from A_1^{--} (Setif *et al*, 1984). A low level of Fe-S_X photoreduction must be possible at cryogenic temperatures as illumination at 9 K generates the g=1.76 resonance characteristic of this reduced iron-sulphur cluster in amounts detectable using cw ESR spectroscopy (Evans *et al*, 1975).

It has been suggested this low temperature inhibition might arise through competition between the forward and back reactions involving A_1. It might also result from competition between the following two forward reactions : A_0^{--} ---> Fe-S_X and A_0^{--} --->A_1working in parallel not in series, or with $P700^+A_0^{--}$ back reaction. This explanation fits far better with the kinetic data - as A_1^{--} reoxidation occurs in about 200 ns and the back reaction with $P700^+$ in 120 μs, it would be expected the forward reaction dominated to give a monophasic kinetic. At cryogenic temperatures it appears the major kinetic phenomenon is the back reaction (or recombination) of A_1^{--} with $P700^+$.

In the following study time resolved pulsed ESR spectroscopy at room temperature and at 4 K was used to confirm an out of phase ESP signal is derived from the same radical pair ($P700^+A_1^{--}$) as the PSI spin polarised signal first described by Thurnauer and Norris,1979 Using chaotrope treatments to selectively remove the iron sulphur clusters from spinach digitonin PSI particles, the identity of the acceptor receiving the electron from A_1 has been unambiguously determined as FeS_X. The 200 ns kinetic has therefore been reliably attributed to the reaction : A_1^{--} ----> Fe-S_X . It is observed in the following that when forward electron transfer is blocked because of chemical pre-reduction of the Fe-S_{AB} clusters, the use of low

temperature or the removal of PsaC, that the decay kinetics of the out of phase ESP signal lengthen from the ns to the μs range.

2.2 MATERIALS AND METHODS

(a) Preparation of Triton X-100 - Fractionated PSI

Chloroplasts were prepared from spinach as described for the preparation of Digitonin PSI particles. For the preparation of Triton X-100 PSI particles the method of Berthold, Babcock and Yocum (1981) with modifications by Ford and Evans (1983) was used. The stacked spinach thylakoids were incubated with 5 % (w/v) Triton X-100 and resuspending medium at a chlorophyll concentration of 2 mg / ml in the dark, on ice for about 25 minutes. This mixture was centrifuged for 2 hours at 40,000 x g to pellet out most of the PSII. The supernatant was centrifuged at 145,000 x g for 2 hours to pellet any residual PSII.

The pH of the PSI - containing supernatant was raised to 8.0 and its concentration adjusted to 20 mM Tris and 100 mM NaCl. The supernatant was then dialysed against 100 mM NaCl and 20 mM Tris pH8.0 in the dark at 4 ^{0}C.

The PSI in this supernatant was then purified by hydroxyapatite column chromatography, which strips away the light - harvesting complex, free chlorophylls and carotenoids and some low molecular peptides.

The packed hydroxyapatite column was equilibrated with 20 mM Tris - HCl pH 8.0 and 100 mM NaCl. The supernatant was loaded onto the column and washed with 20 mM

Tris - HCl pH8.0, 100 mM NaCl and 0.5%Triton until the eluate was clear. It was then washed with 3 column volumes of 0.1 % Triton X-100, 20 mM Tris - HCl pH8.0 and 100 mM NaCl to remove surplus detergent. The PSI was visible as dark green band at the top of the column and was eluted with 5 - 15 mM KH_2PO_4, pH 6.8, 100 mM NaCl and 0.1 % Triton X - 100.

The pH of the eluted PSI was raised to 8.0 by the addition of 20 mM Tris pH 8.0 and dialysed against 20 mM Tris pH8.0 and 100 mM NaCl for 12 hours at 4 ^{0} C in the dark to remove the phosphate. The PSI - containing eluate was concentrated in an Amicon ultrafiltration cell fitted with a YM100 membrane and stored at 77 K until required.

(b) Preparation of Digitonin PSI Particles.

Digitonin PSI particles were prepared according to a method based on that of Boardman (1971). Market spinach leaves were washed and deveined. The leaves were homogenised in a Waring blender in ice cold grinding medium, 20mM Mes-NaOH, 0.2mM $MgCl_2$ pH 6.3. Ascorbate (approx. 5mM) was added to each grind. The homogenate was filtered through 8 single layers of muslin. The filtrate so collected was spun at 3000 x g for 7 minutes in a Mistral centrifuge to pellet the chloroplasts. The chloroplasts were subjected to an osmotic shock by resuspending them in 5 mM $MgCl_2$ for 30 seconds followed by an equal volume of ice cold resuspending medium, 20 mM Mes-NaOH, 25 mM NaCl, 5 mM $MgCl_2$ pH 6.3. The suspension was spun at 3000 x g again for 25 minutes to pellet released thylakoids. This pellet was resuspended in as small a volume as possible of TEM buffer, 50 mM Tris-HCl pH 8.0, 5 mM $MgCl_2$, 2 mM EDTA. The detergent Digitonin (supplied by

Aldrich) and if necessary extra TEM buffer were added to give final concentrations of 1.1%Digitonin and 1.5 mg chlorophyll / ml. It was sometimes necessary to adjust this ratio to maximise the final yield. The mixture was incubated in the dark, on ice for 30-40minutes with stirring. The mixture was spun in a Sorvall RC5B at 10000 x g for 30 minutes and the resulting pellet discarded. The supernatant was spun 50000 x g in a Sorvall ultracentrifuge for 25 minutes and the resulting pellet was once again discarded. These two spins should eliminate any contaminating PSII. The supernatant was finally spun at 150000 x g for 90 minutes. The resulting PSI pellet was resuspended in TEM and stored under liquid nitrogen.

(c) Chlorophyll Assay

This was carried out according to the method of Arnon (1949) and used to determine chloroplast yields and chlorophyll a/ chlorophyll b ratios. 1 ml of 80 % acetone was used to obtain a baseline in the 640-668 nm range using Philips PU 8740 uv/vis scanning spectrophotometer. 25µl of sample was added to 10 ml of 80 % acetone, filtered and 1 ml of it was placed in a cuvette and absorbance readings were taken at the following wavelengths; 663 nm, 652 nm and 645 nm. The measurements were repeated at least once for each sample. The chlorophyll a and b concentrations can be calculated from the equations below : The contributions to absorbance by each the two chlorophylls at 663 and 645 nm is given by

$$A_{663} = 82.04 \text{ Chl a} + 9.27 \text{ Chl b}$$

$$A_{645} = 16.75 \text{ Chl a} + 45.6 \text{ Chl b}$$

The values 82.04 etc. are the chlorophyll extinction coefficients for the wavelengths in question, as determined by MacKinney (1941). A is absorbance , Chl is chlorophyll concentration in mg/ml. When the above equations are solved :

$$\text{Chl a} = 0.0127\ A_{663} - 0.00259\ A_{645}$$

Chl b = 0.0229 A_{645} - 0.00467 A_{663} x 400

A value for total chlorophyll concentration can be obtained as described below :

The optical absorption spectra of chlorophyll a and b intersect at 652 nm. A 1 mg / ml solution of chlorophyll gives an A_{652} reading of 34.5. If 0.1 ml of chloroplast suspension is mixed with 20 ml of 80 % acetone, filtered and the A_{652} reading obtained the concentration of the original chloroplast suspension in mg / ml can be calculated as : A_{652} x 5.8

(d) P 700 Assay

An ascorbate reduced minus ferricyanide oxidised spectrum of P 700 was obtained using an Aminco DW 2000 dual beam scanning spectrophotometer. The absorbance value obtained from the P700 / $P700^+$ difference spectrum for a sample with a concentration of 10 µg / ml is used in the formula below to calculate the number of chlorophylls per P 700 :

14.0625 x optical density from difference spectrum = x

$1/x$ x 10 = number of chlorophylls per P 700 (14.0625 is the factor correcting for the dilution of the sample).

The expected chlorophyll / P 700 ratio for a digitonin PSI particle is 80 to 150.

(e) SDS Polyacrylamide Gel Electrophoresis

The polypeptide composition of the Digitonin PSI particles was analysed using SDS polyacrylamide gel electrophoresis (SDS PAGE). The protocol used was based on that of Laemmli. A 30 ml 15% SDS polyacrylamide gel with the following composition was poured : Resolving Gel

11.3 ml of 40 % bis-acrylamide,

7.5 ml of running gel buffer, 1.5 M Tris, pH 8.8/HCl,

0.3 ml of 10 % of sodium dodecyl sulphate (SDS),

0.014 ml of TEMED,

0.075 ml of 10 % w/v fresh ammonium persulphate solution,

made up to 30 ml with distilled water.

3% Stacking Gel

1.5 ml of 40 %bis-acrylamide,

5.0 ml of stacking gel buffer, 0.5 M Tris, pH6.8,

0.2 ml of 10 % SDS solution,

0.005 ml of TEMED,

0.1 ml of 10 % w/v ammonium persulphate solution,

made up to 10 ml with distilled water.

The gel was run in a tank containing 3.5 litres of 1 X reservoir buffer, 50mM Tris, 40mM glycine and 0.1 % SDS, pH 8.3 approximately. Gels were run at 50 mA/600V for about 3 hours or until the dye front ran to end of the resolving gel. Samples were boiled for 2 minutes in 1 X sample buffer (boiling is necessary to solubilise hydrophobic membrane proteins), 312.5mM Tris pH6.8-HCl, 50 % w/v glycerol, 10 % SDS and 0.025 % bromophenol blue, 25 % β-mercaptoethanol. The markers used were Sigma Dalton Mark VII-L. The run gel was stained for 2 hours in 50 % methanol, 10 % glacial acetic acid and 0.1 % coomassie blue; destained for about 2 hours in several changes 10% methanol, 10% glacial acetic acid.

For a clearer resolution of the polypeptide composition of PSI particles gels were scanned with an LKB Ultrascan X densitometer.

(f) Removal of PsaC/ Fe-S_{AB} - Preparation of Digitonin P700FeS_X PSI Core Particles.

The Fe-S_{AB} clusters were removed from the PSI holocomplex using urea as a chaotrope. The reaction mixture has the following composition : 250 μg chlorophyll/ml, 6.8 M urea, 50mM Tris pH8.0, 0.1%β-mercaptoethanol. The mixture was stirred in the dark, at room temperature under a stream of argon (to protect Fe-S_X from oxidative denaturation). The urea was added drop wise to the mixture as a 9.0 M solution and all the buffers used were thoroughly degassed. The reaction was followed by monitoring the kinetics of $P700^+$rereduction using room temperature kinetic optical spectrophotometer. Fe-S_{AB} clusters were deemed to be completely removed when the half-time for $P700^+$ rereduction of 20ms is replaced by a half-life of 1ms. This corresponds to the loss of the Fe-S_{AB} clusters as the terminal electron acceptor, with the Fe-S_X cluster acting as the terminal acceptor in its place, the back reaction between $P700^+$ and Fe-S_X^{--} having a $t_{1/2}$ of 1ms. At this point the mixture was diluted 10 X by addition of degassed 50mM Tris pH8.0. The mixture was centrifuged at 150,000 x g for 90 minutes in a Sorvall ultracentrifuge. The resulting pellet was resuspended in TEM buffer. The removal of the Fe-S_{AB} clusters was verified using cw EPR and densitometric scans of denaturing gels of treated and control Digitonin particles.

(g) Removal of Fe-S_X - Preparation of P700 A_1 Cores.

Digitonin PSI cores prepared as above were incubated with 3M urea and 5mM potassium ferricyanide, 50mM Tris pH8.3 and a chlorophyll concentration of 100μl / ml. Once again the kinetics of $P700^+$ rereduction were followed. The Fe-S_X is removed by oxidative

denaturation, with its loss A_1 becomes the terminal acceptor and at room temperature the $t_{1/2}$ for the back reaction between $P700^+$ and A_1^{--} is 1.8 to 3.0μs, a rate which is to fast to be resolved by the spectrophotometer used here. When there were no detectable kinetics it was deemed the reaction was over and the mixture was diluted and spun at 150000 x g. The resulting pellet was resuspended in TEM. The ferricyanide was removed by dialysis in 50mM Tris pH8.3, 5mM Tiron (an iron chelator). The Tiron and iron-Tiron chelates were removed by further dialysis in 50mM Tris pH8.3. The resulting PSI cores were stored under liquid nitrogen until needed.

(h) Optical Kinetics Spectrophotometry

homemade

The spectrophotometer used to measure the rate of $P700^+$ rereduction consists of a nitrogen laser and a detection system. The measuring beam is produced by an infrared LED emitting maximally at 820 nm. This measuring beam is then focused, filtered, passed through the cuvette containing the sample and subsequently amplified. The laser flash lasts for 800 ps and the beam has a wavelength of 337 nm. This laser flash excites the sample and induces a charge separation. The apparatus detects time-resolved absorbance changes at 820 nm. The sample was prepared using a chlorophyll concentration of 20μg / ml, 25 mM Tricine-KOH pH 7.8, 6.7mM sodium ascorbate (as an electron donor) and 68μM dichlorophenol indophenol(DCPIP- to facilitate electron donation by ascorbate).

(i) Preparation of Samples. for ESR Spectroscopy

The samples used in room temperature electron spin echo experiments were prepared in silica tubes with an internal diameter of 0.5mm; those used in the low temperature work were prepared in silica tubes with an internal diameter of 3mm. Chlorophyll concentrations of 2 to 5 mg / ml were used in all cases.

Chemical pre-reduction of iron-sulphur clusters, Fe-S_{AB} , was achieved by incubating the PSI particles in the presence 10 mM sodium dithionite (0.2 %w/v), 200mM glycine - KOH pH10.0 for 30 minutes in the dark. The buffer in which the dithionite was dissolved was degassed and the incubation carried out under a stream of oxygen-free nitrogen gas. The reduced samples were frozen in the dark in liquid nitrogen and stored at liquid nitrogen temperatures until required.

For the room temperature observations sodium ascorbate was used as an electron donor at a concentration of 1mM along with 0.1 mM methyl and 0.1mM 2,6-dichlorophenolindophenol present as facilitators of electron transport. This ensured that P700 was reduced and the PSI acceptors were oxidised prior to the exciting laser flash.

The low temperature measurements were made at 4K and the samples were maintained at this temperature by an Oxford Instruments, CF935 flowing gas cryostat.

(j) Induction, Detection and Measurement of the Decay of PSI Electron Spin Polarised (ESP) Signals

The kinetics measurements were made using a Bruker ESP380 X-band pulsed spectrophotometer equipped with a variable Q, dielectric resonator (model 1052 DLQ-H 8907). A doubled Nd-YAG laser (Spectra Physics, model DCR-11) was used to excite the

sample with 532 nm pulses lasting 10 ns. The laser repetition rate and flash energy were set to 1 to 10 Hz and 0.5 to 2 mJ / cm^2 respectively so as to minimise the likelihood of PSI degradation and the photoaccumulation of reduced electron acceptors.

For a 16 ns pulse of microwaves used on a paramagnetic (s=1/2) system occurring in the g=2.002 region, the maximum microwave magnetic field created by a 1 kW travelling wave tube amplifier (model 117) was about 6 Gauss (G) within the 10 mm region of the resonator used.

The microwave pulse sequence used for detection can be represented as follows : (*p-T-2p-T-echo*), where *p* corresponds to the first (90^0) microwave pulse which moves the total magnetisation through an angle of 90^0 from the Z axis, defined by the externally applied magnetic field, to the Y rotating axis corresponding to the in-phase detection channel; *T* (Tau) denotes the time separating microwave pulses, during which the individual magnetisations dephase (i.e. the individual magnetisations segregate into populations with different Larmor frequencies, with some spinning faster than others); *2p* denotes the second (180^0) microwave pulse that moves the magnetisations which will rephase or refocus along the Y axis, releasing a pulse of microwaves after a time *t*, the pulse being detected as a spin echo in the in-phase channel.

At room temperature no signals are seen in PSI particles in the dark in the presence of exogenous electron donors. In PSI preparations in the absence of added reductant, the $P700^+$radical signal can be induced with continuous white light illumination. This photoinduced radical signal can be used to phase the detector. At 4 K the electron spin echo signal arising from the chemically reduced Fe-S_{AB} clusters serves the same function.

The phenomenon of cavity ringing will interfere with whatever spectroscopic measurements are being attempted. The time interval (*T*) between the first and second

microwave pulses is important therefore. At room temperature, ringing is rapidly dampened out and a T of 80 ns is long enough. In this case the pulse sequence from laser flash to echo detection lasts 250 ns. At low temperature ringing is prolonged and a longer T of 112 ns is needed. In these experiments the following pulse sequence was applied to maximise the time resolution : p(16 ns)-T(112 ns)-$2p$(32 ns)-echo. The following pulse sequence was applied, including a longer 90^0 microwave pulse of lower intensity, to improve spectral resolution: p(96ns)-T(224ns)-$2p$(196ns)-echo.

The time resolution of the experiment refers to the step interval between the time of the exciting laser flash and the 90^0 microwave pulse. It can be as short as 8 ns but in practice needs to be extended to 40 ns so as to improve the signal to noise ratio. The signal is displayed only after the pulse sequence is completed, that is not to say the kinetics measured by the instrumentation are those occurring after the so-called dead time of the experiment (corresponding to the length of the pulse sequence). The observed behaviour of the signals correlates with events occurring between the laser flash and the first microwave pulse as the time between them is varied. The behaviour of a radical during the pulse sequence thus determines if it is observable or not. A radical will give rise to an ESP signal only if it persists for the duration of the pulse sequence, in the case of this particular spin polarised signal this condition was met by $P700^+$. Time resolved pulsed ESR kinetic experiments can be used to study a signal formed instantly on the time scale so long as it does not decay too quickly. If its total decay is much faster than the length of the pulse sequence (350 ns), there will be no signal detected. If the decay time is longer than 350 ns, a signal will be detected. For intermediate decay times, measurements can be successfully made providing the original radical concentration was high enough so that a detectable amount of it persists to the end of

the pulse sequence. The time constant for the species in question can then be determined by fitting the data for observable decay. This is why relatively high sample concentrations were used in this experiment, 2 to 5 mg chlorophyll / ml compared with 0.5 to 1.0 mg / ml concentrations routinely used in cw EPR work.

The second situation amenable to this technique is where a signal arises in the ns time domain. in this case the first kinetic data point collected will correspond to any radical formed at the time of the 90^0 microwave pulse, radicals generated after this will not contribute to the observed signal intensity. The kinetics observed will here correlate to events occurring between laser flash and the 90^0 microwave pulse.

(k) The Fitting Procedure - Determination of Rate Constants

The data was fitted according to the non - linear least square method using a Levenburg - Marquand algorithm. An exponential curve was drawn through the data points according to the equation given below:

$I = A + B\ (e^{-1}/T_1)$, where I is intensity , A and B are fitting constants, and T_1 is the relaxation rate. A, B and T_1 are systematically varied by the program until the distances between the curve drawn and the data points has been minimised as much as possible. Once this has been achieved a value for the rate constant, $t_{1/e}$ can be obtained.

This program was written for the fitting of monoexponentials.

(l) $NADP^+$ Reduction Assay

The following reaction mixture was used in every case : 25 mM Tricine-KOH pH 7.8, 6.7 mM sodium ascorbate, 68 μM dichlorophenol indophenol, 0.7 % Triton X-100, 0.1 % β-

mercaptoethanol, digitonin PSI particles (10 μg chlorophyll / ml), 1.5 μM plastocyanin (purified from spinach leaves), 5 μM ferredoxin, 0.5 M $NADP^+$, ferredoxin - $NADP^+$ oxidoreductase. $NADP^+$ reduction was followed by measuring ΔA_{340} after illuminations for 30 s periods. The rate of $NADP^+$reduction in μM $NADP^+$ / mg chlorophyll / hour is calculated using the following formula :

$$\text{Rate} = \frac{A340 \times 3600 \times 1000}{5.85 \times [chl] \times \text{time (s)}}$$

2.3 RESULTS

2.3.1 The Polypeptide Composition of Photosystem I

The polypeptide composition of PSI preparations varies according to the detergent used in the protocol. The composition of PSI preparations used in this study was evaluated on SDS-polyacrylamide gel electrophoresis (SDS-PAGE) and densitometric scans of these gels.

Relative to the digitonin particles, the Triton-X-100 PSI is deficient in the proteins comprising the light-harvesting complex (LHC-I), that run in the 22 - 30 kDa region of the denaturing polyacrylamide gels. It is also clear from densitometric scans (Fig.2.1) that the Triton-X-100 PSI is relatively deficient in other smaller peptides, with PsaC and PsaE significantly less abundant and PsaF not present at detectable levels. This indicates that there is Triton- induced damage of the PSI at both the lumenal and stromal sides of the complex.

2.3.2 $NADP^+$ Reduction Assay

$NADP^+$ is the natural substrate of the PSI complex, being reduced by ferredoxin-dependent NADP-oxidoreductase. Determining the rate of $NADP^+$ reduction by monitoring absorbance changes at 340 nm serves as an indicator of how efficiently the isolated photosystem supports forward electron transfer. Fig.2.2 shows a comparison of the $NADP^+$reduction rates exhibited by Triton-X-100 and Digitonin PSI. The maximal rate of $NADP^+$ reduction for Triton-X-100 is 92.3 μM $NADP^+$mg Chl / hour, for Digitonin PSI, the maximal rate is 483.7 μM $NADP^+$ mg Chl / hour. Fig.2.2(a) shows the $NADP^+$ reduction profile for spinach thylakoids, with a maximal rate of 615 μM NADP / mg Chl/ hour.

Digitonin PSI is a more intact preparation than PSI isolated using Triton-X-100 PSI and functionally is more representative of the *in vivo* situation. For this reason PSI isolated using Digitonin was chosen for the kinetic studies, because it was reasoned that the kinetics observed in these complexes reflects more accurately what occurs *in vivo*.

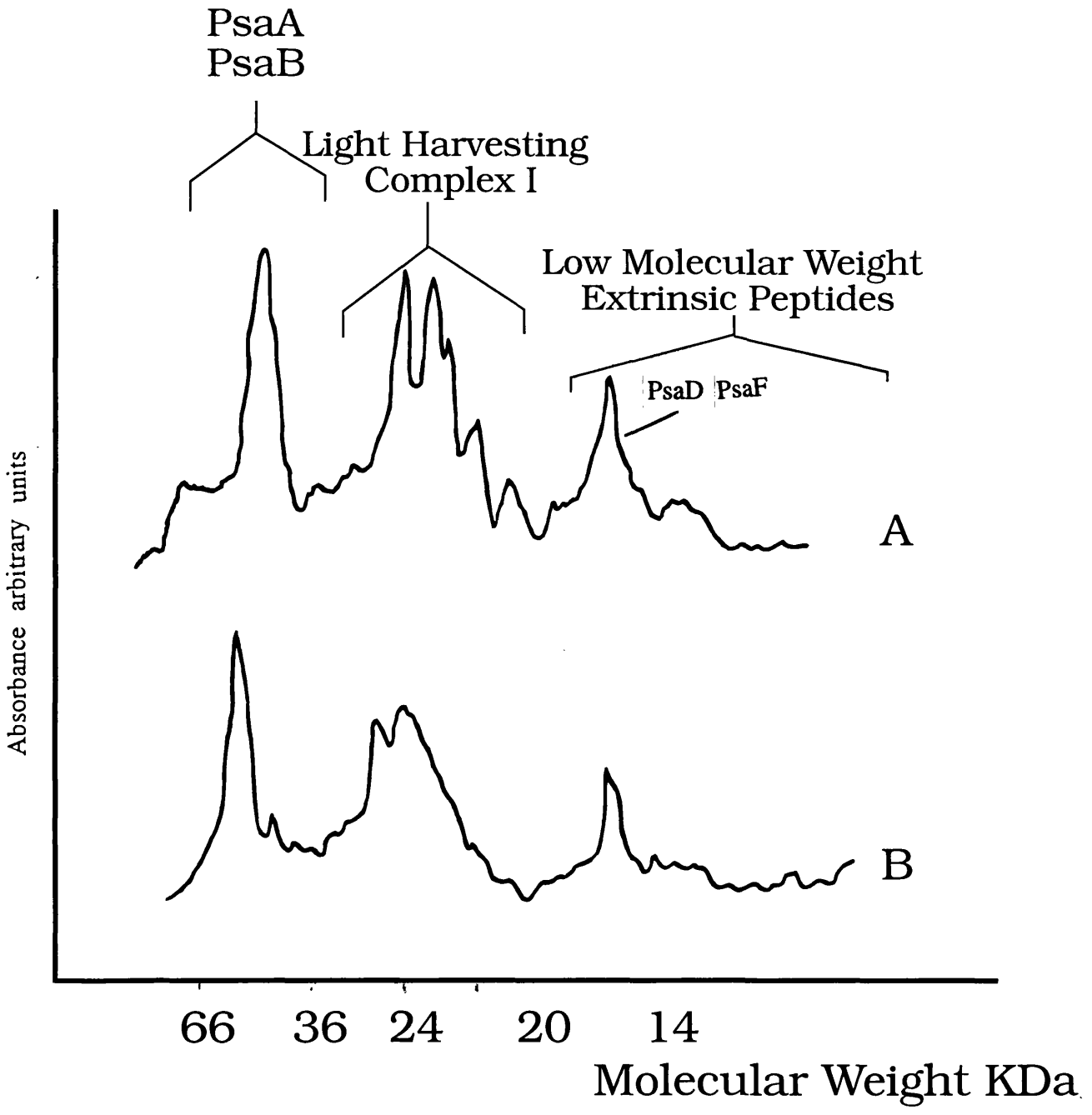

Figure 2.1, Laser densitometric scans of denaturing protein gels
a) Intact digitonin PSI particles
b) Intact Triton PSI particles
Sample concentration: 0.5 microgrammes per lane

0.5 micrograms of chlorophyll per lane. The molecular weight scale is derived from SDS PAGE molecular weight markers run on the same gel.

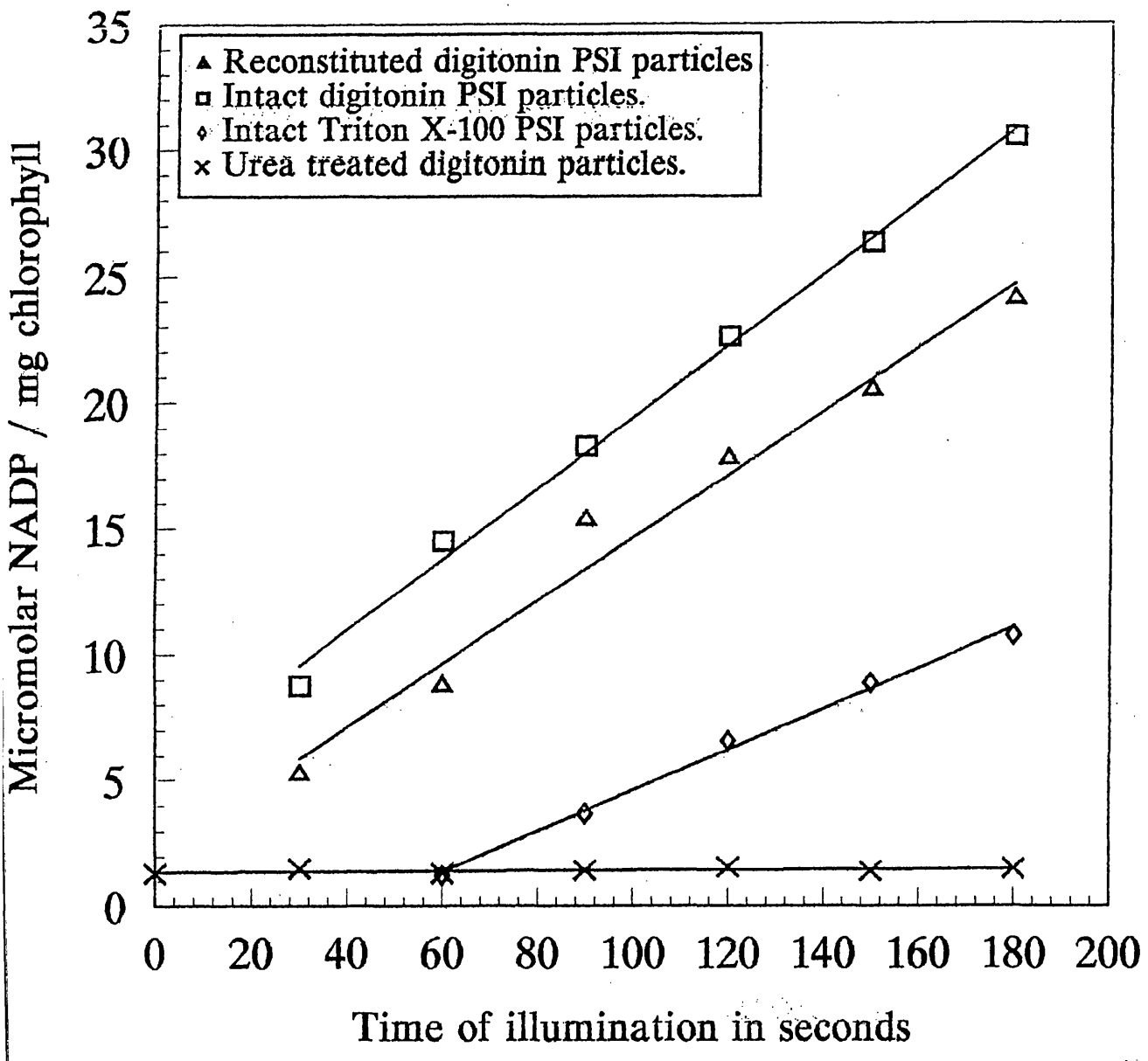

Figure2.2. Plots of NADPH concentration against time of illumination of various PSI samples. The sample concentration in each case is 12 μg chlorophyll / ml. The reaction mixture composition is as follows : 6.7mM sodium ascorbate, 68 μM dichlorophenol indophenol, 1.5 μM plastocyanin, 5 μM ferredoxin, 0.5 mM $NADP^+$and ferredoxin - $NADP^+$reductase to excess. The following rates of $NADP^+$ reduction were determined in μMNADP / mg chlorophyll / hour :
Intact digitonin PSI - 615.67; reconstituted digitonin PSI - 482.0; intact Triton X-100 PSI - 216.0.

2.3.3 The Removal of PsaC (Fe--S_{AB})

(a) Optical Kinetic Spectroscopy

The iron-sulphur clusters, Fe-S_{AB}, were removed according to the method described in materials and methods. The removal was followed optically. The rate of flash-induced $P700^+$ rereduction was determined for the reaction mixture after increasing periods of incubation to establish when the reaction has gone to completion.

Fig.2.3(a) shows the rereduction kinetics trace for untreated Digitonin PSI particles. The half-life of rereduction is 20 ms which is characteristic of a back reaction between the reduced iron-sulphur clusters, Fe-S_{AB}^{--} and $P700^+$.

(b) shows the rereduction kinetics trace of the Digitonin PSI core, i.e. urea treated, so as to remove the iron-sulphur clusters, Fe-S_{AB}. The half-life of rereduction is about 1 ms, typical of a back reaction between $P700^+$ and the reduced ion-sulphur cluster, Fe-S_X^{--}, which acts as the terminal acceptor in the PSI core preparation.

(c)The rereduction kinetics trace of Digitonin PSI core reconstituted with purified butanol extracted PsaC, PsaD and PsaE. The control-type kinetics are restored to about 80 % of the untreated sample.

The removal of the iron - sulphur clusters, Fe-S_{AB}, is further verified using densitometric scans of gels on which urea - treated PSI particles have been run, and by cw electron spin resonance spectroscopy (ESR).

(b) Ultrascan Densitometry of Protein Gels

Figure 2.4 compares the densitometric scan profiles of intact digitonin PSI particles and digitonin PSI cores (i.e. urea treated so as to extract the iron-sulphur clusters). The

intensity peak corresponding to PsaC peptide (which coordinates the iron-sulphur clusters, Fe-S_{AB}), that runs at about 10kDa) is absent in the urea-treated sample. Additionally the peaks occurring at about 20 and 18 kDa, corresponding to the extrinsically bound peptides PsaE and PsaF, respectively which are also removed from the PSI particles by treatment with urea. This demonstrates iron sulphur cluster depletion at the protein level, it can also be demonstrated spectroscopically.

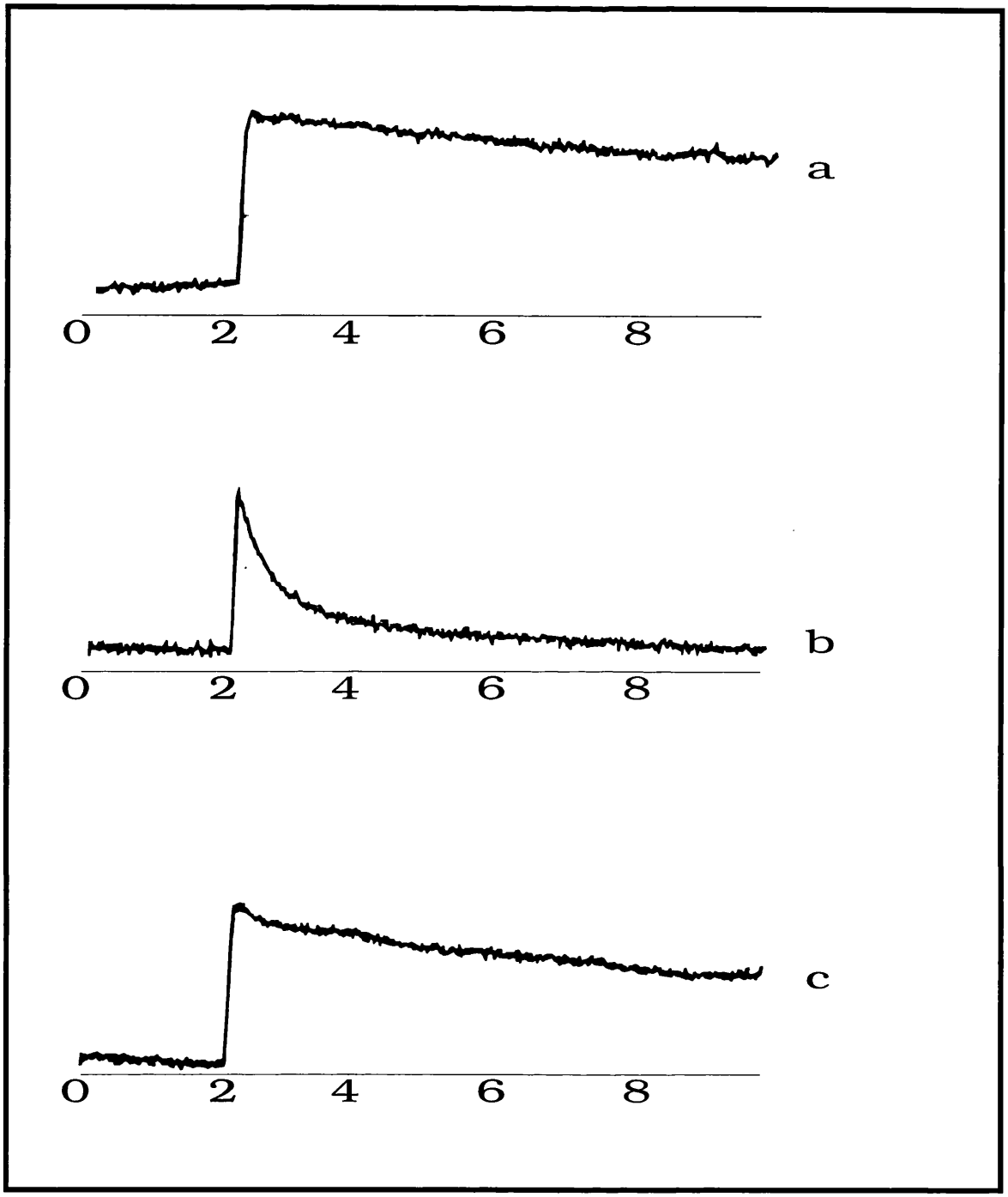

Figure 2.3 Room temperature optical kinetic traces showing the rate of $P700^+$ rereduction in the following samples:
(A) Intact digitonin PSI, with a $P700^+$ rereduction half-life of 20 ms;
(B) Digitonin PSI core particles resulting from a 30 min. incubation of intact PSI with 6.8M urea. $P700^+$ rereduction half-life of 1ms.
(C) Digitonin PSI core particles reconstituted with a mixture of the extrinsic peptides, PsaC, D, and E, which restores the 20ms half-life.
The reaction is intiated by the addition of urea.

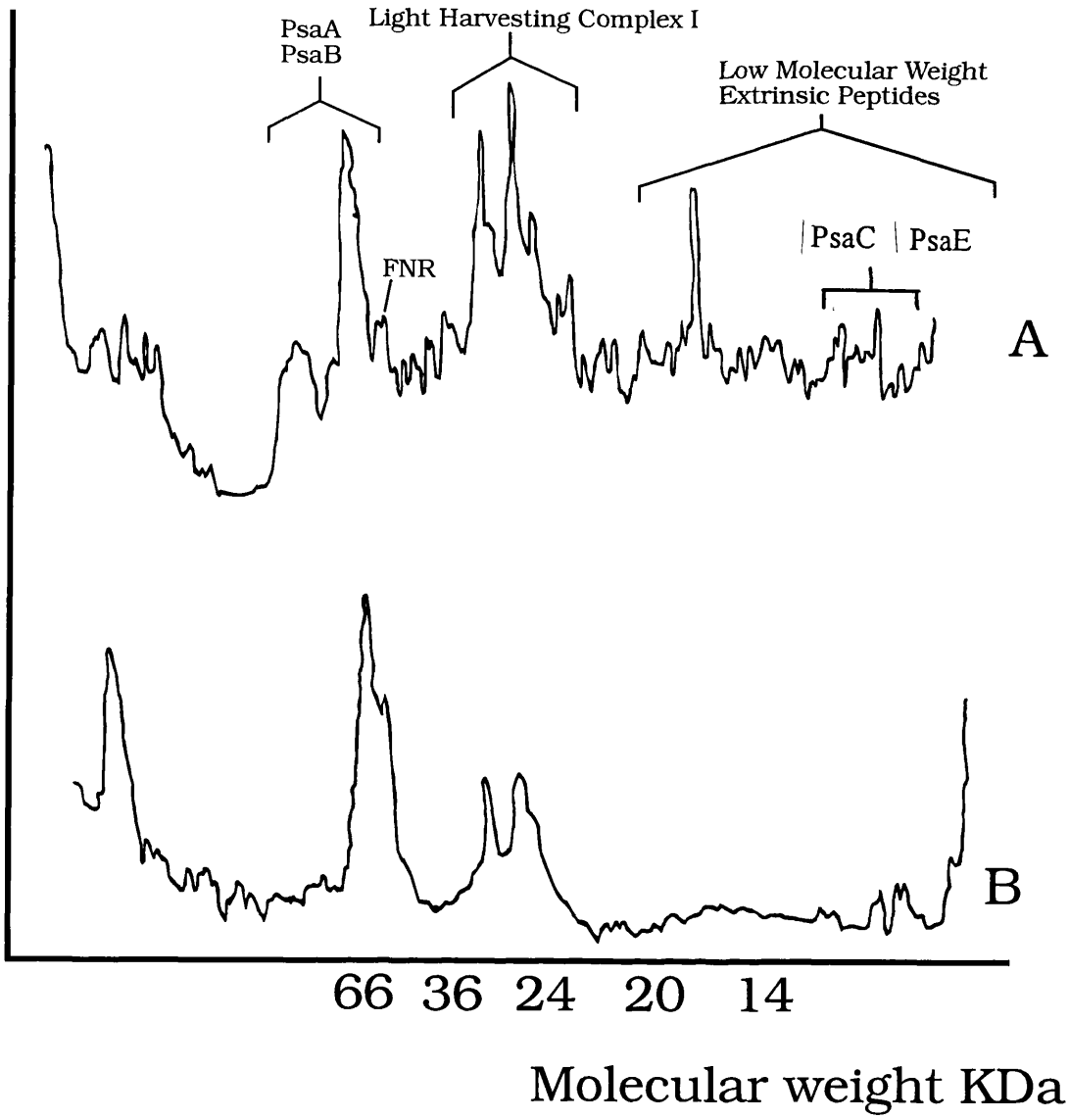

Figure 2.4, Laser densitometric scans of denaturing protein gels
a) Intact digitonin PSI particles
b) Digitonin PSI particles after treatment with 6.8 molar urea
Sample concentration: 0.5 microgrammes per lane

Peak assignments are based on work in which particular protein bands were shown to light up when probed with the appropriate specific antibodies.

(c) Cw Electron Spin Resonance (ESR) Spectroscopy

Figure 2.5 (a) shows the cw ESR light minus dark spectrum of Fe-S_A^{--} as observed in ascorbate reduced untreated Digitonin spinach PSI particles. The spectrum is a classical axial signal with resonances occurring at g=1.95, g=2.05 and g =1.87. The g=2 (radical) region of the spectrum has been deleted for the sake of clarity.

Figure 2.5 (b) shows the spectrum recorded under the same experimental conditions but for PSI particles incubated in 6.8 M urea. The resonances that are characteristic of the reduced iron -sulphur clusters are not observed.

Figures 2.6 (a) and (b) depict the light minus dark spectral characteristics of the same samples (but with sodium dithionite used as the reductant) in g=2.00 region of the spectrum. In the urea - treated PSI particles, illuminated in the pesence of the reductant sodium dithionite, the light - inducible, reversible $P700^+$ signal is observed as it is in the untreated PSI particles. The reversible nature of this signal is attributed to the back reaction that occurs between $P700^+$ and reduced iron-sulphur cluster, Fe - S_X^{--}, indicating that this intrinsically bound iron sulphur cluster is retained by centres depleted of their extrinsically bound iron sulphur clusters. The removal of the clusters, Fe-S_{AB} results in a broadening of the cw ESR spectrum of the cluster, Fe-S_X, probably due to a change in g-strain parameter, induced by the removal of PsaC. However the altered signal for the reduced cluster, Fe-S_X^{--} can be detected in depleted samples under condition that are optimal for observing the unaltered spectrum, as depicted in figure (c).

Figure 2.5 ESR spectra of digitonin PSI particles which have been reduced with 30 mM sodium ascorbate, illuminated at room temperature and then frozen under illumination. (a) Untreated PSI particles. (b) PSI particles after incubation with 6.8 M urea. Sample concentration : 1.0 mg / ml. Microwave power - 10 mW; operating temperature : 15 K; modulation width : 1.25 mT; instrument gain : 500.

Figure 2.6 The g =2.00 region of the ESR spectrum of a urea treated digitonin PSI sample that has been reduced with 0.2 % sodium dithionite. The sample was illuminated in the instrument cavity. (a) light on; (b) light off. Temperature : 18 K; power : 20 mW; gain : 500. (c) The g = 1.76 region of a urea treated PSI particles illuminated in the presence of sodium dithionite, indicating the presence of photochemically reduced FeS_X. Recording temperature : 8 K.

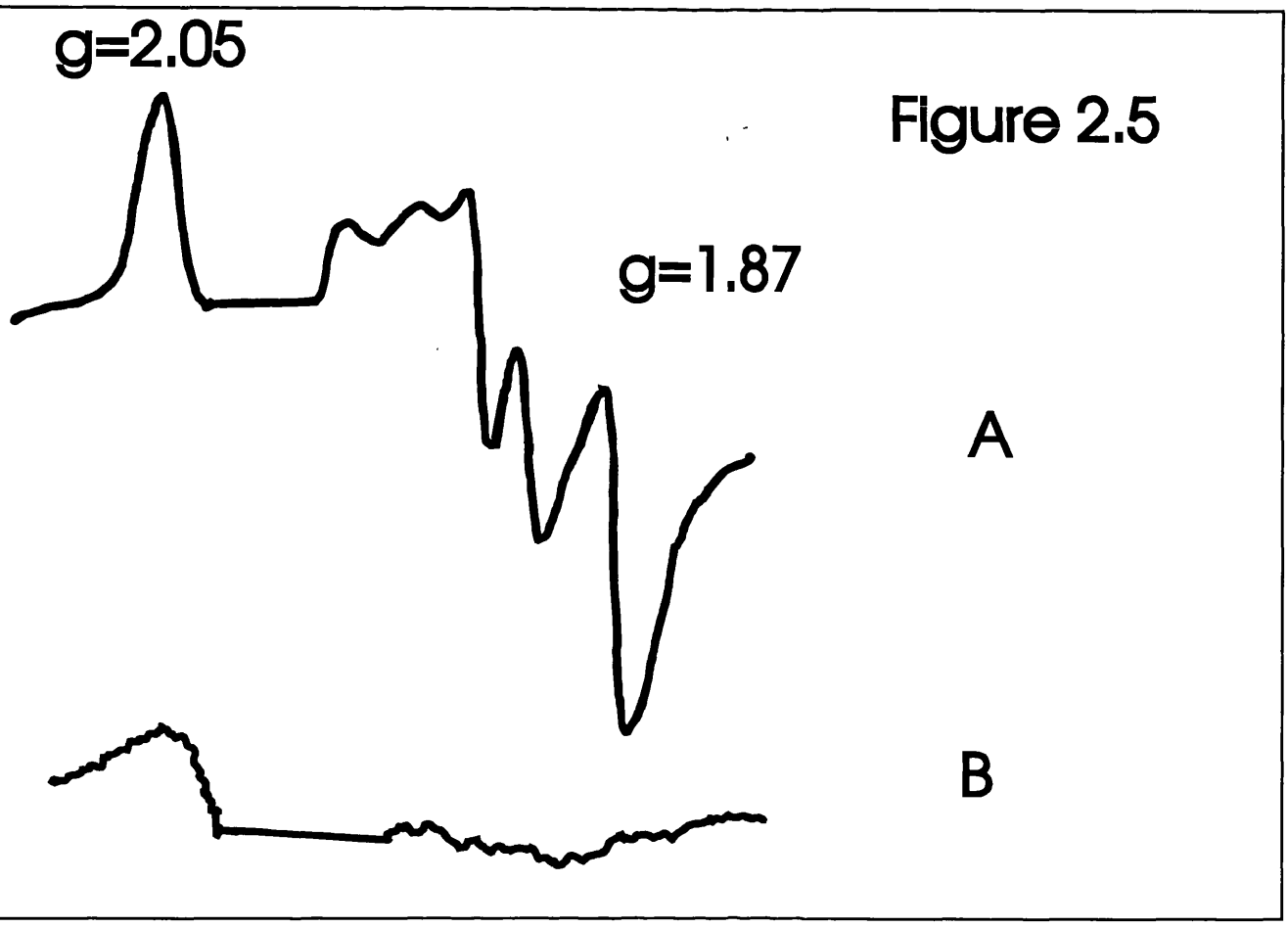

Figure 2.5

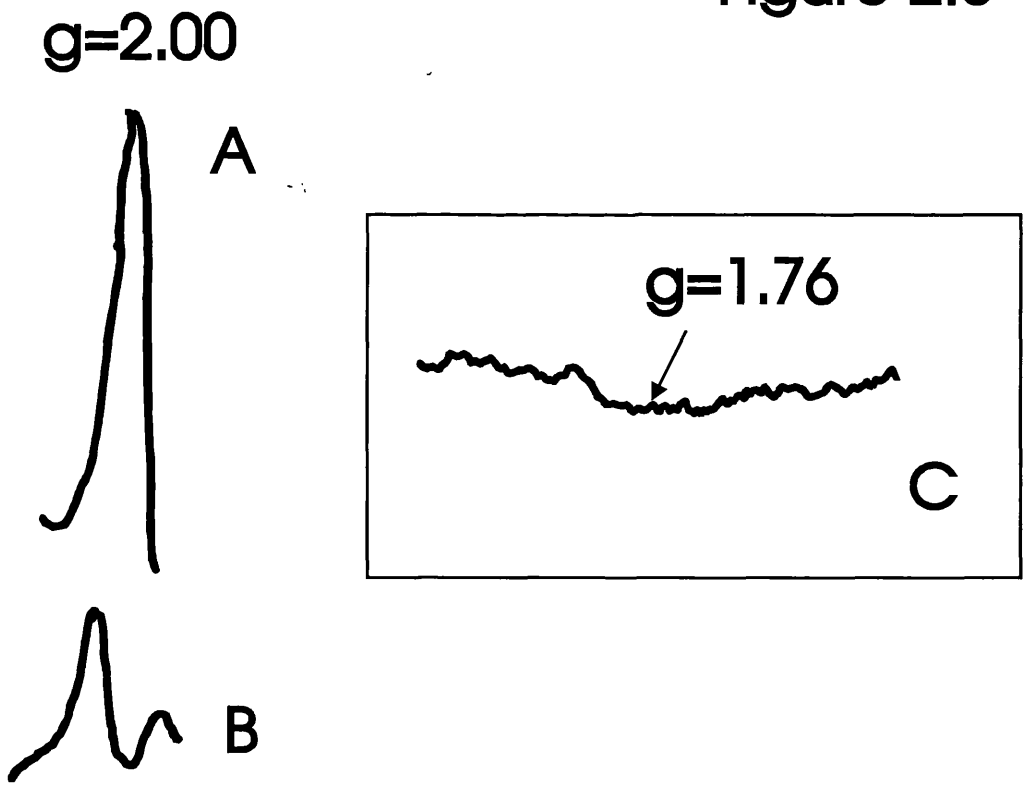

Figure 2.6

2.3.4 Oxidative Denaturation of Fe-S_X

Room Temperature Optical Spectroscopy

The iron sulphur cluster, Fe-S_X, was removed from digitonin PSI core according to the method described. As with the extraction of Fe-S_{AB}, the progress of the reaction was followed by monitoring the rereduction kinetics of flash-induced $P700^+$.

Figure 2.7 shows a series of kinetics traces taken at 5 minute intervals from a reaction mixture in which digitonin PSI core particles were incubated with 3.5 M urea and 5 mM potassium ferricyanide. The topmost trace shows rereduction kinetics that are typical of the PSI core , with a half - life 1 ms which corresponds to the room temperature back reaction between $P700^+$ and Fe-S_X^{--}. The final figure shows the trace for the reaction mixture after about 25 minutes incubation, there are no detectable kinetics. This corresponds to a state of affairs in which the iron-sulphur cluster, Fe-S_X, has been removed from most if not all centres, with the quinone acceptor, A_1, replacing it as the terminal acceptor. At room temperature the half - life of the recombination between $P700^+$ and A_1^{--} is determined to be 1.5 to 3μs, which is too rapid to be resolved on the optical spectrophotometer used here.

This is in contrast to the findings of Golbeck *et al* who extracted the iron-sulphur cluster, Fe-S_X, from PSI prepared from *Synechocystis* sp.. They found the core particles needed to be incubated for as much as three hours for the thorough removal of the cluster, meaning the core is exposed to high concentrations of urea for far longer, increasing the likelihood of urea - induced damage to the acceptors preceding iron-sulphur cluster, Fe-S_X.

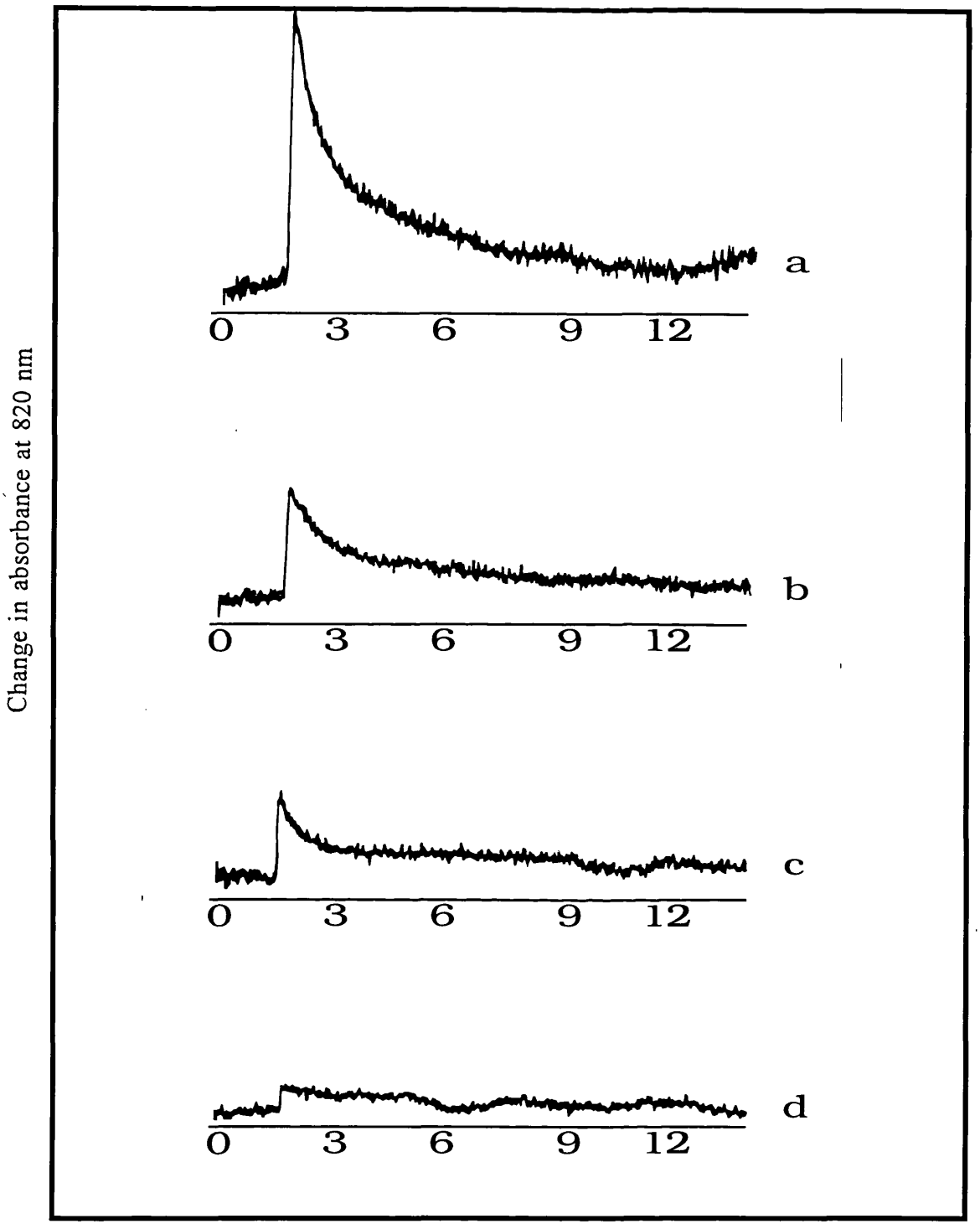

Figure 2.7. Room temperature optical kinetic traces demonstrating the removal of FeS_x from PSI core particles. The rate of $P700^+$ rereduction increases from $t_{1/2}$=1ms to a rate that is too fast to be resolved by the spectrophotometer. Samples were taken from the reaction mixture prior to addition of urea,
(A) After 10 min. incubation.
(B) After 20 min. incubation.
(C) After 30 min. incubation.
(D) After 40 min. incubation.

ESR spectra of the reduced radicals, A_1^{--} and A_0^{--} in PSI cores depleted of their iron-sulphur cluster, Fe-S_X, are very similar with respect to linewidth and lineshape, as the equivalent spectra observed in untreated particles, i.e. they present recognisable quinone and monomer chlorophyll spectra. This suggests that the removal of the Fe-S_X cluster in this way does not do any significant, irreversible damage to the binding sites of these acceptors.

2.3.5. PULSED ELECTRON SPIN RESONANCE (ESR) KINETICS MEASUREMENTS

(a) Low Temperature (4 K)

Figure 2.8 shows a field swept spin echo ESR spectrum for intact spinach digitonin PSI in which the iron sulphur clusters, Fe-S_{AB}, have been chemically pre-reduced by sodium dithionite. The broad signal which dominates the in - phase field sweep, centring on 3600 G, corresponds to the reduced iron - sulphur clusters. In the dark (figure 2.8a), there is a small g=2 radical signal (centring on 3475 G). The intensity of this radical spike is increased when the sample is exposed to laser pulse (figure 2.8b).

In the dark (figure 2.8d) there is no signal observed in the out - of - phase field swept spectrum. When the laser is activated, a flash induced g=2 radical signal, of greater magnitude than that observed in the in - phase channel, is detected.

When the microwave pulse sequence is triggered after the exciting laser flash, an in -

phase radical signal, is detected immediately after the laser flash (figure 2.9bi). The in - phase signal is almost instantly, converted into a broad absorption signal, observed in the out - of - phase channel (figure 2.9bii).

Figure 2.9a shows a kinetic trace depicting the decay of the out - of - phase signal, taken at a point on the field swept spectrum shown in figure 2.8c. The signal decays with a half - life ($t_{1/e}$) of 23 μs. The field swept spectrum remains constant during the decay of the out - of - phase signal. The rise time kinetics of the in - phase signal are faster than the response time of the instrument and so the kinetic trace it produces is spurious.

Figures 2.10a and b depict field swept spectra of the signals generated using two different pulse patterns at 4 K. When a microwave pulse of relatively short duration and relatively high intensity is used to probe the sample, a purely absorptive out - of - phase signal is seen to dominate (figure 2.10a). When microwave pulses of relatively long duration and relatively low intensity probe the sample, spectral resolution is enhanced and an in phase emissive / absorptive / emissive signal centring on g=2 dominates (figure 2.10b) at the expense of the out - of - phase signal, which is diminished. It is this in - phase signal which produces a spectrum typical of the spin - correlated radical pair $P700^{+}A_1^{-}$, first described by Thurnauer *et al*, 1979 and further reviewed by Hore *et al*, 1987. The kinetic traces for this in - phase signal, taken at different positions along the field swept spectrum yield a half - time of 23 μs, the same as the half - time determined for the out - of - phase signal.

Kinetic measurements were carried out on a number of other different PSI preparations at 4 K. These results are shown in figure 2.11 / 12. Figures 2.11depicts the kinetic trace for spinach digitonin PSI which has been depleted of all its iron - sulphur clusters, Fe-S_X and Fe-S_{AB}, prepared in pH 8.0 Tris - HCl buffer. An average half - life of 16.93 μs was determined for the decay of the out - of - phase signal, generated using the same pulse sequence that was

used on the intact digitonin particles.

Figures 2.12a and b give the field swept spectrum of the out - of - phase signal and out - of - phase signal kinetic trace for spinach digitonin PSI depleted of its iron - sulphur clusters, Fe-S_{AB}. An average half - time for the decay of the out - of - phase signal of 50.7 μs +/_ 5μs.

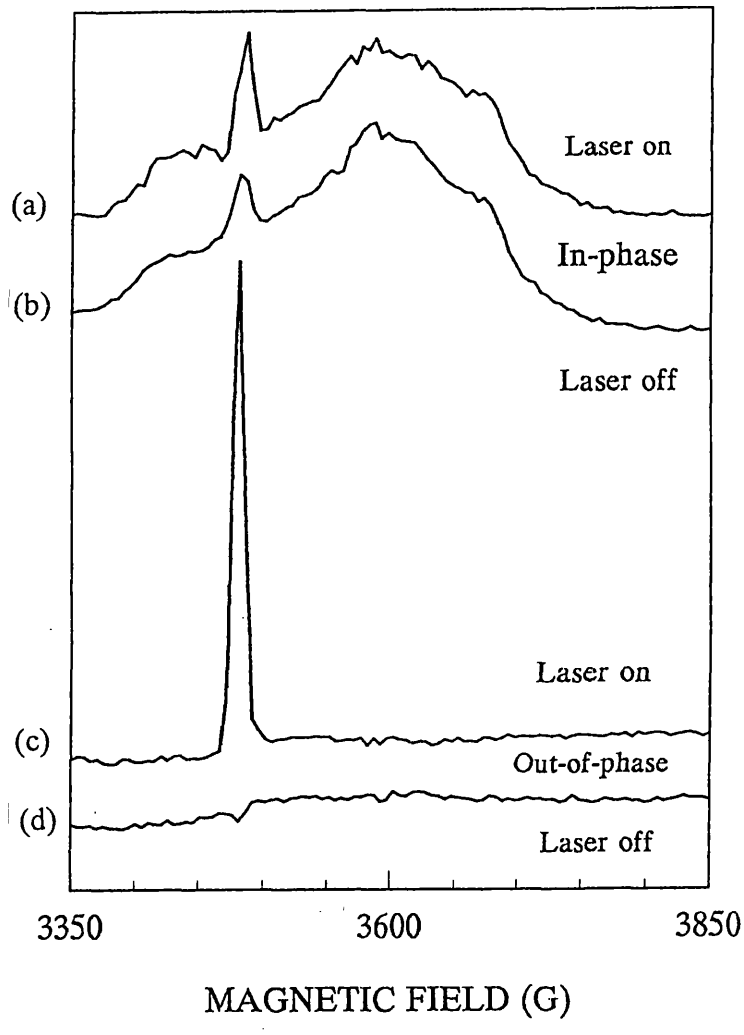

Figure 2.8: Field sweep spin echo EPR spectra of prereduced PS1 particles at 4K. Laser repetition rate of 10Hz; microwave pulse sequence : p/2 pulse=16ns , t=112ns; 5 Gauss per points, 10 added sequence per point; delay between laser pulse and microwave sequence: t_0=1500ns.

Top to bottom: (a) IN phase, laser ON

(b) IN phase, laser OFF

(c) OUT of phase, laserON

(d) OUT of phase, laserOFF

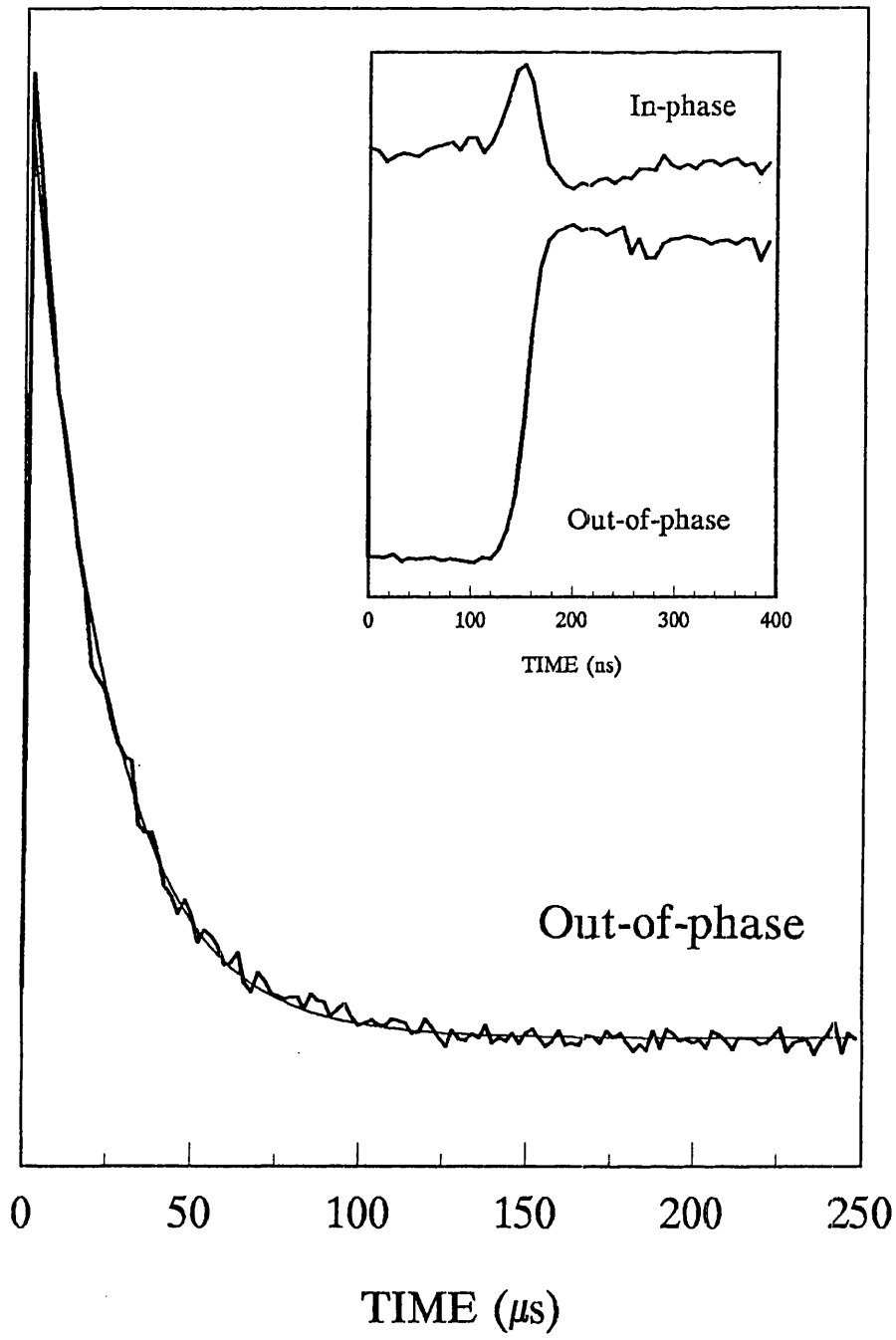

Figure 2.9:(A) Out of phase kinetic trace at H_0=348.0mT in PSI particles in which iron sulphur clusters are chemically prereduced. t_0 is incremented with 2ms steps, 125points and 10 added sequence per point. Fit: $t_{1/e}$=23μs.(B) The inset is the in phase kinetic trace observed in the same conditions excepts 8ns increment of t_0 has been used.

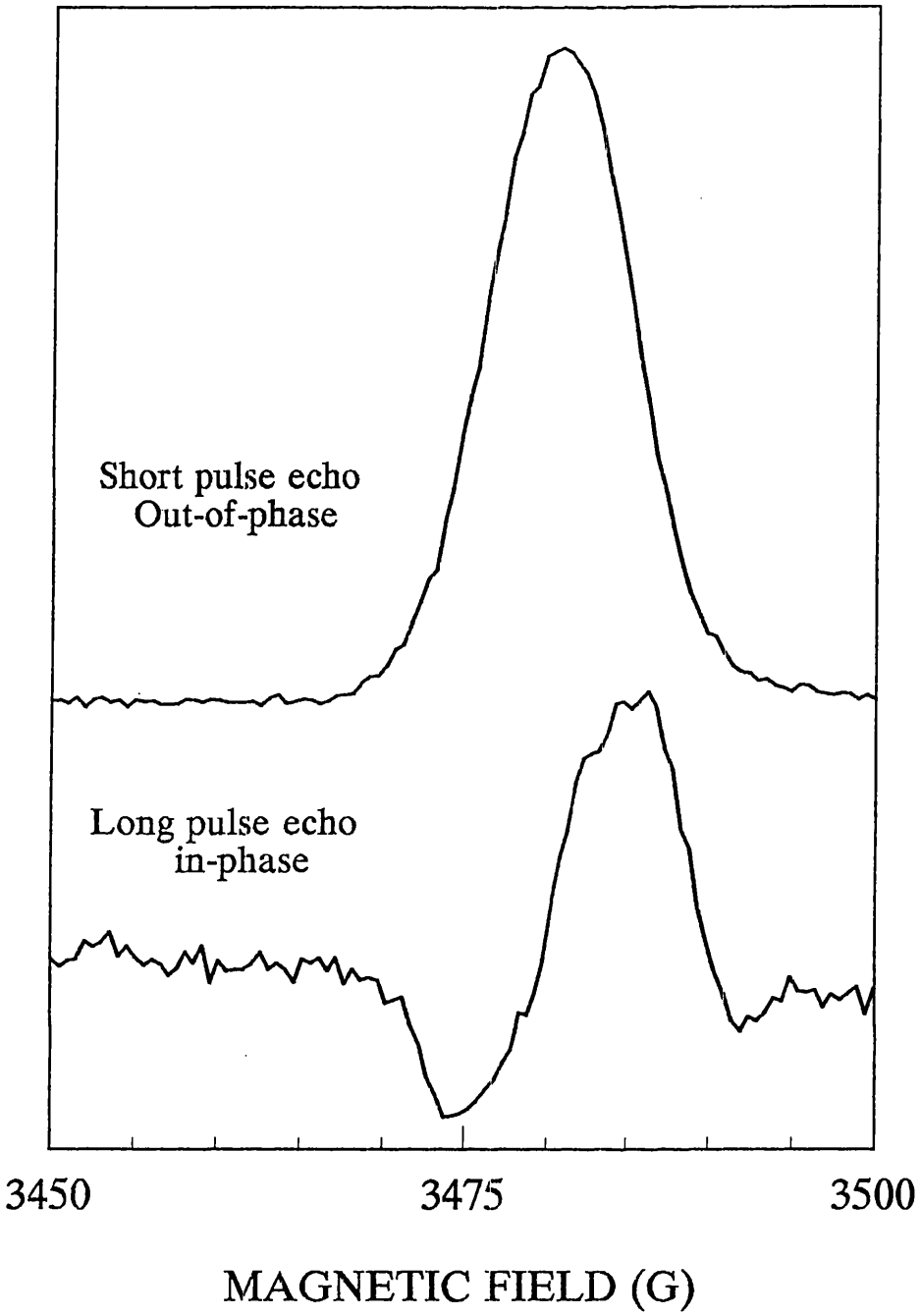

Figure 2.10: Laser-induced signal (ON-OFF, $t_0=1\mu s$) in prereduced PS1 at 4K.

(a)Top spectrum: out of phase signal obtained with short pulse of high intensity (p/2 pulse=16ns). 00.5mT per points. 20 added sequence per point.

(b)Bottom spectrum : in phase signal obtained with longer pulses of lower intensity (p/2 pulse=96ns). 0.05mT per points. 40 added sequence per point.

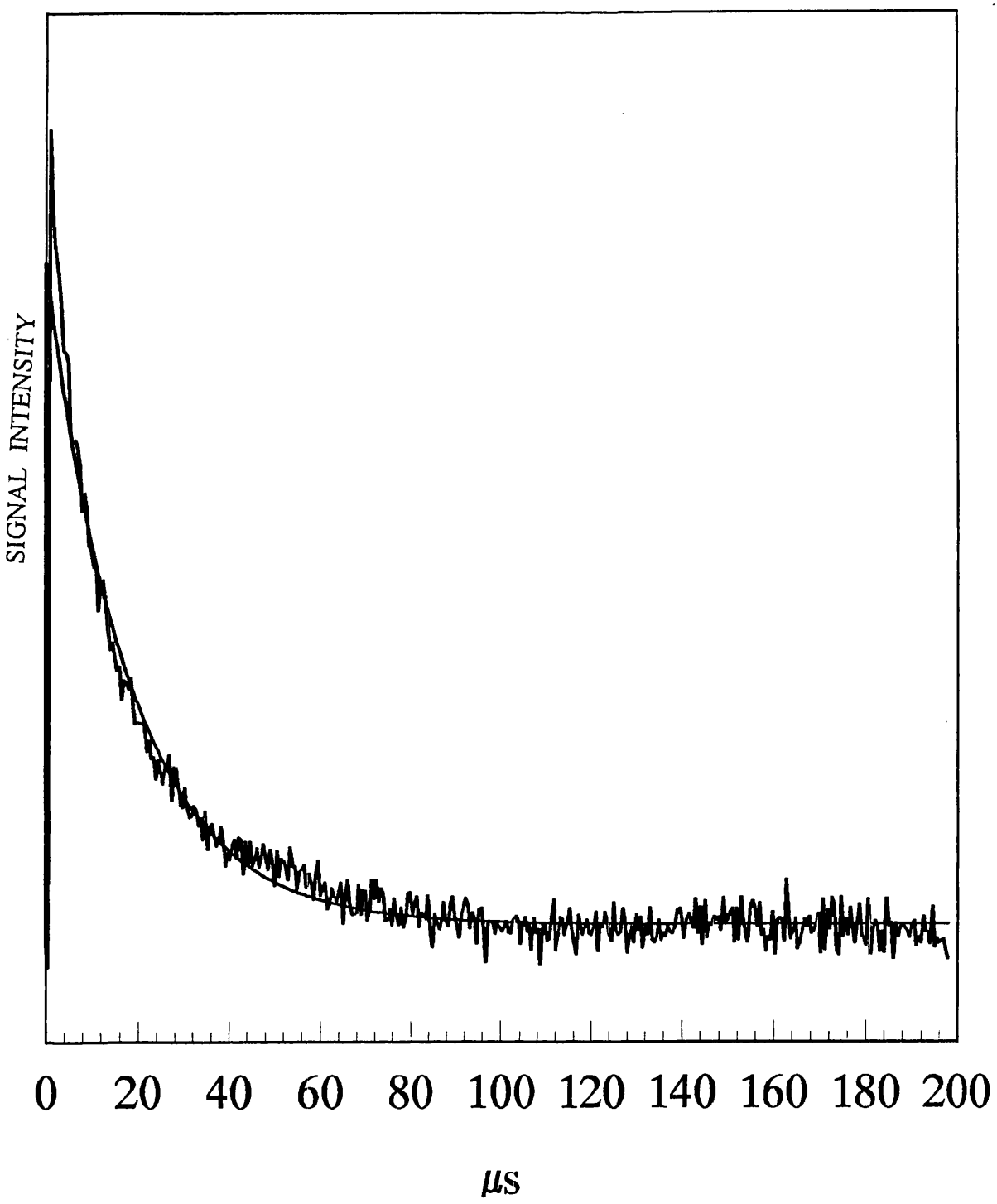

Figure 2.11 Out - of - phase kinetic trace at 4 Kof the laser flash induced signal at H_0 = 348.0 mT in PSI particles depleted of all their iron - sulphur clusters. Fit : $t_{1/e}$ = 16.93μs.

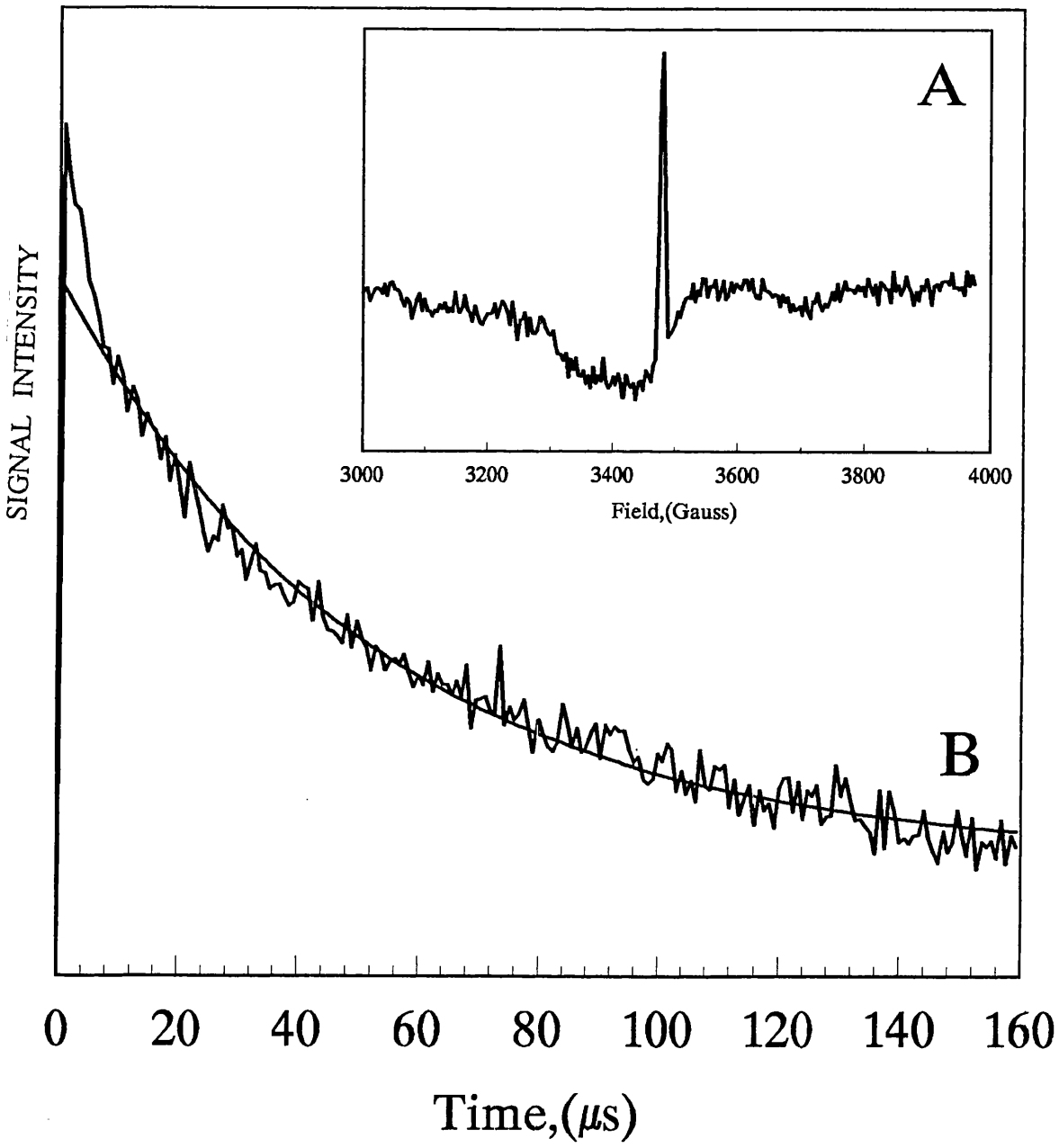

(A)

Figure 2.12. (A) Out - of - phase field sweep at 4 K of spinach digitonin core particles, pH 8.0. Sample concentration: 2 - 4 mg / ml. (B) 4 K kinetic trace of same sample. Fit yields a $t_{1/e}$ = 51 +/_ 5μs. Pulse parameters are the same as those used in the other low temperature experiments.

(b) Room Temperature Kinetic Measurements.

Figure 2.13 a and b show field swept electron spin echo (ESE) spectra of the flash induced signals detected at different time intervals after the laser flash in intact spinach digitonin PSI particles in the presence of an external electron donor, sodium ascorbate and 2,6-dichlorophenolindophenol and methyl viologen as facilitators of electron transfer, at room temperature. In these samples P700 is reduced and the iron sulphur clusters are oxidised prior to laser flash. Both signals are centred at about g=2. In the out - of - phase channel an absorption signal is measured 20 ns after the laser flash (figure 2.13a). In the in - phase channel, an emissively polarised signal is measured 1500 ns after the laser flash (figure 2.13b). Spectrally, the room temperature out - of - phase signal is identical to its 4 K equivalent. The kinetic traces of both the in - and out - of phase signals can be recorded simultaneously, a feature which is important for the room temperature measurements.

The electron spin echo kinetic traces for intact digitonin particles at room temperature are shown figure 2.14. In the in-phase channel there is an initial transient spike followed by the appearance of an emissive signal (represented by the field sweep in figure 2.13b) which has a rise time $t_{1/e}$ of 160 ns +/_ 50 ns and which decays with a $t_{1/e}$ of 2000 ns +/_ 100 ns (figure 2.14ai). In the out - of - phase channel, there is observed a signal (represented by the field sweep in figure 2.13a) which decays with a half - life of 130 ns +/_ 50 ns (figure 2.14aii). A small component of this signal decays more slowly with a $t_{1/e}$ of 1400 ns +/_ 100 ns. The slower - decaying component comprises less than 5% of the original signal intensity. Within the error margin of the experiment the rise - time kinetics of the in - phase signal correlate with the decay - time kinetics of the out - of - phase signal.

The electron spin echo kinetic traces for depleted digitonin PSI particles are given in

figures 2.14b and c. The kinetic trace detected in the in - phase channel for digitonin particles depleted of their iron - sulphur clusters, Fe-S_{AB} is given in figure 2.14bi. The rise time for the in- phase signal in this sample has a $t_{1/e}$ of 170 ns +/_ 50 ns and decays with a $t_{1/e}$ of 2000 ns +/_ 100 ns. The out - of - phase signal decays with a $t_{1/e}$ of 190 ns +/_ 50 ns (figure 2.14bii). There is a component of the out - of - phase signal, comprising less than 10% of the original signal intensity, which decays about ten times more slowly with a $t_{1/e}$ of 1500 ns +/_ 10 ns. In this depleted sample the intensity of the in - phase signal relative to the out - of - phase signal is smaller than it is in the untreated, intact digitonin particles.

The kinetic traces for digitonin PSI cores depleted of their iron - sulphur cluster, FeS_X, are given in figure 2.14c. In this sample the emissive in - phase signal is abolished, resulting in a "flat" kinetic trace (figure 2.14ci). The out - of - phase signal decays monophasically with a $t_{1/e}$ of 1250 ns +/_ 50 ns (figure 2.14cii).

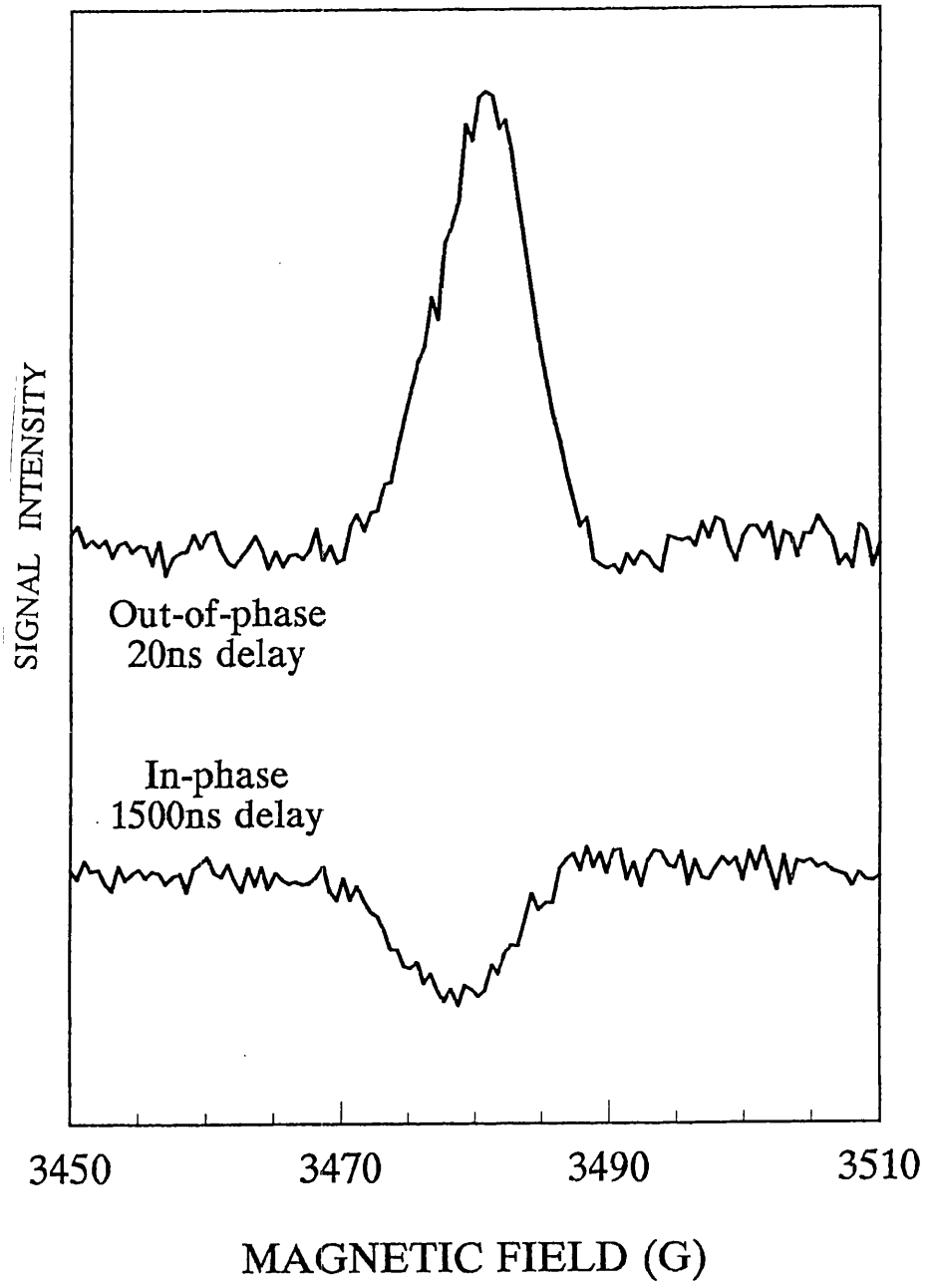

Figure 2.13: Room temperature ESE signals obtained in untreated PS1 particles.

Laser repetition rate of 2.4Hz; microwave pulse sequence : p/2 pulse=16ns , t=80ns; 1Gauss per points, average of 10 sweeps per point

Top spectrum: out of phase signal, t_0=20ns.

Bottom spectrum: in phase signal, t_0=1500ns.

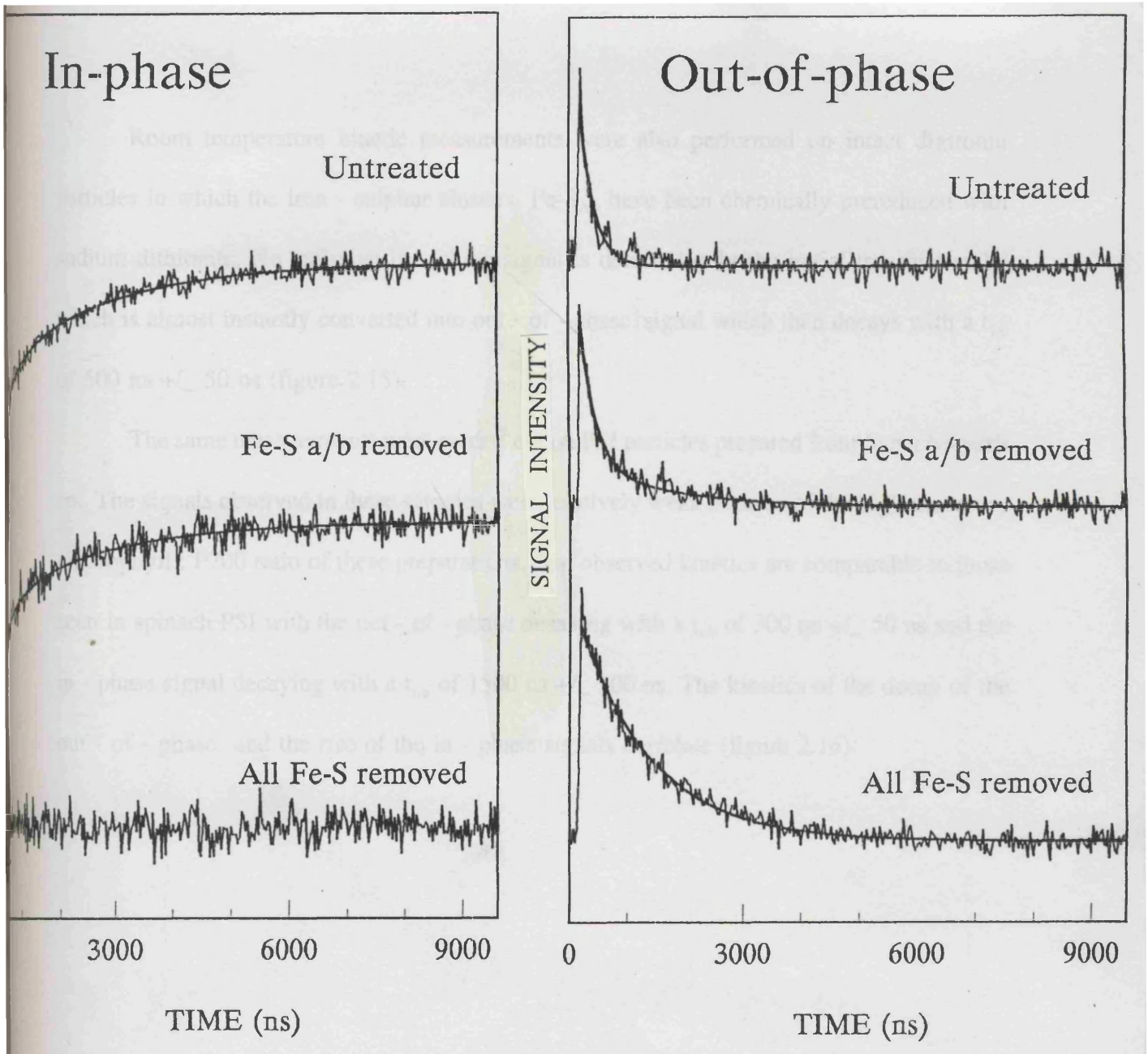

Figure 2.14: In phase (left) and out of phase (right) kinetic traces at H_0=348.05mT, t_0 is incremented with 32ns steps, 300points and 40 added sequence per point, of untreated PS1, F_aF_b depleted PS1, and $F_aF_bF_x$ depleted PS1, from top to bottom respectively. In phase top, untreated, $t_{1/e}$ = 160+/_50 ns(rise), 200+/_100 ns(decay). Middle, FeS_{AB} depleted, $t_{1/e}$=170+/_50 ns(rise), 2000+/_100ns(decay).Bottom:all FeS clusters depleted. Out of phase, top:untreated, $t_{1/e}$=130+/_50ns,middle: FeS_{AB} depleted,$t_{1/e}$=190+/_50ns, bottom:all FeS clusters depleted, $t_{1/e}$=1250+/_50ns.

Room temperature kinetic measurements were also performed on intact digitonin particles in which the iron - sulphur clusters, Fe-S_{AB} have been chemically prereduced with sodium dithionite. No emissive in - phase signal is detected only the initial transient spike which is almost instantly converted into out - of - phase1signal which then decays with a $t_{1/e}$ of 500 ns +/_ 50 ns (figure 2.15).

The same measurements were carried out on PSI particles prepared from *Synechocystis* sp.. The signals observed in these samples were relatively weak because of the high accessory chlorophyll : P700 ratio of these preparations. The observed kinetics are comparable to those seen in spinach PSI with the out - of - phase decaying with a $t_{1/e}$ of 300 ns +/_ 50 ns and the in - phase signal decaying with a $t_{1/e}$ of 1500 ns +/_ 100 ns. The kinetics of the decay of the out - of - phase and the rise of the in - phase signals correlate (figure 2.16).

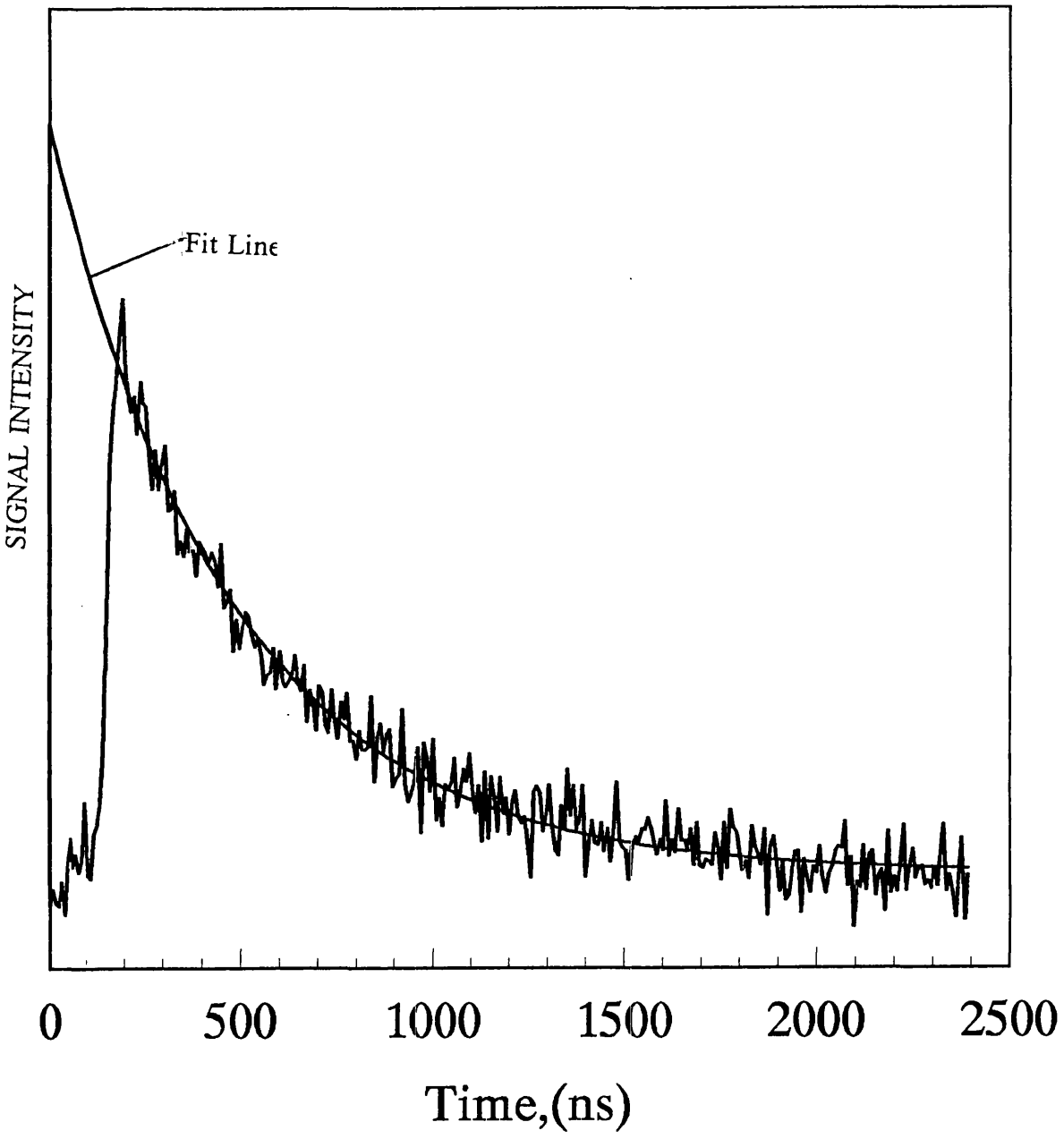

Figure 2.15. Room temperature kinetic trace of spin polarised signal observed in the out - of - phase channel for intact digitonin spinach PSI that has been prereduced by incubation in 100 mM glycine - KOH, pH = 10.0, 0.2 %(w/v) sodium dithionite, sample concentration of 4 - 5 mg chlorophyll / ml. Fit gives $t_{1/e}$ =500 +/_50 ns.

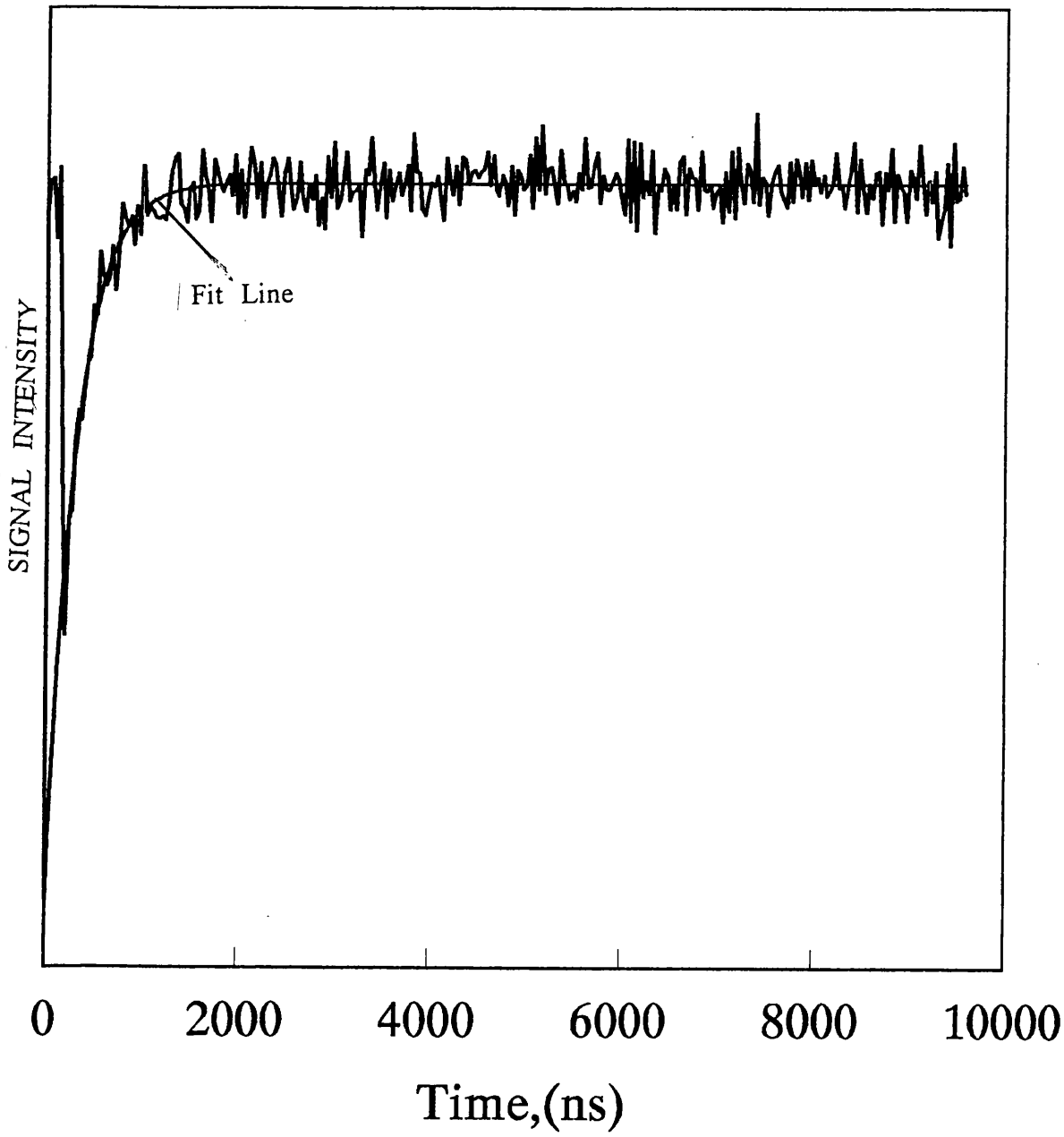

Figure 2.16. Room temperature kinetic trace of in - phase phase spin polarised signal in intact PSI particles of the cyanobacterium, *Synechocystis*. Sample concentration : 4-5 mg chlorophyll / ml. 50 mM Tris-HCl, pH8.0, 1 mM sodium ascorbate, 0.1mM 2,6-dichlorophenol indophenol, 0.1mM methyl viologen. Fit yields a $t_{1/e}$ = 300 +/_50 ns.

2.4 DISCUSSION

(a) Low Temperature Kinetics

The out - of - phase signal observed in these experiments at both 4 K and room temperature exhibits the same spectral features as the signal described by Thurnauer and Norris (1980). The kinetics of this signal have been shown to vary with experimental conditions. They interpreted the echo shift associated with this spin polarised signal in terms of an interaction argument - the shift arising because forward electron transfer from A_1^{--} during the first microwave pulse, means the radical of the radical pair, $P700^+A_1^{--}$, can no longer interact magnetically. This interpretation is not compatible with the results presented here, in which the ESP radical pair signal is observed at 4 K, even though forward electron transfer is inhibited or non - existent at this temperature. Secondly the duration of the radical pair signal is long relative to the length of the microwave pulse sequence, which also conflicts with this explanation for the signal's origin. This spin polarised signal is exclusive to PSI samples which contain an external electron donor, either sodium dithionite or ascorbate, so cannot be a laser artefact, nor can it be a low temperature artefact. The shift effect would appear to depend on the intensity of the microwave pulses. When pulses of relatively low intensity are used it is the typical electron spin polarised signal that is detected (figure $3b). As with the spin polarised signal described by Thurnauer and Norris, it is assumed the signal detected in this study arises from the radical pair, $P700^+A_1^{--}$.

From the 4 K measurements it can be seen that the in - phase spin polarised signal produced using low intensity microwave pulses and the out - of - phase signal produced by high intensity pulses cover the same spectral region; their intensities correlate; they decay at the same rate. Additionally deuteration of phylloquinone has been shown to narrow the linewidth of both these signals (Heathcote *et al*, 1994 in press). These lines of evidence

suggest that the out - of - phase signal can also be attributed to the $P700^{+}A_{1}^{--}$, as was suggested by Thurnauer and Norris.

In samples containing prereduced iron sulphur clusters at 4 K the out - of - phase signal decays with a half - life of 23 μs. There are two modes by which this signal could decay : through relaxation of spin polarisation or through a recombination reaction within the radical pair, $P700^{+}A_{1}^{--}$. Setif *et al*, 1984 used flash absorption to measure the rate of back reaction in spinach PSI particles with prereduced iron sulphur clusters at 10 K and obtained a half - life value of 120 μs. We repeated our measurements of the decay of the out - of - phase signal at 10 K and 20 K and the $t_{1/e}$ obtained was the same as that at 4 K, this is not surprising for a process which is not diffusion - dependent. The difference in the determined decay rates of the same flash induced radical pair signal may reflect differences inherent in the two techniques applied, but this is unlikely. Both the determined rates are in the μs time scale and within the margins of error of the two techniques differences in the determined decay rates could be negligible. T_1 relaxation rate measurements carried out on radicals at 4 K gave rate constants that were in the ms time range. If the spin polarised signal detected at 4 K in these experiments decayed by spin polarisation relaxation or forward electron transfer were occurring, half - lives in the ms or ns range respectively would be expected and so the value of 23 μs fits far better with the recombination model. The fact that no $P700^{+}FeS_{X}^{--}$ spin polarised signal is observed in the in - phase detection channel further confirms that no forward electron transfer is occurring at 4 K.

4 K measurements performed on PSI particles which have not been prereduced, in the presence of external donor and acceptor, are not possible because after a single laser flash an irreversible charge separation takes place with the formation of the $P700^{+}Fe\text{-}S_{A}^{--}$ charge pair without the detectable formation of any $P700^{+}A_{1}^{--}$ spin polarised signal. The work of Wynn

and Malkin (1988) suggests that forward electron transfer between A_1 and Fe-S_X is inhibited at low temperature even in the presence of oxidised iron - sulphur clusters, Fe-S_{AB}.

For PSI particles, in the presence of sodium dithionite and depleted of their iron-sulphur clusters, FeS_{AB}, a half - life of 51μs +/_ 5μs was obtained. This is closer to the 120 μs value determined by flash absorption. The difference between this half-life and that determined for the chemically prereduced intact PSI particles 23 μs can be explained in terms of columbic repulsion with the negative charge on the reduced iron - sulphur clusters increasing the rate of back reaction between $P700^+$ and A_1^{--}. In the absence of the Fe-S_{AB} clusters this repulsion effect is not exerted and the radical pair recombines more slowly with a $t_{1/e}$ of 23 μs. However the fact that the decay rates of the observed out - of - phase signals are all in the μs range indicate that the spin polarised radical pair signal is decaying by recombination in all the cases. Similarly the lack of any in - phase signal attributable to the spin polarised radical-metal pair indicates that no forward electron transfer beyond A_1 is occurring in any of these samples at 4 K. The $P700^+A_1^{--}$ triplet is only observed in samples in which the FeS_X cluster has been photochemically reduced prior to laser flash excitation. As this condition does not apply to any of the samples discussed here, decay of the triplet should not be a feature of the interpretation of the observed kinetics.

(b) Room Temperature.

At room temperature intact PSI particles supplied with an external electron donor and acceptor exhibit an out - of - phase signal typical of the radical pair $P700^+A_1^{--}$, which decays with a half - life of about 130 ns +/_ 50 ns. This kinetic has traditionally been assigned to

forward electron transfer from A_1 to the tertiary electron acceptor, generally assumed to be Fe-S_X. The decay half - life determined for this reaction has been found to vary according to the technique being used and the source of the PSI, but the value obtained here is comparable to those obtained with time resolved cw ESR(Bock *et al*, 1989), pulsed ESR (Thurnauer *et al*, 1979) and optically (Brettel *et al*, 1988). As the out - of - phase signal decays, a second signal arises in the in - phase channel with kinetics that correlate with those of the decay of the out - of - phase signal. On this basis the in - phase signal can be reasonably attributed to the radical pair comprising the P700 cation and reduced tertiary acceptor. Depleting the PSI of its iron-sulphur clusters, Fe-S_{AB}, essentially had no effect on the observed kinetic behaviour, with the out - of - phase signal decaying at the rate seen in intact PSI, and the appearance of a second spin polarised radical pair signal in the in - phase channel. Depleting PSI particles of the Fe-S_X cluster abolished the in - phase signal and slowed the decay rate of the out - of - phase signal by ten fold both of which indicate the elimination of forward electron transfer from the reduced secondary acceptor. These observations firmly establish the identity of the tertiary acceptor as the iron - sulphur cluster, Fe-S_X, and enable the unambiguous assignment of the 130 - 200 ns kinetic to the reaction : A_1^{--} --------> Fe-S_X.

The decay of the out - of - phase signal in PSI particles depleted of the iron-sulphur clusters, Fe-S_{AB}, shows some biphasic character with a slower decaying component comprising about 10 % of the total signal intensity. This slower component could arise from two possible sources : it could be contributed by a small proportion of centres containing urea - damaged Fe-S_X, or which are depleted of this cluster; secondly it could be because removal of the PsaC results in structural changes to FeS_X, which in turn lead to altered kinetic behaviour (it is known that the rate of electron transfer is sensitive to the orientation of a radical's electron orbitals). A slower decaying component is also detected in the out - of - phase signal of intact

PSI particles at room temperature comprising less than 5 % of the original signal intensity which might be contributed by a small sub-population of centres which are inherently inefficient in forward electron transfer.

The in - phase signal observed at room temperature appears to be analogous to the electron spin polarised signals observed using time - resolved cw ESR (Blankenship *et al*, 1975, Dismukes and Sauer, 1978, and Bock *et al*, 1989). This signal decays with a half - life of 2 μs. This agrees with the decay rate determined by Bock *et al*, 1989, which was attributed to the relaxation of P700 cation spin polarisation by means of transient cw ESR measurements in which they varied the microwave power.

Bock *et al* explained the origin of the in - phase signal in two ways : that it was either the electron spin polarised signal corresponding to the P700 cation within the radical pair $P700^{+}Fe\text{-}S^{-}$, which does not exhibit any detectable contribution from the iron sulphur radical due to the latter's large g-anisotropy, although the signal's spectral characteristics are influenced by the interaction with the iron-sulphur radical; or that it represents undecayed spin polarisation of the P700 cation persisting after reoxidation of A_1^{-}. It would follow on from the second explanation that the intensity of the in - phase signal would correlate with that of out - of - phase signal. However in this present study in particles depleted of their $Fe\text{-}S_{AB}$ the intensity of the in - phase signal is increased relative to that of the out - of - phase signal in comparison with intact PSI particles. It is quite conceivable that the loss of the $Fe\text{-}S_{AB}$ clusters could induce changes to the spin - spin interactions of the $P700^{+}FeS_X^{-}$ and so affect the signal intensity ratio. Therefore these observations favour the first of the two explanations put forward by Bock *et al*. It is generally agreed that there is a direct correlation between the distance separating two acceptors and the rate of electron transfer. According to the emerging X-ray crystal structure of PSI (Krauss *et al*, 1993) there is a distance of 15-22 A between the

iron sulphur clusters, Fe-S_X and Fe-S_{AB}. It would be expected that the rate of electron transfer between these clusters was in the ns range and so the in - phase signal decay rate of 2μs is not easily reconciled with this first explanation. It may be that some other less straightforward explanation is applicable to the origin of this signal, however the in - phase is still a useful probe of forward electron transfer. The results presented here demonstrate that the emissive in - phase signal stems from the $P700^+ FeS_X^-$ radical pair.

When PSI particles are deprived of all their iron sulphur clusters and there is no forward electron transfer the out - of - phase signal decays far more slowly than in intact particles, with a half - life of 1.3 μs. This decay could be either due to spin polarisation relaxation or a back reaction within the radical pair. From optical work carried out on the P700-A_1 core particles by Warren *et al*, 1993 it has been established that the $P700^+A_1^-$ radical pair decays by charge recombination to the ground state of P700. They determined the half - life of decay as 10 μs. The difference between this and the rate determined by pulsed ESE kinetics could be due to inherent differences in the two techniques but this does not seem very probable. Within the error margins encountered in the two techniques it is quite possible that these two decay rates are comparable, although the 1.3 μs rate obtained here is closer to the 3 μs half-life optically determined for intact PSI particles with prereduced Fe-S_{ABX} clusters (Golbeck *et al*, 1990, Parrett *et al*, 1990) which was attributed to a charge recombination to the P700 triplet state. However it has been established that the presence of prereduced Fe-S_X is required for the formation of P700 triplet and so it is most likely that the decay rate observed in this study arises from a charge recombination to the P700 ground state. However at room temperature chlorophyll radical relaxation might well be expected to lie in the μs time range and so this cannot be entirely discounted as the mode of decay in this case. In the present study when intact PSI particles were prereduced with sodium dithionite, the emissive

in - phase signal corresponding to the $P700^{+}FeS_{X}^{--}$ radical pair is not detected. This indicates that the presence of the reduced iron-sulphur clusters, Fe-S_{AB}, is inhibitive to forward electron transfer from A_1^{--}. In such prereduced samples the decay rate of the out - of - phase signal is faster than in samples with unreduced iron - sulphur clusters, with a half - life of 500 ns. This faster decay rate can be explained in terms of columbic repulsive effects exerted by the reduced iron - sulphur clusters. This is in accord with the decay rate half-life of 750 ns determined for $P700^{+}A_1^{--}$ in the same sort of samples by Setif and Bottin, 1989. From this it would seem that the decay of the out - of - phase signal in intact chemically prereduced PSI and FeS_{AB}- depleted PSI is occurring by the same mechanism i.e. most probably a charge recombination within the $P700^{+}A_1^{--}$ radical pair.

At low redox potentials as low as - 550 mV a reduction of the intensity of the out - of - phase signal was observed by Thurnauer *et al*, 1982. This is the sort of redox potential which exists in the sodium dithionite reduced pH 10.0 PSI particles used here and a similar reduction of intensity was observed. Thurnauer *et al* explained this reduction of intensity in terms of an increase in the lifetime of the radical pair in - phase signal. This explanation stems from their account of the origin of the out - of - phase signal and the phase shift effect and the results presented here do not support this account. An alternative explanation must be provided therefore. Low potential mediators were present in their pH11.0 samples and under these conditions the double reduction of A_1 is possible. If this double reduction occurred in a fraction of centres this would provide a valid explanation for the intensity reduction of the out - of - phase signal observed in their samples. Loss of the spin polarised signal through the double reduction of A_1 has been previously established by Snyder *et al*, 1991. In the work presented here low potential redox mediators were not used and so quinone double reduction should not be a significant factor and so this explanation cannot apply to the

reduction of intensity of the out - of - phase signal observed here.

Room temperature kinetic investigations carried out using time - resolved flash absorption spectroscopy (Setif and Brettel, 1993) showed that forward electron transfer from A_1 gives a biphasic kinetic trace, with one component decaying with a half - life of 150 ns and a faster decaying component with a half - life of 25 ns. The decay of the out - of - phase signal observed here was unambiguously monophasic and it is probable that the "25 ns component" cannot be resolved using our instrumentation, the 25 ns decay rate being considerably shorter than the pulse sequence. Setif and Brettel found that the forward transfer that gives this 25 ns half - life was not inhibited by chemical prereduction of the Fe-S_{AB} clusters, with the result that about 40 % of centres in prereduced digitonin particles formed the $P700^+Fe\text{-}S_X^-$ radical pair. If 40 % of the centres were exhibiting this kinetic behaviour we would expect to detect the 25 ns decay rate. It was suggested by Setif and Brettel that this faster component was an artefact of detergent - induced structural damage, but represented the formation of the $P700^+FeS_X^-$. However it is just as likely that this decay represents centres in which A_1^- is more accessible to the external acceptor. The absence of this faster kinetic in any of the samples examined here at room temperature suggests its existence is preparation sensitive.

Setif and Brettel (1993) assigned the 25 ns kinetic to the A_1^- ---->Fe-S_X reaction, and the 200 ns kinetic to the A_1^- ----->Fe-S_{AB} reaction, with Fe-S_X by-passed. The pulsed ESE kinetic results presented here show that this interpretation must be incorrect as the 200 ns kinetic survives the removal of the iron - sulphur clusters, Fe-S_{AB}, but not the removal of the iron - sulphur cluster, Fe-S_X.

The room temperature kinetic experiments carried out on PSI prepared from *Synechocystis* and exhibited an out - of - phase signal decaying with a $t_{1/e}$ of 300 ns +/_ 50

ns, which is very similar to the decay rate for the out - of - phase signal observed in spinach PSI particles indicating that the kinetics of the reaction $A_1^{\cdot-}$ ---->FeS_X and therefore the distance between these two acceptors are conserved between eukaryotic and prokaryotic PSI.

Our results obtained using pulsed ESR concur with those of a study using flash absorption methods carried out independently by Lunneberg *et al*, 1993. They found that the removal of the iron - sulphur clusters, Fe-S_{AB} did not affect the kinetic behaviour of the $A_1^{\cdot-}$ reoxidation process as observed in *Synechococcus* sp. PSI.

The spin polarised signals described in this work are useful markers for assessing whether or not electron transfer is blocked beyond the phylloquinone acceptor, A_1. The signals can therefore be used to test the potency of putative inhibitors of electron transport, such as herbicides. The effect of substituting modified quinones for phylloquinone on the kinetics of electron transfer to the iron - sulphur clusters could also be studied using these spin polarised signals, although subject to the same limitation as other studies of this sort, i.e. competition between the specific and adventitious binding of the modified quinone.

An analogous flash - induced, spin - polarised oxidised primary donor / reduced quinone signal can be observed in purple bacterial reaction centres. As for example in the reaction centres of *Rhodobacter sphaeroides* W58 in which the non - haem iron has been replaced by zinc. The signal is not observed when the semiquinone is coupled to the iron. This means that similar kinetics measurements could be performed on purple bacteria for which there is already a high resolution crystal structure, enabling a synthesis of kinetic and structural data.

3.0 DISTANCE DETERMINATION IN PSI USING PULSED ESR SPECTROSCOPY.

3.1 Sub-Introduction II

Use of T_1 Saturation Recovery Measurements to Study the Structure of Photosystem I

At the present time there is no complete high resolution X - ray crystal structure of photosystem I or any of its bacterial analogues, such as green sulphur bacterial reaction centres. The PSI of *Synechococcus* sp. has been crystallised but to date the structure has only been solved to a resolution of about 6 Å, which is too low for the reliable identification of chlorophyll much less of quinone molecules (Krauss *et al*, 1993). However the structure of part of the acceptor side can be accurately solved and this is because the three iron - sulphur clusters located there represent electron - dense regions which diffract X - rays well. This portion of the structure is shown schematically in figure 3.1, giving the distances in angstroms between the iron - sulphur clusters. The rest of the structure cannot be accepted with such confidence at this resolution and there is scope for the application of techniques other than X - ray crystallography to estimate the distances separating the other acceptors.

Hecks *et al*, 1994 have used picosecond photovoltage measurements to make deductions about the positions of the A_0 and A_1 acceptors relative to P700. Electroluminescence kinetics studies have also been used to obtain structural information about the PSI reaction centre (Vos and van Gorkom, 1988). In the following section a study

using T_1 saturation recovery measurements to gain structural insights into higher plant PSI is presented.

3.1.1 The Principles of Saturation Recovery

The saturation of paramagnetic spin systems by microwave irradiation has been widely used to study electronic and structural aspects of such systems. In a saturation recovery experiment a spin system is irradiated with a short-lived high intensity microwave pulse, the kinetics of the recovery process by which the magnetisation reestablishes its thermal equilibrium are followed. Equilibrium is restored by *relaxation*, which can be defined as an energy exchange occurring either between spin systems (as in spin-spin coupling) or between a spin system and the surrounding crystal lattice (as in spin-lattice relaxation). Measuring the kinetics of the former yields a value for the parameter T_2; measuring the kinetics of the latter yields a value for T_1. There are a number of unquantifiable factors that influence T_2 relaxation kinetics and for this reason T_1 is a purer parameter.

The radical is exposed to a pulse of high intensity microwaves for long enough to saturate the bulk magnetisation of the radical. The bulk magnetisation consists of the net contribution from electron spins, including those spins which are aligned against the applied magnetic field. Probing microwave pulses of lower intensity are used to phase the relaxing magnetisation. When the system is restored to equilibrium the input microwaves are released in a burst which results in a spin echo. The increase in the intensity of this echo is measured against time. This is represented schematically in figure 3.2. The technique originates from the nuclear magnetic resonance work of Bloembergen *et al* (1948). The situation for a simple two - level spin system can be represented by the following rate equation:

$$dn/dt = n -- n_0 / T_1 \quad ,$$

where n is the instantaneous difference in populations of the two energy levels; n_0 is the Boltzmann - determined equilibrium difference of the populations. Signal recovery can be represented by the following equation:

$$S(t) = S_{LP} -- \Delta S_{exp.} [-- t / T_1] \quad ,$$

where S_{LP} is the signal amplitude at $t = \infty$, ΔS is the difference in signal amplitudes at t=0 and $t=\infty$. After a saturating pulse the pulse grows back in an exponential fashion. These equations are appropriate for an ESR transition of two levels and do not accommodate other ESR transitions or the presence of magnetic nuclei. Both of these result in complications, namely cross-relaxation and spectral diffusion which are time - dependent effects. For accurate T_1 measurements the spin - lattice relaxation must be separated from the time - dependent phenomena. There are four basic conditions which need to be fulfilled to ensure this separation:

(1)Detected signals should exhibit a single exponential behaviour.

(2)The later part of the recovery curves should be taken to obtain the relaxation rate constants, as this data is the most reliable.

(3)Relaxation constants should be independent of the duration of microwave pumping.

(4)They should also be independent of observing microwave power.

If the simplest case does not apply it may still be possible to extract rate constants by a number of strategies. For example by only fitting the latter part of the saturation curve which is the least susceptible to these time - dependent effects, or by use of a multiexponential fitting program which fits data over the entire time range.

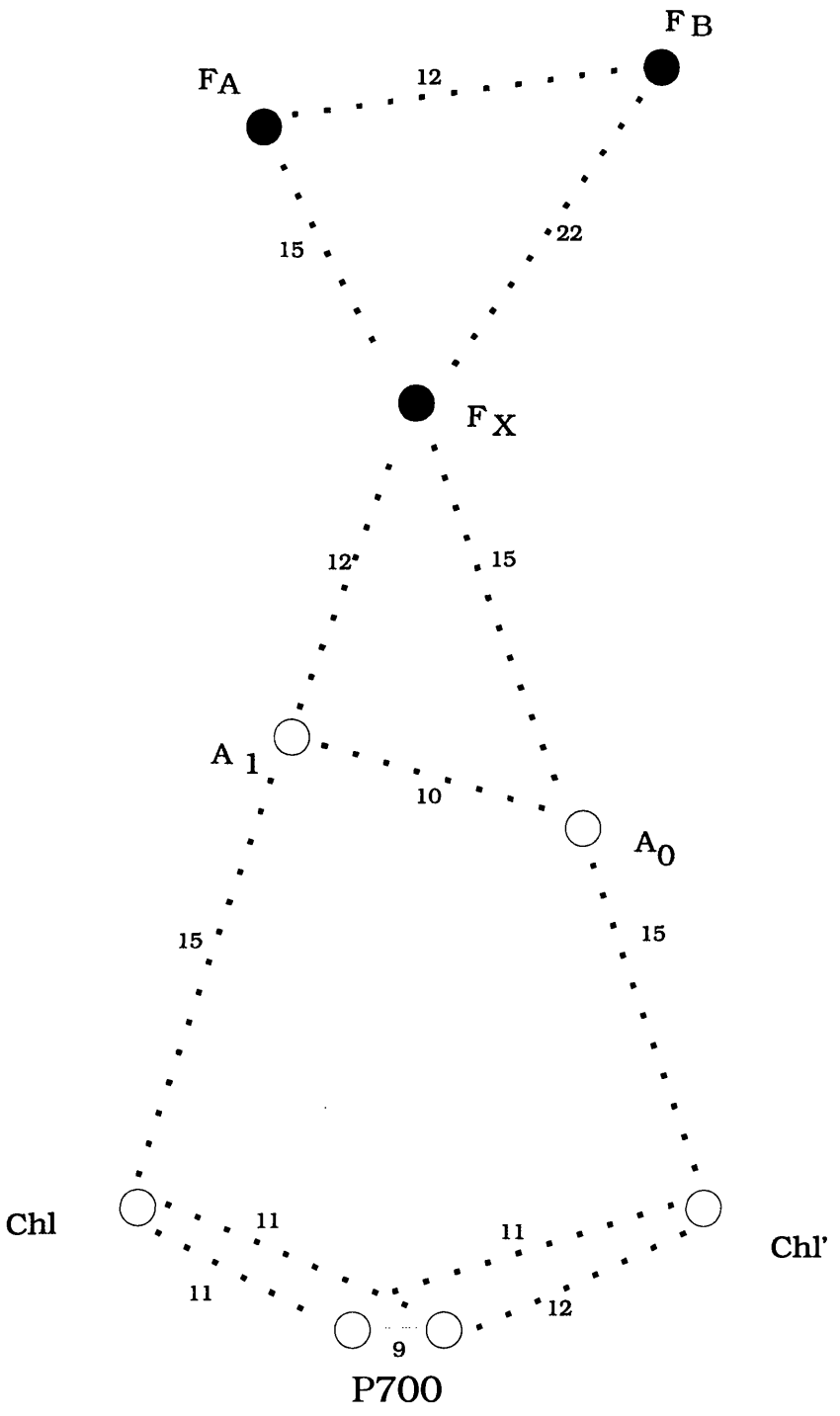

Figure 3.1 6 Å X - Ray Crystal Structure of *Synechococcus* Photosystem I Reaction Centre.

Figure 3.2

SP - saturating microwave pulse.

SE - spin echo. Tau is the time interval between the saturating and 90^0 microwave pulses. T is the time interval between the 90^0 and 180^0 microwave pulses.

The 2000 ns microwave pulse saturates the bulk magnetisation corresonding to a paramagnet so that the recovery of the bulk magnetisation can be measured. A microwave pulse with a duration of 16 ns is used to flip the recovering magnetisation through 90^0. After a time interval, T, a microwave pulse with a duration of 32 ns is used to flip the magnetisation through $180,^0$ so it lies along the y axis and can be detected. As the magnetisation relaxes microwave energy is released as a spin echo. It is the recovery of this spin echo which is determined spectroscopically.

The Measurement of Spin Lattice Relaxation Times

Method
The Pulse Saturation and Recovery Experiment

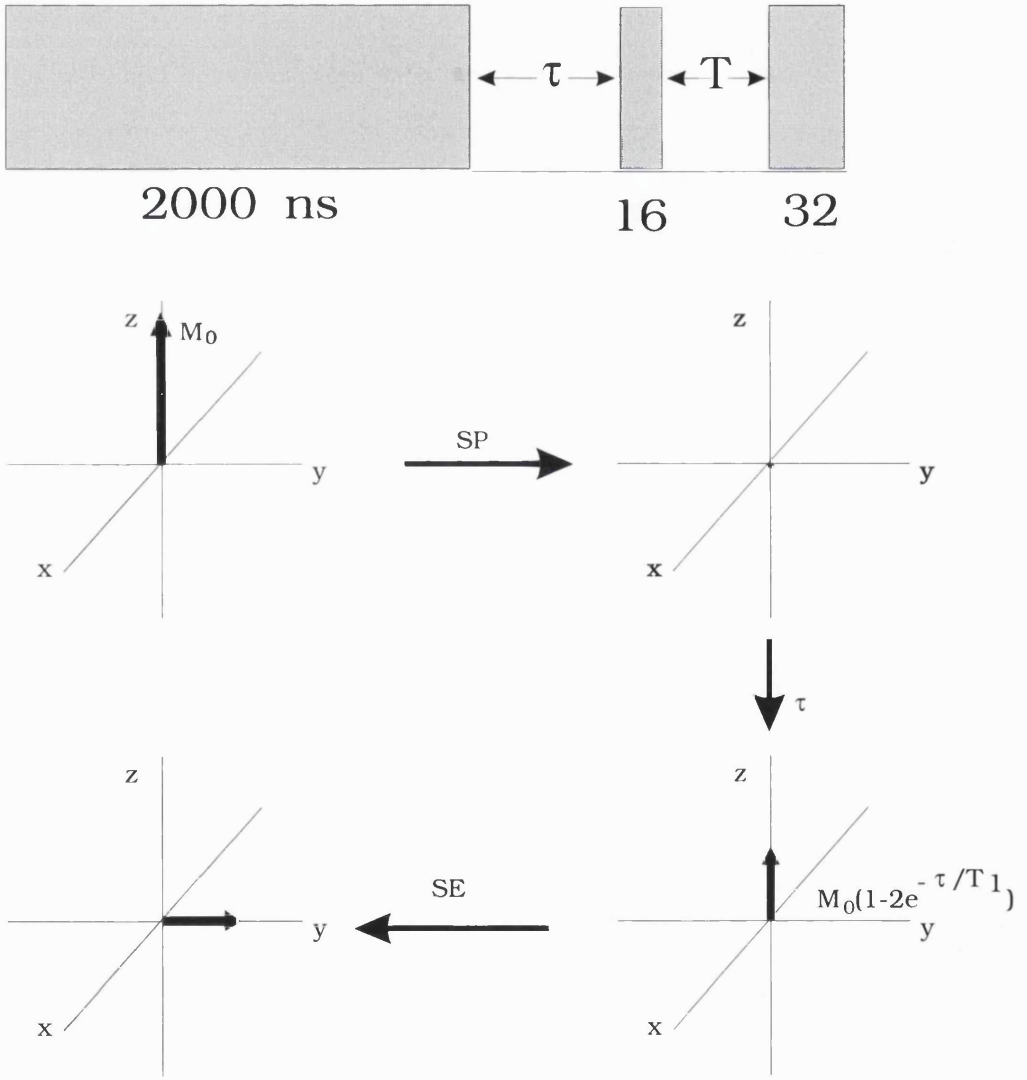

Figure 3.2

3.1.2 Relaxation Enhancement as a Method of Distance Determination in Photosystem I

The anionic radicals generated by the reduction of the chlorophyll, and quinone acceptors of photosynthetic reaction centres are intrinsically slow relaxing species giving spin - lattice relaxation rate (T_1) values which are typically in the ms range, while those generated by the reduction of metal centres are intrinsically fast - relaxing species giving T_1 values in the μs / ns range. Within a spin system containing both types of component, a paramagnetic metal centre and a non - metallic radical can interact magnetically, resulting in an increased rate of spin - lattice relaxation of the slow - relaxing species. In systems where such an interaction is taking place the saturation recovery transient of the slow relaxing species behaves non - exponentially. This is because there is what is termed a dipole - dipole interaction between these species, giving a dipolar relaxation rate that is orientation - dependent. Samples of the sort used in the present study contain thylakoid membrane fragments arranged randomly in many different orientations with respect to the applied magnetic field. This means that in such samples the magnetic dipole moment between interacting paramagnets within the membrane fragments are similarly arranged in many different orientations relative to the applied magnetic field. For each different orientation there is a different spin lattice relaxation rate. Therefore the net spin lattice relaxation rate of the enhanced radical is equal to the sum of these different rates, resulting in a spin lattice recovery curve which is multiexponential. In a highly ordered structure like a protein crystal, the positions of reaction centres are fixed and there is only one orientation of the magnetic dipole moment relative to the external magnetic field. In this case the spin lattice saturation recovery curve of a paramagnetic species is monoexponential. This relaxation rate

enhancement effect is distance dependent and can be formulated. By making T_1 measurements of both the fast and slow - relaxing species, it is possible to estimate the distances separating them and make inferences about the relative positions of the components of the system. There are several practical precedents for this kind of study, e.g. the determination of the distance between the tyrosine radical (Y_D) and the non - haem iron atom of PSII (Hirsh *et al*, 1989) and between tyrosines, Y_D and Y_Z in the same system, Astashkin *et al*, 1994.

3.2 Materials and Methods

(a) Preparation of Photosystem I Particles Containing Radicals, Under Different Redox Conditions

All the samples were prepared using both digitonin and Triton X-100 spinach PSI particles. The iron - sulphur clusters, Fe-S_{AB}, were chemically pre-reduced by incubating PSI with 0.2 % sodium dithionite and either 50 mM Tris-HCl pH8.0 or 200 mM glycine-KOH pH10.0 in the dark for 30 minutes at room temperature. The buffers were degassed beforehand and the sample was incubated under a stream of oxygen - free nitrogen gas. The sample concentration used was 1.0 mg chlorophyll / ml. The samples were frozen in the dark in liquid nitrogen. The iron - sulphur cluster, Fe - S_X, was photochemically reduced prior to the photoaccumulation of the other radical species. Because the pulsed ESR spectrometer is less sensitive than the cw ESR spectrophotometer stronger signal intensities are required for the saturation recovery measurements and so the sample concentration used was twice that routinely used in cw ESR spectrophotometry.

Strong signals were particularly important for the T_1 measurement of the reduced iron - sulphur cluster, Fe-S_X, because the rate of this radical's relaxation is close to the resolution

limit of the instrument. A relatively strong Fe-S_X signal was photoaccumulated by illuminating the sample with high intensity white light (150 Watt lamp) for 2 minutes in liquid nitrogen vapour. The samples were then frozen either in the dark or under illumination. In such samples a mixed g=2 radical was also produced with contributions from A_0 and A_1. The other radical signals were generated as follows :

(1)Reduced quinone acceptor, $A_1^{\cdot-}$, was produced by illuminating spinach PSI with its iron sulphur clusters chemically prereduced, in an unsilvered dewar containing a solid CO_2 / ethanol mixture for 2 minutes. The sample buffer was 50 mM Tris HCl pH 8.0.

(2)A mixture of reduced quinone and chlorophyll radicals was generated by illuminating the PSI sample for 10 minutes at 230 K.

(3)A pure A_0 spectrum was produced by first illuminating the sample in an unsilvered dewar at 4 ^{0}C for 2 hours with white light in the presence of 0.2 % sodium dithionite, 200 mM glycine - KOH pH10.0 under a stream of oxygen - free nitrogen. During this prolonged illumination a copper sulphate filter was positioned between sample and lamp to reduce infrared heating effects and the likelihood of photoinhibition. This illumination was carried out to double reduce both the quinone molecules present in each reaction centre. Double reduction was confirmed by attempting to generate the singly reduced quinone. Double reduced quinone is ESR silent. The double - reduced PSI was then illuminated for a further 10 - 20 minutes at 230 K in order to produce $A_0^{\cdot-}$.

(4)The $P700^+Fe\text{-}S_A^{\cdot-}$ charge pair was produced using ascorbate dark reduced samples. Spinach PSI samples were prepared in the dark containing 20 mM ascorbate, dark adapted for 20 minutes and frozen in the dark. The samples were then illuminated for 4 minutes either in the instrument cavity at 8 K or in liquid nitrogen vapour. This results in an irreversible charge separation.

(5)The $P700^{+}Fe\text{-}S_X^{-}$ charge pair was produced by continuous illumination of a dithionite dark reduced PSI sample in the cavity of the spectrophotometer at 8 K. This charge separation is reversible and rapidly recombines in the dark.

The T_1 measurements of the unrelaxed quinone and chlorophyll radicals, i.e. of radicals in the absence of fast - relaxers, were carried out on PSI particles which had been depleted of all their iron - sulphur clusters. These depletions were carried out in accordance with the methods already described.

Unrelaxed $P700^{+}$ was produced by illuminating spinach PSI particles without the addition of exogenous reductant at room temperature for 2 minutes, followed by freezing in liquid nitrogen. In this case the electron on the primary donor passes through the acceptors of the core, leaving the system, to be either solvated or to reduce a Tris molecule in the surrounding medium. This results in a g=2 radical signal but no iron - sulphur cluster radical signal. These samples were made using Triton X - 100 PSI particles which were treated with 6.8 M urea to remove residual plastocyanin not removed on the hydroxyapatite column. The $P700^{+}$ T_1 so obtained is not enhanced by the fast - relaxing copper II atom of oxidised plastocyanin. All the illuminations were carried out using a quartz halogen lamp producing an incident photon flux density of 1500 μmol / m^2 / s. A water filter was placed between sample and light source to limit heating effects during the shorter illuminations. The temperature of the solid CO_2 / ethanol bath was monitored during the illumination. All the samples were prepared in quartz tubes with 3 mm internal diameter.

The identity of the radicals formed was verified by a combination of cw and pulsed ESR spectra in which the radicals have characteristic linewidths and resonance g values and ESEEM (electron spin envelope echo modulation).

(b) Electron Spin Envelope Echo Modulation (ESEEM) Spectroscopy

ESEEM spectroscopy was carried out as a three pulse experiment. The radical - containing sample was subjected to three 90^0 microwave pulses (i.e.pulse with a duration of 16 ns). The time interval (tau) used to separate the first and second pulses was 112 ns. This generated a stimulated echo signal the decay of which was followed from 0 to 8000 ns. The modulation this echo exhibits arises because of dipolar interactions with surrounding nuclei. The ESEEM data were then fourier transformed to convert it from a time domain into a frequency domain. The technique can be diagnostic as certain nuclei and certain radical species give resonances at characteristic frequencies and / or characteristic spectral profiles. ESEEM experiments were carried at 8 K.

(c) Saturation Recovery Measurements

The determination of spin - lattice relaxation times was carried out using the following pulse sequence :

$[P1\text{-}t\text{-}(\pi/2 - T\text{-}\pi\text{-}T\text{-}Echo]n$

where P1 is a microwave pulse of sufficient duration to saturate the energy level transition of the signal of interest. The duration of P used here was 2000 ns. The progress of bulk magnetisation back to equilibrium was detected using the Hahn spin echo sequence after a variable time, *t*. The value of *T*, i.e. the time interval between the probing microwave pulses, was 112 ns. Measurements of relaxation transients were made at the following field positions : 348 mT for the non - metallic radicals, 359 mT for iron -sulphur cluster, Fe-S_A, 381.5 mT

for iron - sulphur cluster, Fe-S_X. The relaxation data was fitted using Bruker software for fitting multi-exponentials and software written by P. Bratt.

(d) CW Microwave Power Saturation Measurements

Power saturation measurements were made on PSI particles that had been chemically prereduced by incubation with sodium dithionite as already described, and which were then frozen at 77 K under illumination. The sample concentration was 0.5-1.0 mg chlorophyll / ml.

The peak to peak amplitudes of the g = 1.76 FeS_X signal observed in this sample, were measured on a cw ESR spectrometer at various microwave powers. These measurements were carried out at 8 K.

3.3 Theory

In the following section a study is presented in which spin - lattice relaxation rates were determined by saturation recovery for two types of spins in spinach PSI involved in a dipole - dipole interaction, namely a slow - relaxing chlorophyll or quinone radical and the fast relaxing reduced iron - sulphur cluster, Fe - S_X. The intrinsic relaxation rates of the non - metallic radicals were also determined using the saturation recovery method. The saturation recovery data was fitted to the powder model developed by Hirsh *et al*, 1992, for the dipole interaction between the non - haem iron (II) and tyrosine radical of PSII. For any one orientation of the interspin vector, the saturation recovery transient is described by a single exponential, theta - angle between magnetic dipole moment of the interacting

$k_{1obs}(\theta) = k_{1scalar} + k_{1\theta}$. radicals and the moment of the externally applied magnetic field.

The relaxation rate is a function of θ and in the powder sample and in our PSI samples there is a random distribution of orientations and so the observed saturation recovery transient is

the sum of many different exponentials described by the equation below :

$$I(t) = 1 - N \int_0^{\pi} \sin\theta \, [e^{-(k_{1scalar} + k_{1\theta})t}] \, d\theta$$

where $I(t)$ is the intensity of the saturation - recovery transient at time t and N is an adjustable scaling factor. Our saturation recovery data for the slow relaxing radical in the presence of reduced iron - sulphur cluster, Fe-S_X was found to fit with this non -(single)- exponential recovery curve, indicating that a dipole - dipole interaction is taking place and the same relaxation enhancement theory used by Hirsh *et al* can be applied here to calculate distances between Fe-S_X and the preceding acceptors. From the fit a value can be obtained for the rate constant, $k_{1\theta}$ and therefore for the dipolar rate constant, k_{1d} , because of the following relationship :

$$k_{1\theta} = k_{1d}(1 - 3\cos^2\theta)^2$$

the value the dipolar rate constant can be included in the equation given below :

$$k_{1d} = \gamma_s^2 \mu_f^2 / 6r^6 \, \omega_s^2 \, (1 - g_f/g_s)^2 \, T_{1f}$$

T_{1f} is the spin - lattice relaxation rate of the fast relaxing species which can be determined directly or indirectly by experiment, along with the dipolar rate constant. The other terms are constants with known values, γ_s is the magnetogyric ratio for the slow relaxing spin, μ_f is the magnetic dipolar moment, g_f and g_s are the g values of the fast and slow - relaxing spins respectively, ω_s is the Larmor frequency of the slow-spin. By rearranging this equation it should be possible to calculate a value for r , the interspin distance.

Spin - lattice relaxation measurements were made at cryogenic temperatures ranging from 4 K to 16 K. The temperature chosen for a particular radical was determined by the resolving capacity of the instrument and the fact that there is a "blind spot"meaning that

radicals relaxing in the time range 260 μs to 1ms cannot be measured. Accurate determination of the T_1 of Fe-S_X could only be made at between 4 K to 6 K. For the $P700^+Fe\text{-}S^{--}_A$ charge pair the temperature had to be raised to 10 K so that the iron - sulphur radical was relaxing fast enough to enhance the $P700^+$ T_1 and no longer fell within the blind spot. The T_1 values of the unenhanced slow relaxers could not be determined reliably at temperatures much below 8 K because otherwise they were too long to resolve accurately.

It should be emphasised that it is possible to use the pulsed ESR spectrometer to measure relaxation rates that lie in the nanosecond time range. However the instrument uses a spin - spin coupled relaxation rate (T_2) detection system. Spin - spin relaxation rates are significantly faster than their spin lattice equivalents and at temperatures greater than 5 K intensity corresponding to FeS_X was not detectable in the field swept spectrum even when the shortest possible tau (time interval between the first and second probing microwave pulses) was employed. In practice this places a restriction on the measurement of spin - lattice relaxation transients.

3.4 Results

3.4.1 Saturation Recovery Experiments on the Reduced Iron - Sulphur Centre, Fe-S_X Over a Range of Cryogenic Temperatures.

Preliminary measurements of spin - lattice (T_1) relaxation rates were made on PSI particles reduced with sodium dithionite and frozen under strong illumination. Samples prepared in this way reproducibly gave the strongest g = 2 radical and reduced iron - sulphur cluster, Fe-S_X^{-}, signal. The g = 2 radical signal in such samples is thought to contain

contributions from both the A_0^{--} and A_1^{--} radicals. Because of the mixed nature of the g = 2 signal, these samples are not suitable for distance determination work but do provide particularly strong signals and so increase the likelihood of accurate T_1 determinations for the species, Fe-S_X^{--} and for establishing the optimal instrumental and sample conditions for saturation recovery experiments using this particular biological system.

Figure 3.3 shows a field swept spectrum for a dithionite dark reduced (pH8.0) PSI sample frozen under illumination.

Figure 3.4 shows the saturation recovery curves for the g = 1.76 radical signal in this sample at 3.7 K and 5.5 K. The saturation recovery experiments were carried out at a field position of 389 mT.

Table 3.1 gives the T_1 values determined for the g = 1.76 signal (Fe-S_X^{--}) for a range of cryogenic temperatures, 3.7 K -- 8.0K.

At 3.7 K, the T_1 of Fe-S_X is determined as 109μs.

The most reliable T_1 measurements for Fe - S_X^{--} were obtained between 4.4 K to 5.5 K -- 12.3 μs to 5.88μs respectively. At temperatures higher than 5.5 K the rate of Fe - S_X^{--} spin lattice relaxation showed no marked increase. This cannot reflect what is actually happening to the relaxation rates of this radical and must mean that at temperatures above 5.5 K Fe - S_X^{--} is relaxing too rapidly to be measured on the fast time scale of the instrument used here. The quality of the saturation recovery data collected for Fe - S_X^{--} for the temperature range 4.5 K to 5.5 K was considerably better than that collected outside this range, as judged by the fact that recovery curves within this temperature range exhibited the expected exponential shape. The Fe - S_X^{--} radical recovery curves obtained outside this

temperature range were not so convincingly exponential.

The T_2 (spin - spin relaxation transient) value for a given radical is always significantly smaller than the corresponding T_1 value. The T_2 of Fe - S_X^{--} at a given temperature proved to be extremely difficult to measure. At 5 K, a T_2 of 1.4 μs was obtained but it is possible that this value is spurious, the actual spin - spin relaxation rate might well be considerably faster than this.

In theory it is possible to measure spin lattice relaxation transients that lie in the ns time range using pulsed ESR spectroscopy. However the instrument employs a spin - spin relaxation (T_2) detection system. At any given temperature the spin lattice relaxation rate of a paramagnetic species is about an order of magnitude slower that its spin - spin coupled relaxation rate. At 8 K the T_2 of FeS_X must be considerably faster than 50 ns because there is no detectable intensity corresponding to this species when a tau of 50 ns (the smallest possible) is used. This limits the measurement of T_1 in practice.

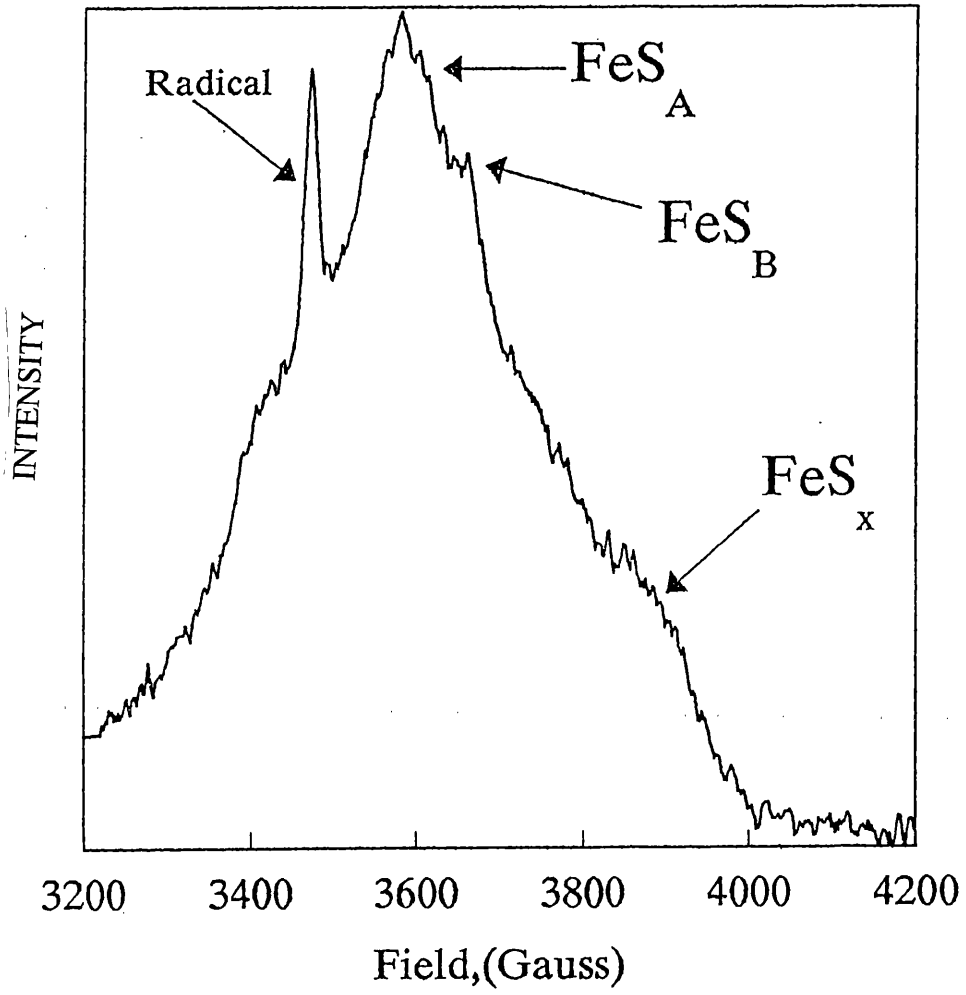

Figure 3.3. Field sweep of pulsed ESR spectrum taken at 4 K of Triton PSI pH 10.0 (chlorophyll concentration 1.0 mg / ml), incubated in the dark with 0.2 % sodium dithionite and frozen under illumination.
Pulse parameters - 16 sweeps per experiment; 4 shots per loop; shot repetition time of 20.480 ms; pulse resolution in X - 500 points.
Field parameters - Centre field at 3718 G; sweep width of 1000 G; field sweep : on.
Microwave frequency of 9.745 GHz.

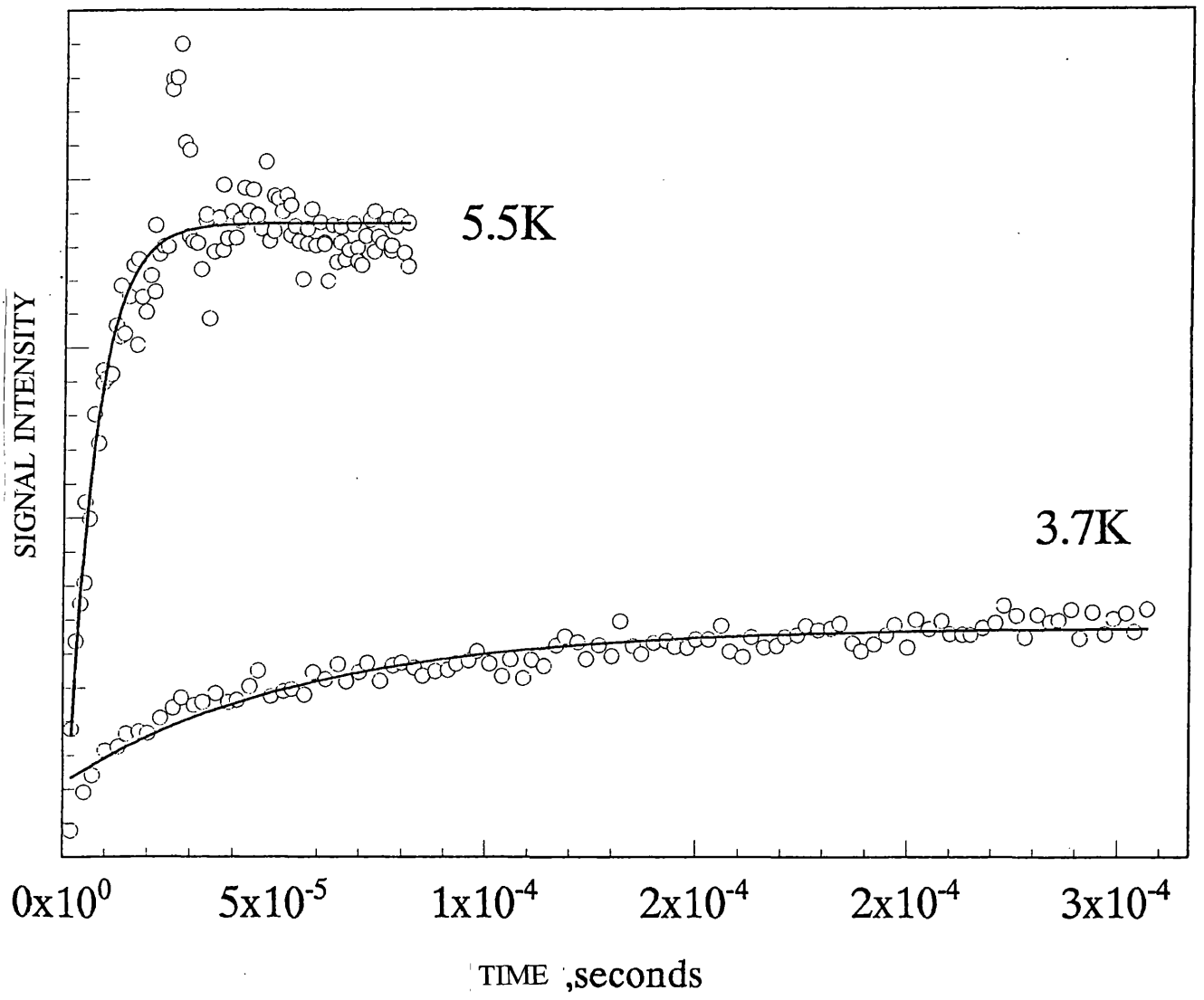

Figure 3.4 Saturation recovery curves of the iron - sulphur cluster, FeS_x, at 3.7 and 5.5 K, in PSI samples prereduced with sodium dithionite, frozen under illumination. Sample concentration 1.0 mg / ml. Fitted to single exponentials. At 3.7 K, T_1 = 109μs +/_ 10μs ; at 5.5 K, T_1 = 6μs +/_ 1μs.

Temperature / K	Spin Lattice RelaxationTransient (T_1) / μs
3.7	109.0
4.4	12.3
5.0	7.15
5.5	5.88
6.2	5.88

Table 3.1

Tabulated spin - lattice relaxation rates of the iron sulphur cluster, F_X, measured at a field position of 389 mT in digitonin PSI particles (1.0 mg chlorophyll / ml) that were frozen under illumination with white light. The values cover the narrow temperature range over which the T_1 of this cluster was measurable. It was not possible to measure the spin - spin relaxation transient (T_2) for this cluster even at 3.7 K as it was too fast to be resolved.

The T_1s of the g = 2 radical in these samples were measured at different temperatures across the same range as for the Fe-S_X^{-} radical. The spin - lattice relaxation mechanism is known to be highly temperature dependent. The observed variation in the FeS_X^{-} enhanced T_1 values for the g = 2 radical, ranging from 48 ms to 17 ms, may be explicable largely in terms

of temperature dependence rather than increases in relaxation enhancement as the sample temperature is raised. It is possible that the degree of relaxation enhancement changes relatively little with increases in temperature. That the T_1s of the g = 2 radical are being enhanced by the fast relaxing species is indicated by the fact that the saturation recovery data for the g = 2 mixed radical collected at the different temperatures fits closely the non - (single) exponential powder model formulated by Hirsh *et al*, 1992. Secondly the corresponding T_1 values of the pure g = 2 radicals in samples containing no paramagnetic fast relaxer are considerably longer (this data is presented later in the section).

It has been assumed for some time that the iron - sulphur cluster radical, Fe-S_X^{-} , relaxes very rapidly. The evidence for this comes from cw ESR spectroscopy - the Fe - S_X^{-} spectrum is only observed at very low temperature and high microwave powers are needed to saturate the signal. This assumption is confirmed by the T_1 and T_2 measurements we have made on Fe - S_X^{-} and by the power saturation data that has been obtained for this cluster at 8 K.

In these measurements made to determine degrees of relaxation enhancement we have discounted the influence of the reduced iron - sulphur clusters, FeS_{AB}, because at 8 K the spin lattice relaxation rate of these extrinsic iron sulphur clusters is very much slower than that of the intrinsic iron sulphur cluster, FeS_X. Additionally FeS_{AB} is about two times further away from the nearest slow relaxing species. The assumption has therefore been made that at 8 K, in samples in which FeS_X is photochemically reduced, FeS_{AB} are not making a significant contribution to spin lattice relaxation enhancement.

The next step was to repeat the saturation recovery measurements on "pure" radical signals both in the presence and absence of the fast relaxing paramagnet, i.e to obtain the enhanced and the intrinsic spin - lattice relaxation rates for each of the PSI acceptors

preceding the iron - sulphur cluster, Fe - S_X. PSI particles were prereduced by incubation with sodium dithionite. The desired radical was then photoaccumulated as described in the materials and methods section. The identity of the radicals was confirmed by a combination of cw ESR and electron spin envelope echo modulation (ESEEM) spectroscopies.

3.4.2 cw ESR Spectroscopy of the Chlorin and Quinone Acceptors in Intact PSI Particles

The chlorophyll anion, $A_0^{\cdot-}$, and the semiquinone radical, $A_1^{\cdot-}$, both give cw ESR spectra with characteristic linewidth, lineshape and g - values.

Figure 3.5(a) shows the ESR spectrum of the $A_1^{\cdot-}$ radical formed in intact digitonin PSI particles at a chlorophyll concentration of 0.5 mg / ml in 50 mM Tris - HCl pH 8.0. The recording conditions are given in the figure legend. The spectrum has a linewidth of 0.8 mT(peak to peak distance). The pure $A_1^{\cdot-}$ spectrum is smaller and more symmetrical than the $A_1^{\cdot-}$ / $A_0^{\cdot-}$ spectrum though both spectra centre at about g = 2.0048.

Figure 3.5(b) shows the cw ESR spectrum of the $A_0^{\cdot-}$ radical formed in intact digitonin PSI particles at a chlorophyll concentration of 0.5 mg / ml in 200 mM glycine - KOH pH 10.0. The $A_0^{\cdot-}$ spectrum is broader than that of $A_1^{\cdot-}$, having a linewidth of 1.3 mT and the spectrum centres at g = 2.0037. The formation of an $A_0^{\cdot-}$ only spectrum as opposed to a combined $A_0^{\cdot-}$ / $A_1^{\cdot-}$ spectrum, depends on the thorough double reduction of A_1 in all centres. The quinol form of A_1 is diamagnetic and will not give an ESR spectrum. PSI particles that have been thoroughly doubly reduced, when illuminated for 2 minutes at 205 K did not produce the A_1ESR signal but did give a very low intensity broader chlorophyll - type spectrum.

3.4.3 ESEEM Spectroscopy of the A_0 and A_1 Anions

Further confirmation of the identities of these two radicals can be obtained using ESEEM spectroscopy. A_1 is now known to be a phylloquinone molecule. Phylloquinone contains no nitrogen atoms being comprised of carbon, hydrogen and oxygen atoms only.

Figure 3.6(b) shows the ESEEM spectrum of a putative $A_1^{\cdot-}$ signal. The spectrum contains no appreciable nitrogen modulations which characteristically occur in the frequency range 0 to 2.5 MHz, but does exhibit strong proton resonances centred at around 15 MHz indicating that this spectrum is predominantly made up of a non - N - containing species. The low intensity nitrogen modulations observed between 0 and 5 MHz may reflect the presence of a small percentage of $A_0^{\cdot-}$ radical or these nitrogen modulations might be contributed by amino acid ligands in close proximity.

Figure 3.6(a) shows the ESEEM spectrum of a combined $A_1^{\cdot-}$ / $A_0^{\cdot-}$ signal, formed by illumination of digitonin PSI particles (0.5 mg chl / ml) in 200 mM glycine - KOH pH10.0 at 230 K for 10 minutes. This spectrum displays obvious nitrogen resonance as would be expected if there were significant contributions from a chlorophyll radical, the chlorin ring containing 4 nitrogen atoms. There is also a very low intensity peak at around 14 MHz, reflecting a minor contribution of proton resonance to the spectrum.

Figure 3.6(c) shows the ESEEM spectrum of a sample in which A_1 has been double reduced and the A_0 anion has been accumulated by a 20 minute illumination at 230 K. The spectrum is very similar to that obtained for the A_0 / A_1 signal, but the signal to noise ratio is much greater. For example the nitrogen peaks occuring at about 1.5 MHz are better defined than in the A_0 / A_1 spectrum. The intensity of the major nitrogen peak occuring at about 2.5 MHz is much greater than in spectrum (a).

Figure 3.5. (A) Continuous wave ESR spectrum of the radical, A_1^-. Digitonin PSI particles. Sample concentration: 1.0 mg/ml. pH 8.0. 0.2 % w/v sodium dithioninite dark reduced. Illuminated at 205K for 2 minutes. (B) Continuous wave ESR spectrum of the radical, A_0^-. Digitonin PSI particles. Sample concentration 1.0 mg/ml. pH 10.0 0.2% sodium dithionite, dark reduced. Illuminated at 230K for 20 min. Running conditions: 77K, microwave power: 5 microwatts, modulation width: 0.2mT

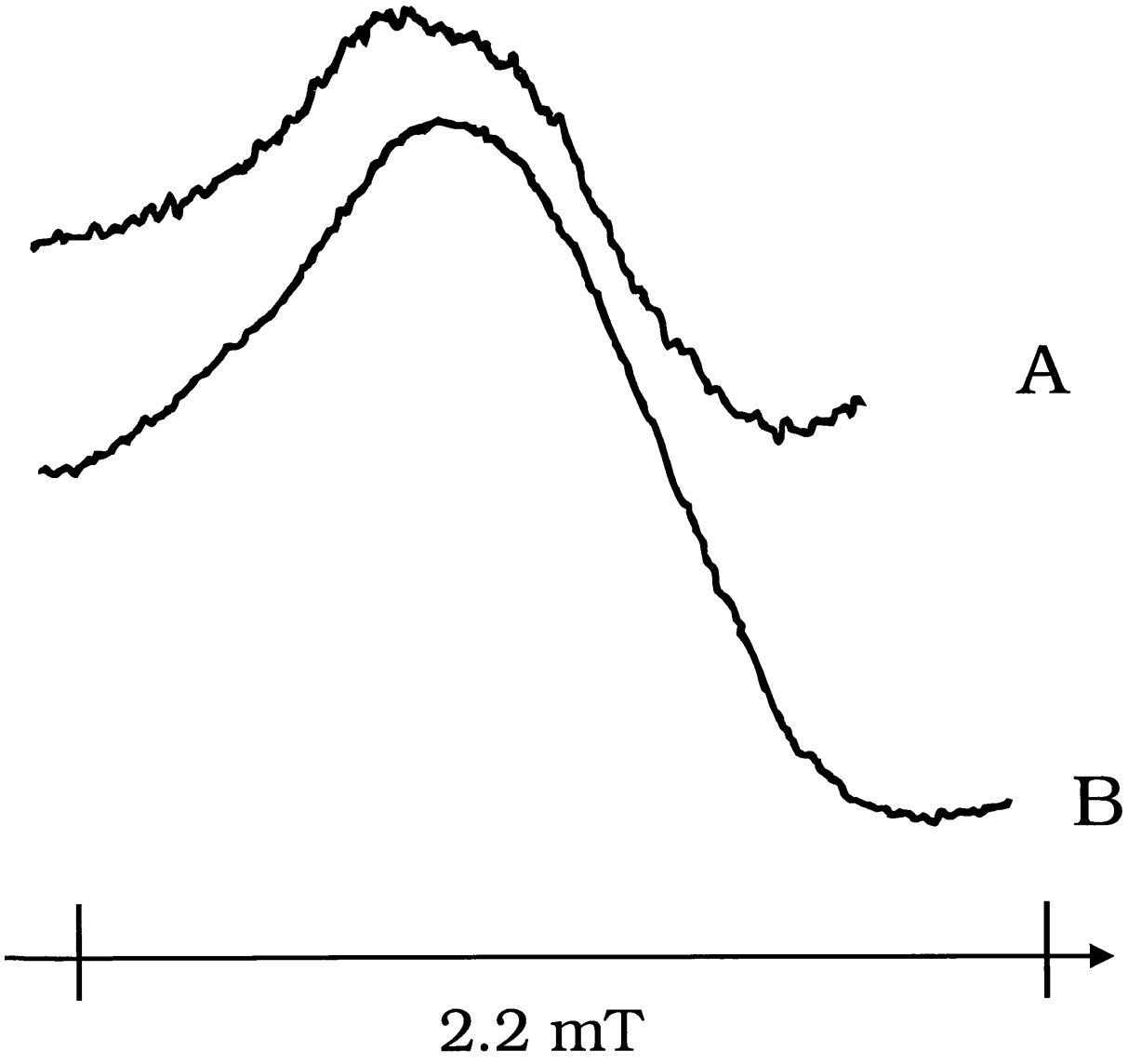

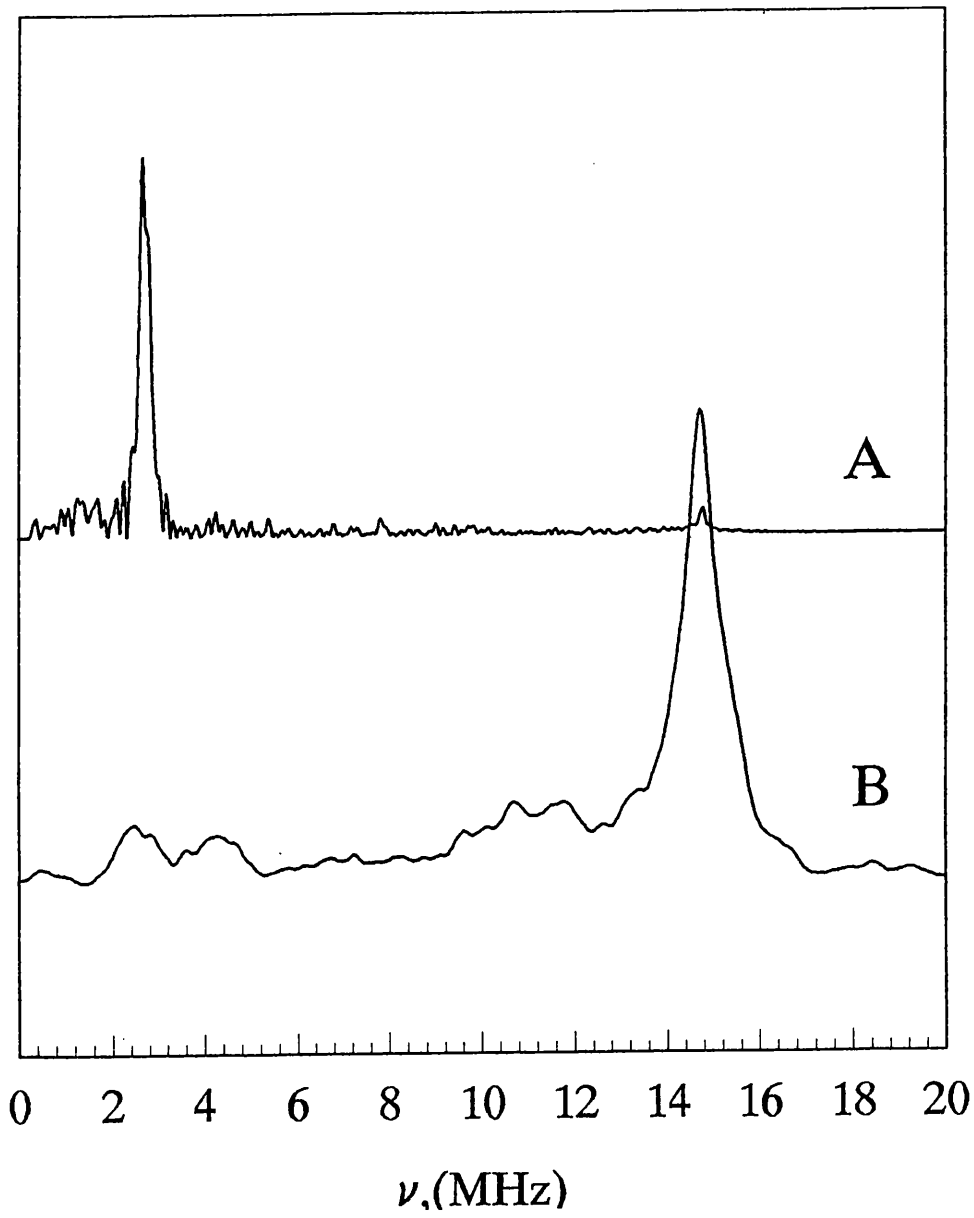

Figure 3.6 (A) The ESEEM spectrum of a mixed A_0/ A_1 signal in digitonin PSI particles (1.0 mg chlorophyll / ml) pH 10.0 illuminated at 230 K for 10 minutes.
(B) The ESEEM spectrum of A_1formed in digitonin PSI particles (1.0 mg chlorophyll / ml) pH 8.0 illuminated for 2 minutes at 205 K.
Pulse parameters : 1 sweep; 12 shots per loop; shot repetition time of 30.72 ms; pulse resolution in X of 2048 points.
Field parameters : field centred at 3464.0 G; sweep width of 0 G.
Frequency of microwaves - 9.716 GHz.

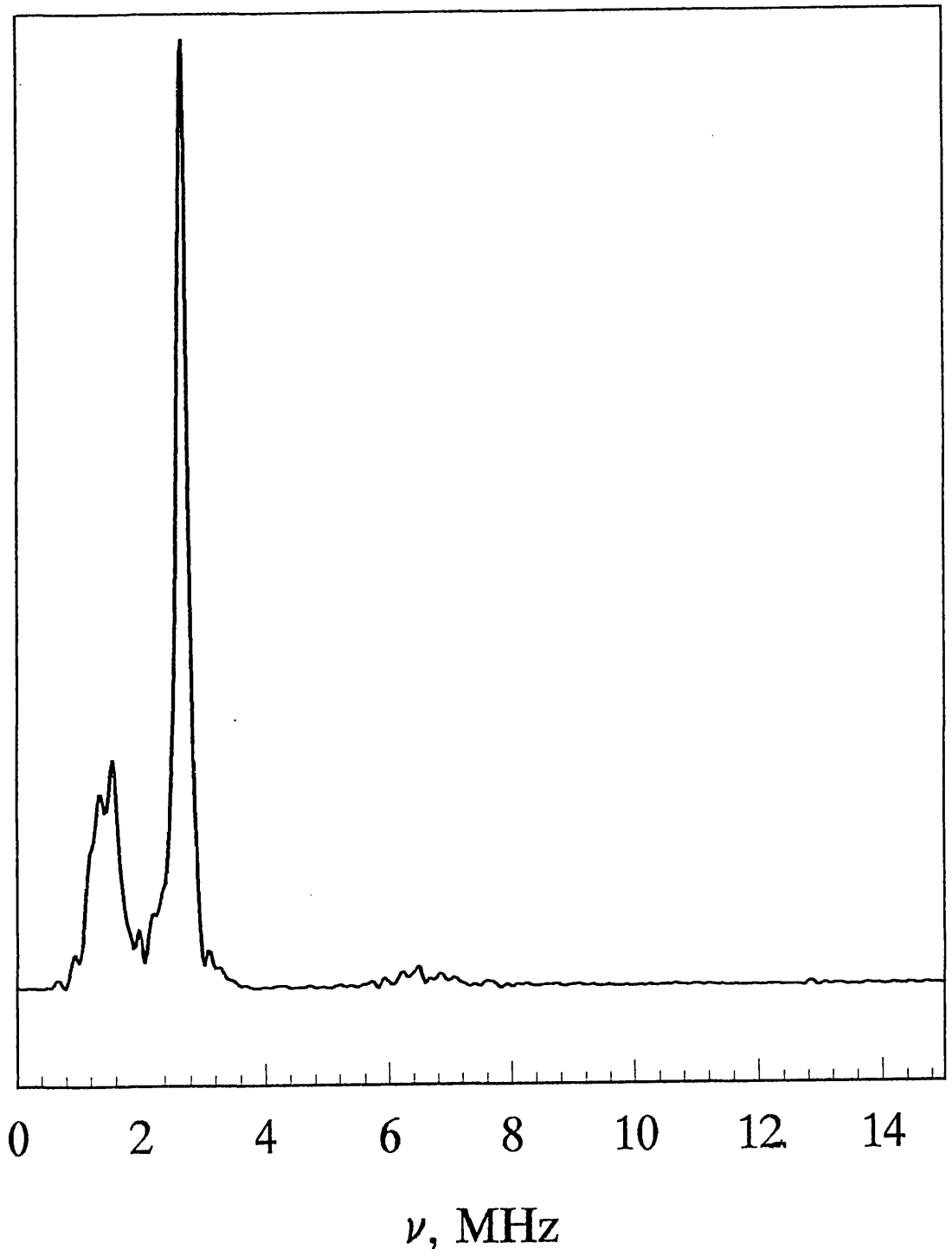

Figure 3.6 (c) One dimensional ESEEM spectrum of the A_0^- radical formed in digitonin PSI in which A_1 was double reduced by a 2 hour illumination at 4°C in the presence of sodium dithionite, pH 10.0. The A_0 spectrum was produced by a 20 minute illumination of the doubly reduced PSI sample at 230 K. Pulse parameters were the same as those used in (a) and (b).

Figure 3.7(a) shows the field swept spectrum for a digitonin PSI sample with its iron - sulphur clusters, Fe-S_{AB}, chemically prereduced and illuminated at 205 K so as to photoaccumulate A_1^{--} and Fe - S_X^{--}. A_1^{--} radical appears as a spike at g = 2. The Fe - S_{AB}^{--} signals cover that part of the spectrum that spans the magnetic frequency from 3500 gauss to 3760 gauss. The main peaks occur at g = 1.95 (Fe-S_A) and g = 1.90 (Fe-S_B). The Fe - S_X^{--} signal appears as a shoulder - like feature stretching from about 3755 gauss to about 4000 gauss. This feature has its point of inflection at g = 1.76.

Figure 3.7(b) is a derivatised version of the preceding spectrum, in which the data has been differentiated. This effectively generates the equivalent of a cw ESR spectrum. The FeS_X^{--} signal now appears as region of declining intensity, centring at about 3885 gauss (g = 1.76). This signal is noticeably weaker than its equivalent formed in the sodium dithionite reduced PSI samples frozen under illumination.

Figure 3.8 shows the field swept spectrum for $P700^+Fe\text{-}S_X^{--}$ formed by continuous illumination of the sample in the cavity at 8 K. The g = 2.0 signal is produced in low yield and this reflects the difficulty of light penetrating the sample in the cavity. The g = 2 radical signal decays as soon as the light is switched off. The spectrum is dominated by reduced iron - sulphur clusters, Fe - S_{AB}^{--}. The Fe - S_X^{--} signal is correspondingly weak.

Figure 3.9 shows the field swept spectrum for the charge pair $P700^+Fe\text{-}S_A^{--}$ produced in an ascorbate dark reduced digitonin PSI sample. The iron - sulphur region of the spectrum contains only the g = 1.95 resonance of reduced Fe-S_A.

3.4.4 ESEEM Spectroscopy of the P700 Cation.

Because there are other oxidisable chlorophylls bound to the PSI core the identity of the putative P700 cation in the $P700^+FeS_X^{--}$ samples was verified using ESEEM. The oxidised chlorophyll dimer, $P700^+$, gives a diagnostic one - dimensional ESEEM spectrum and the g

= 2 radical in these samples produced the spectrum that is expected for $P700^+$.

Figure 3.10(a) shows the 1D ESEEM spectrum for g = 2.0 signal observed in a putative $P700^+Fe\text{-}S_X^{--}$ sample, this signal is light induced and quickly decays away in the dark.

Figure 3.10(b) is the ESEEM spectrum of the P700 radical formed by illumination of ascorbate reduced PSI. This treatment results in an irreversible charge separation with the radical pair, $P700^+FeS_A^{--}$, formed. A much stronger echo is generated in this sample than in the former but the ESEEM spectra given by the g=2 radicals in both samples share almost every feature.

Figure 3.10(c) shows the 1D ESEEM spectrum for the cationic bulk chlorophyll monomer, Chl^+, prepared in PSII, for comparative purposes. The differences between this spectrum and the first two reflect differences in electron spin distribution between a chlorophyll dimer and monomer. Chl^+ was generated in Tris - washed PS2 by illumination in liquid nitrogen (77 K) with an unfiltered 300 Watt white light source (Rigby *et al*, 1994).

Table 3.2 presents the T_1 values for the g = 2 radical and the Fe - S_A^{--} in an ascorbate dark reduced PSI sample, containing the charge pair, $P700^+Fe\text{-}S_A^{--}$ over the temperature range 4 K to 14 K. It is not until the temperature is raised to around 10 K, that the Fe - S_A^{--} T_1s resemble those of the Fe - S_X^{--} at around 8 K.

In all cases the saturation recovery of the "enhanced" g = 2 radicals is found to be non exponential, indicating a dipolar interaction between the slow and fast relaxers in each case. This means that in principle the theory formulated by Hirsh *et al*, and used by them to determine the distance separating the tyrosine residue, Y_D^+, and the non - haem iron atom in PSII can be applied in this instance to calculate the distances between the iron - sulphur cluster, FeS_X, and the preceding acceptors.

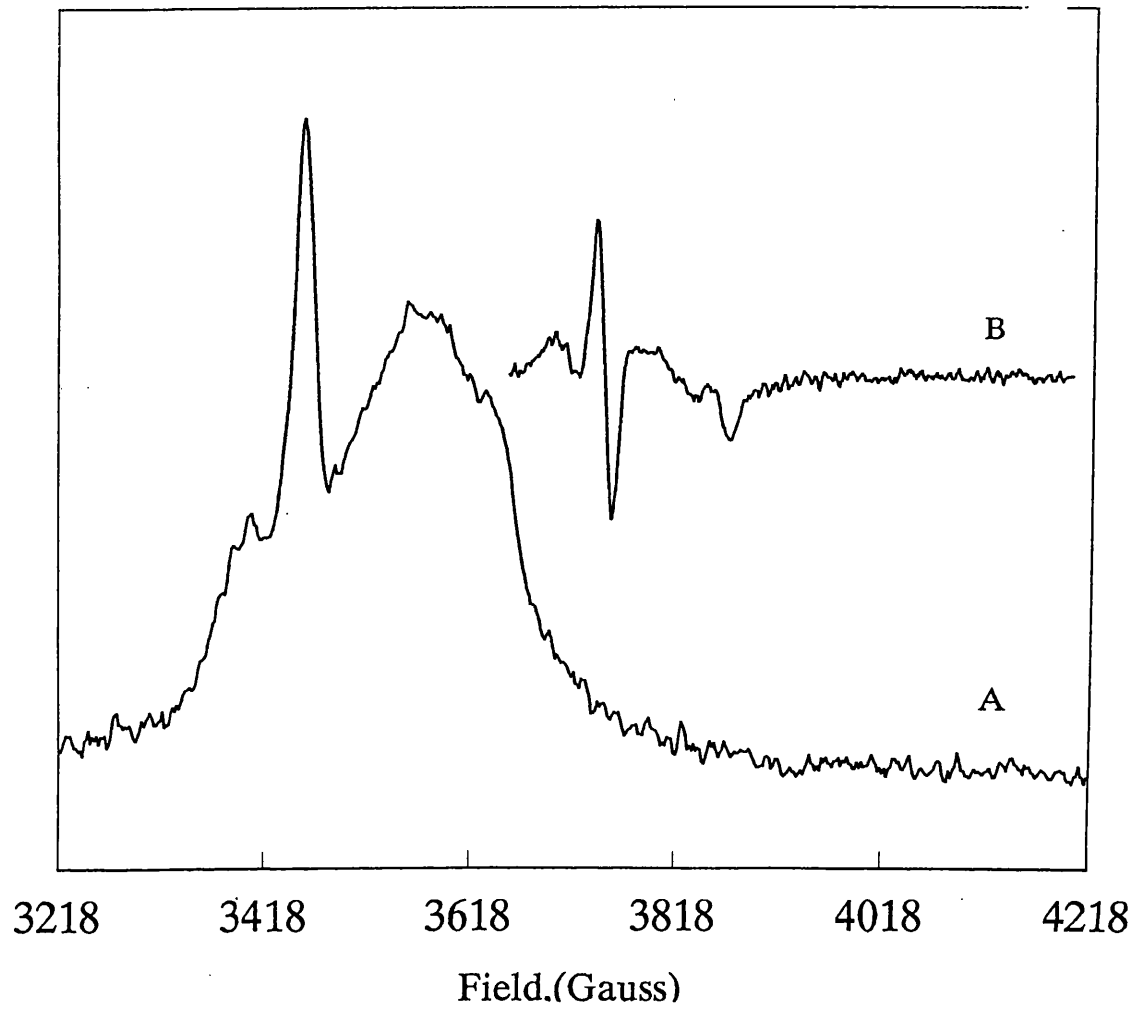

Figure 3.7(A) Field sweep of digitonin PSI sample that has been prereduced by dark incubation in presence of 0.2 % sodium dithionite and illuminated at 205 K for 2 minutes to form the A_1^- radical. (B) The same spectrum, on the same scale, that has been integrated. Pulse parameters : 16 sweeps per experiment; 4 shots per loop; shot repetition time of 102.4 ms. Field centred at 3718 G. Sweep width 1000 G. Microwave frequency 9.7053 GHz; microwave power 0.2μW.

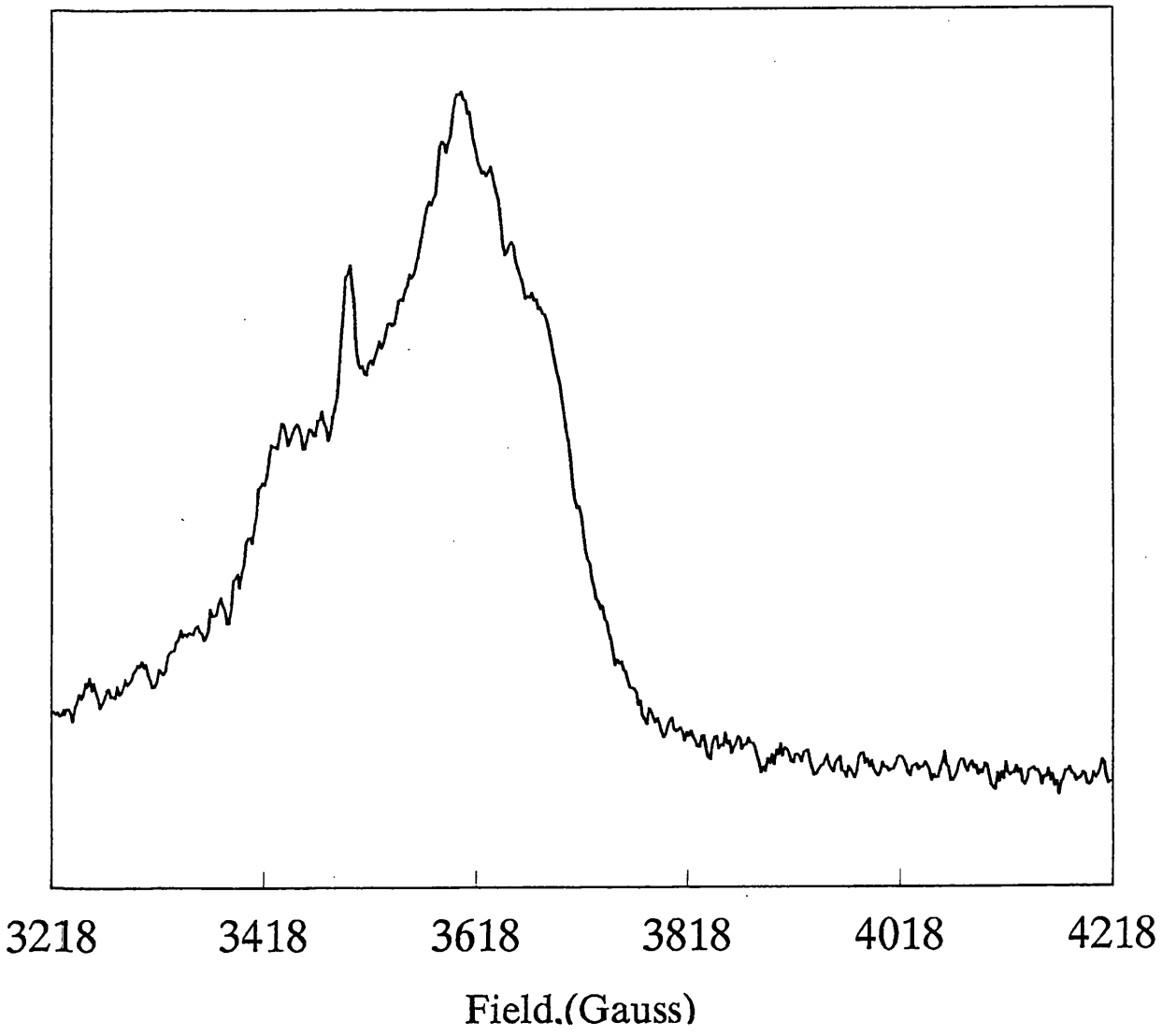

Figure3.8 Field sweep of Triton PSI sample prereduced by dark incubation in 0.2 % sodium dithionite and continuously illuminated in the instrument cavity at 8 K to form the radical pair, $P700^{+}FeS_{x}^{-}$. Pulse parameters : 100 sweeps per experiment; 4 shots per loop; shot repetition time of 51.2 ms. Field centred at 3718 G; sweep width of 1000 G. Microwave frequency of 9.18 GHz; microwave power of 0.2 μW.

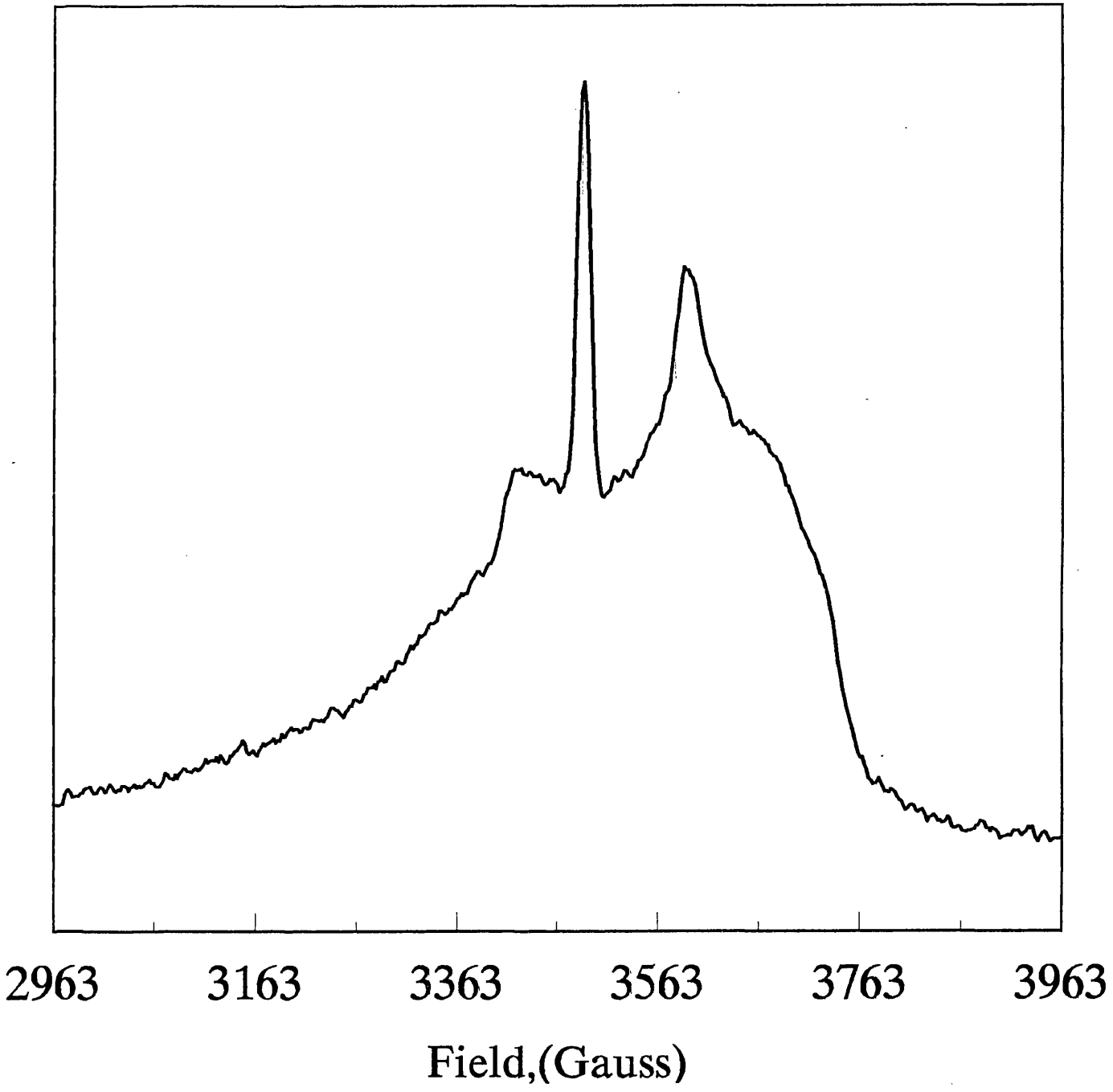

Figure 3.9 Field swept spectrum of ascorbate dark reduced PSI particles, illuminated at 77 K, to form the radical pair $P700^{+}FeS_{A}^{-}$. Pulse parameters as for figure 3.8.

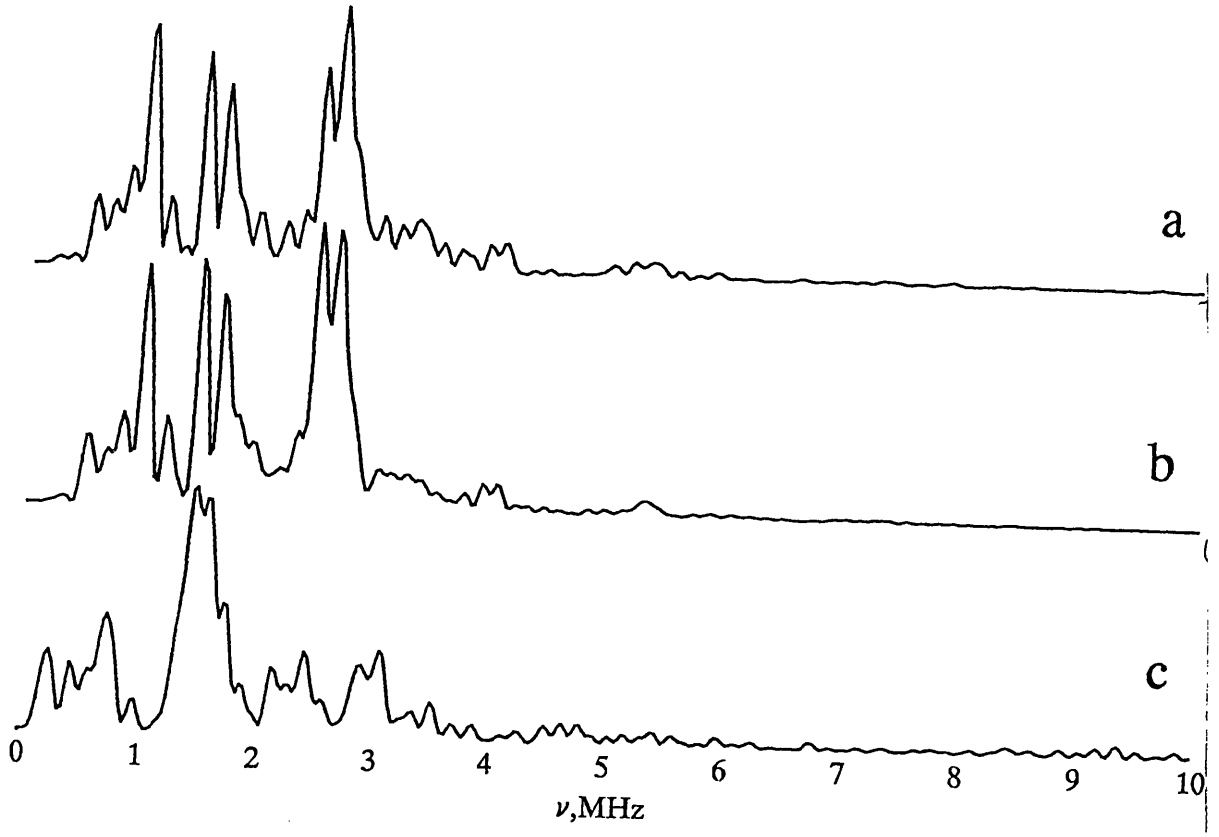

Figure 3.10. 3 pulse ESEEM spectra of chlorophyll cations : (A) Light - inducible, reversible $P700^+$ radical formed by illumination of dithionite dark reduced Triton PSI particles, pH8.0. Chlorophyll concentration 1.0 mg / ml. (B) $P700^+$ radical irreversibly formed in ascorbate reduced digitonin PSI particles by illumination in liquid nitrogen vapour. Chlorophyll concentration 1.0 mg / ml. (C) Bulk monomeric chlorophyll cation (Chl^+) formed in Tris - washed PSII reaction centres by illuminating at 77 K with an unfiltered 300 W white light source. Chlorophyll concentration ?mg / ml. The vertical scale of spectrum (A) has been compressed relative to that of (B) to make comparison easier.
Pulse parameters : 1 sweep per experiment; 6 shots per loop; shot repetition time of 30.72 ms; tau value of 112 ns. Field centred at 3463 G. Microwave frequency of 9.711 GHz.

Table 2.2

Temperature / K	T_1 of P700 radical/ms	T_1 of FeS_A^-/ ms
3.7	109.0	52.0
5.0	84.0	20.0
8.0	60.0	5.0
11.2	50.0	0.011
12.2	46.2	0.013
14.0	38.0	0.006

3.4 5 Saturation Recovery Measurements of the g=2.00 Radicals

The intrinsic spin lattice relaxation rates of each g = 2 radical signal were determined in PSI particles that have been depleted of all their fast relaxing species. The chaotrope urea was used as before to remove the iron - sulphur clusters, Fe - S_{ABX}.

Figures 3.11(a) - (f) compare the relaxation recovery curves of the different g = 2.00 radicals as measured in PSI particles at 8 K, in the presence and absence of the fast relaxing radical. The "unenhanced" data fits better to an exponential model of spin lattice relaxation, indicating the disruption of the dipole interaction caused by the removal of the fast relaxing species from the system.

Figures 3.12(a) and (b) show the cw ESR spectra of the A_1^{--} and A_0^{--} radicals respectively in digitonin PSI particles that have been depleted of all their iron - sulphur clusters. The spectra of the unenhanced g = 2 radicals retain similar linewidth and lineshape of their equivalents in intact PSI particles. From these results it is clear that the magnetic interaction between A_0^{--} and A_1^{--} and the reduced iron - sulphur cluster, FeS_X^{--} detected by means of pulsed saturation recovery measurements cannot be detected through linewidth changes observed using cw ESR spectroscopy. Our saturation recovery measurements indicate that both these radical species interact magnetically with FeS_X in contrast with Mansfield and Evans, 1988, who only observed an interaction with A_0.

Tables 3.3(i) and (ii) present the intrinsic and Fe - S_X^{--} - enhanced spin lattice relaxation rates (T_1) for the various g = 2.00 radicals at 8 K for digitonin and Triton X-100 PSI particles. In each case the T_1s resulting from crude and refined fits of the saturation recovery data are quoted. There are two omissions. Firstly there is no intrinsic T_1 for A_1^{--} in Triton X-100 PSI particles. This is because in Triton X-100 PSI samples which have been depleted of their iron - sulphur clusters, Fe-S_{ABX}, no A_1^{--} signal is formed - a broader

chlorophyll - type spectrum is detected in samples of this type when illuminated at 205 K. This observation supports the work of Golbeck *et al*, who found that the detergent, Triton X-100, extracted A_1 from PSI core particles depleted of the iron - sulphur cluster, Fe - S_X.

Secondly it was not possible to determine spin - lattice relaxation rates for the P700 cation, either intrinsic or enhanced, in digitonin PSI particles because the g = 2 radical was too weak for the extraction of a rate constant. This was the case even with extended scanning. The weak signal observed in these samples is not unexpected given the low P700 / chlorophyll ratio typically found in these preparations.

Intrinsic P700 T_1 measurements were carried out initially on Triton X-100 PSI particles in the absence of any exogenous reductant and unexpectedly short T_1s (in the 20 ms range) were obtained. Almost certainly this was due to the presence of plastocyanin not removed on the hydroxyapatite column during purification, and the oxidised copper ion residing in this metalloprotein will act as a fast relaxer. In order to avoid the problem of plastocyanin enhancement, the Digitonin PSI particles were first subjected to a brief treatment (10 minutes) in 3M urea to remove any residual plastocyanin and the saturation recovery measurements were then repeated and a long T_1 of about 90 ms was determined.

From the similarity of the A_0 radical T_1s in the digitonin and Triton X-100 PSI particles (which are reproducibly very close to each other and within error, identical in the two types of particle) we conclude that while the Triton X-100 particles are deficient in both stromal - and lumenal - side extrinsically bound peptides, they have not undergone any gross structural changes which would result in significant differences in the distances separating the acceptors. We have combined the relaxation rate data for the two types of PSI particle for the distance calculations.

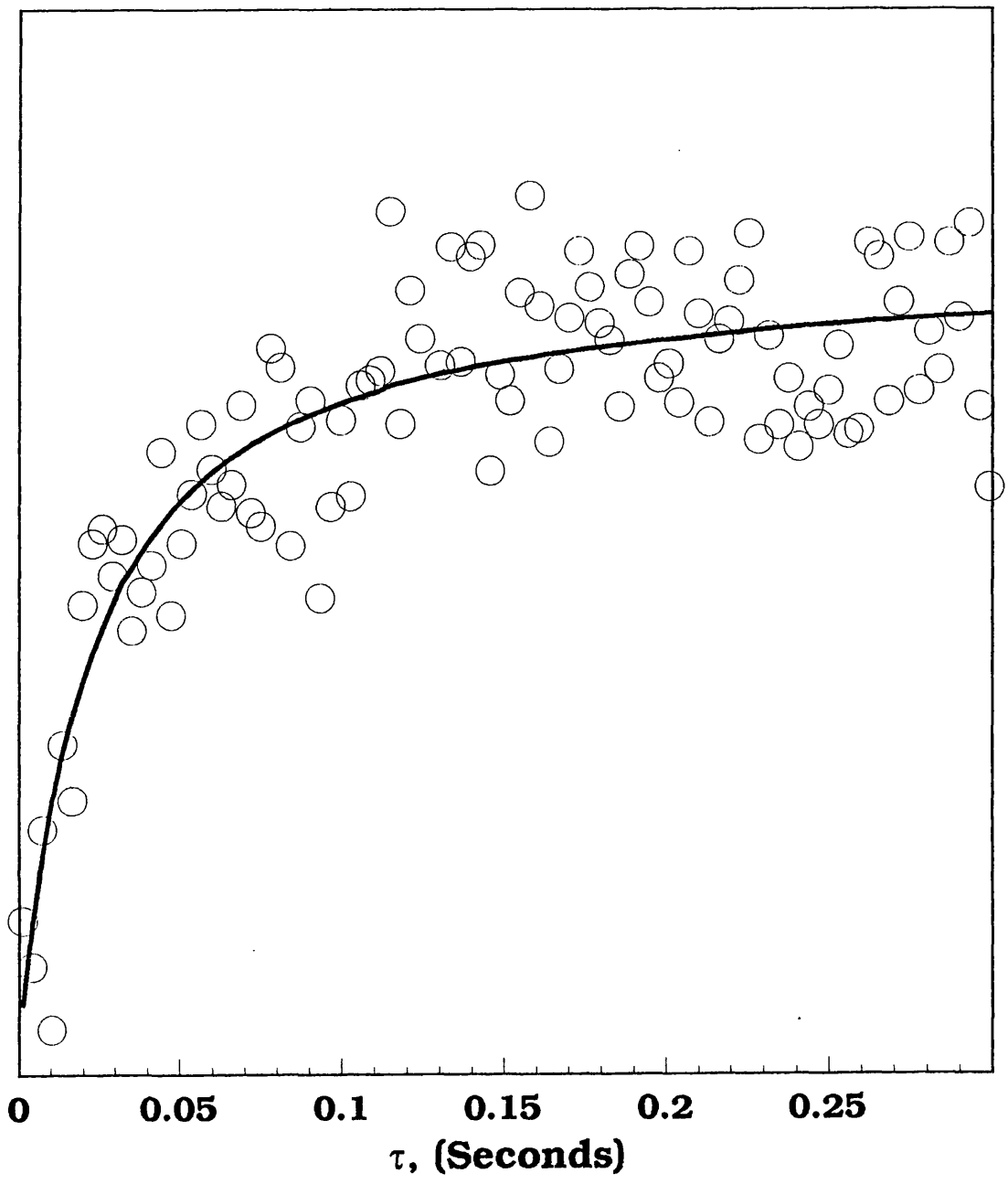

Figure 3.11a Saturation recovery curve of enhanced $P700^+$ radical, 8 K. Fitted to a multiexponential. $K_{1D}=50.128$. Standard deviation +/_ $12_{S^{-1}}$ s^{-1}

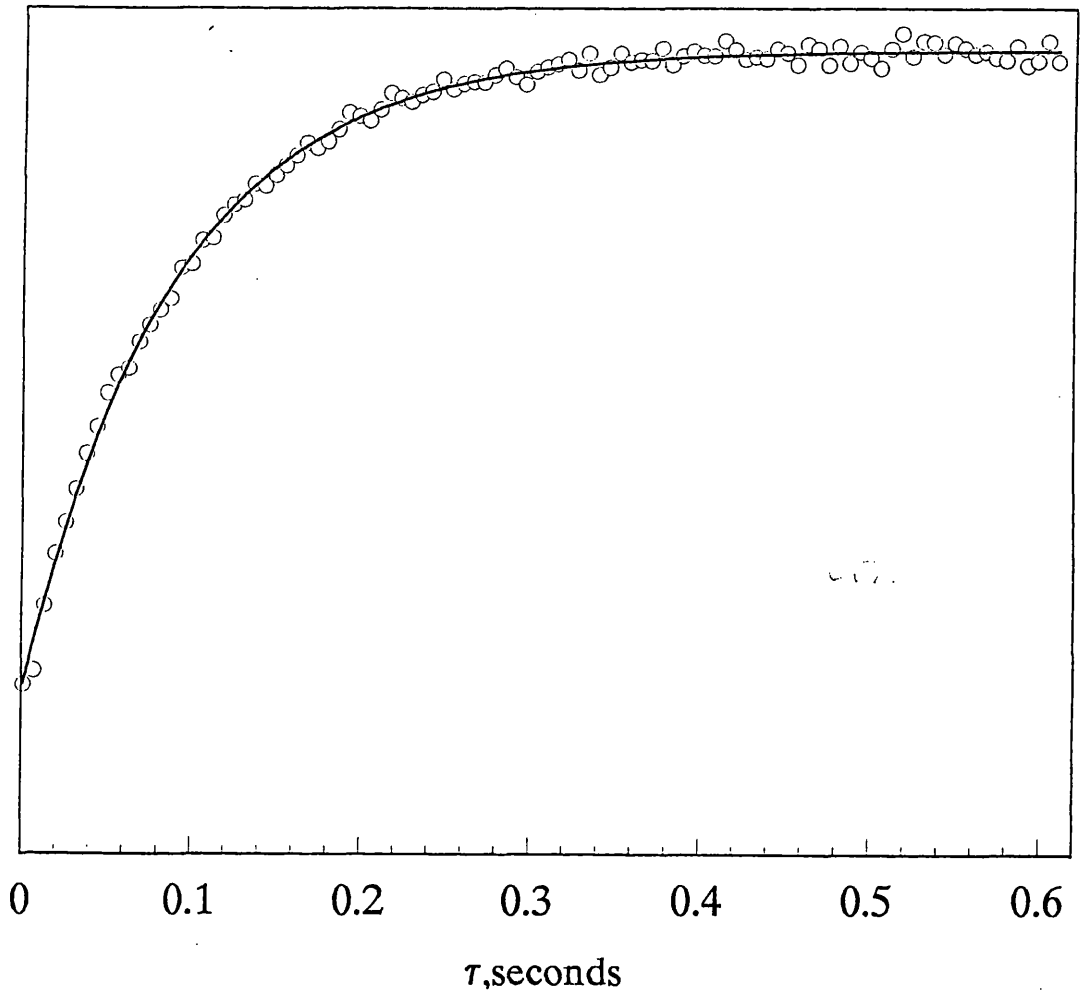

Figure3.11(b) Saturation recovery curve of the unenhanced $P700^+$, 8 K. Fitted to a single exponential. R1(rate constant)estimate=11.41. Standard deviation 0.13355 s^{-1}

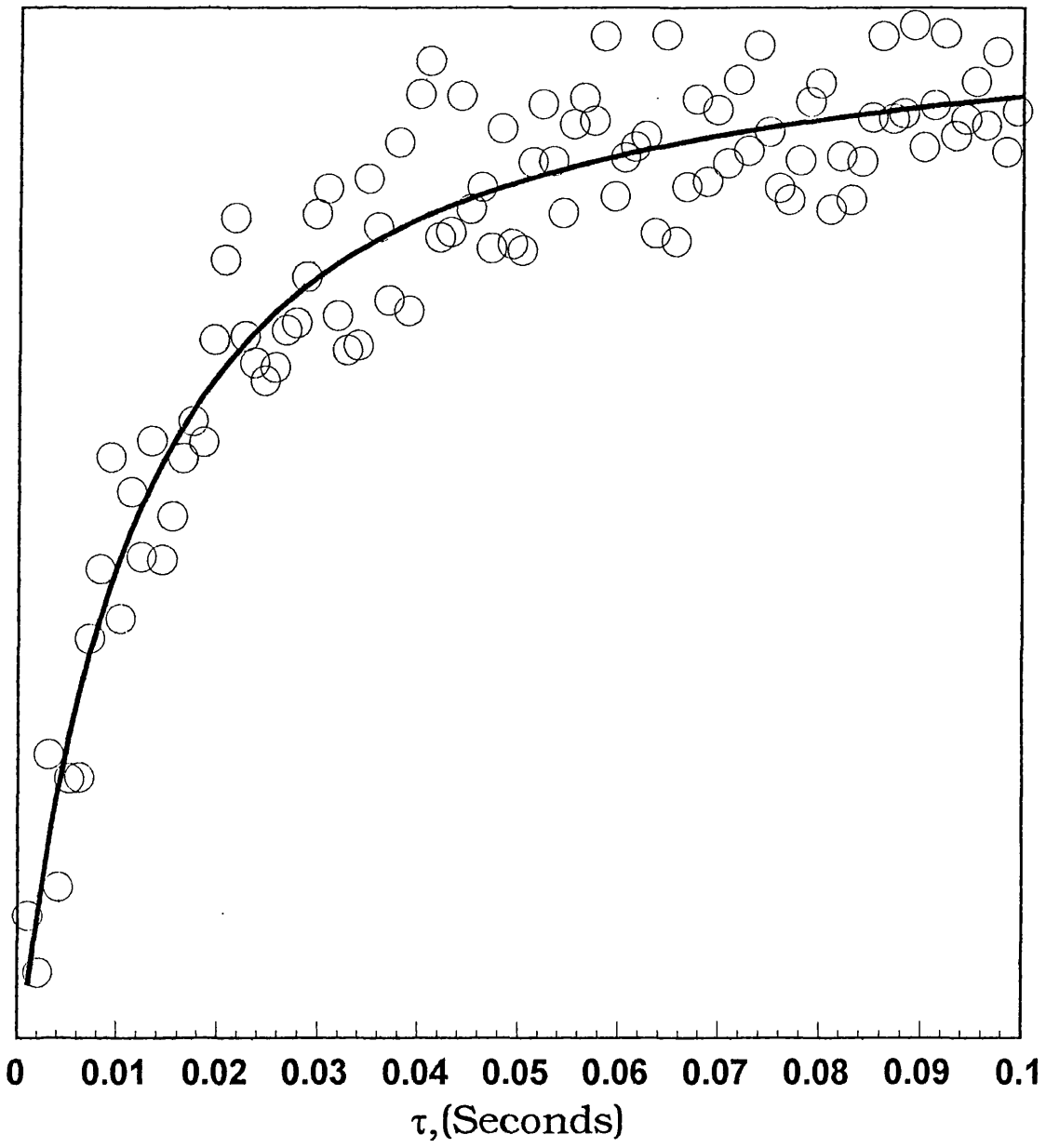

Figure 3.11(c) Saturation Recovery Curve of FeS_x- enhanced A_1 radical, 8 K, fitted to a multiexponential powder model. K_{ID}(dipolar rate constant) = 100.87. Standard Deviation of +/_ 13.6 s^{-1}

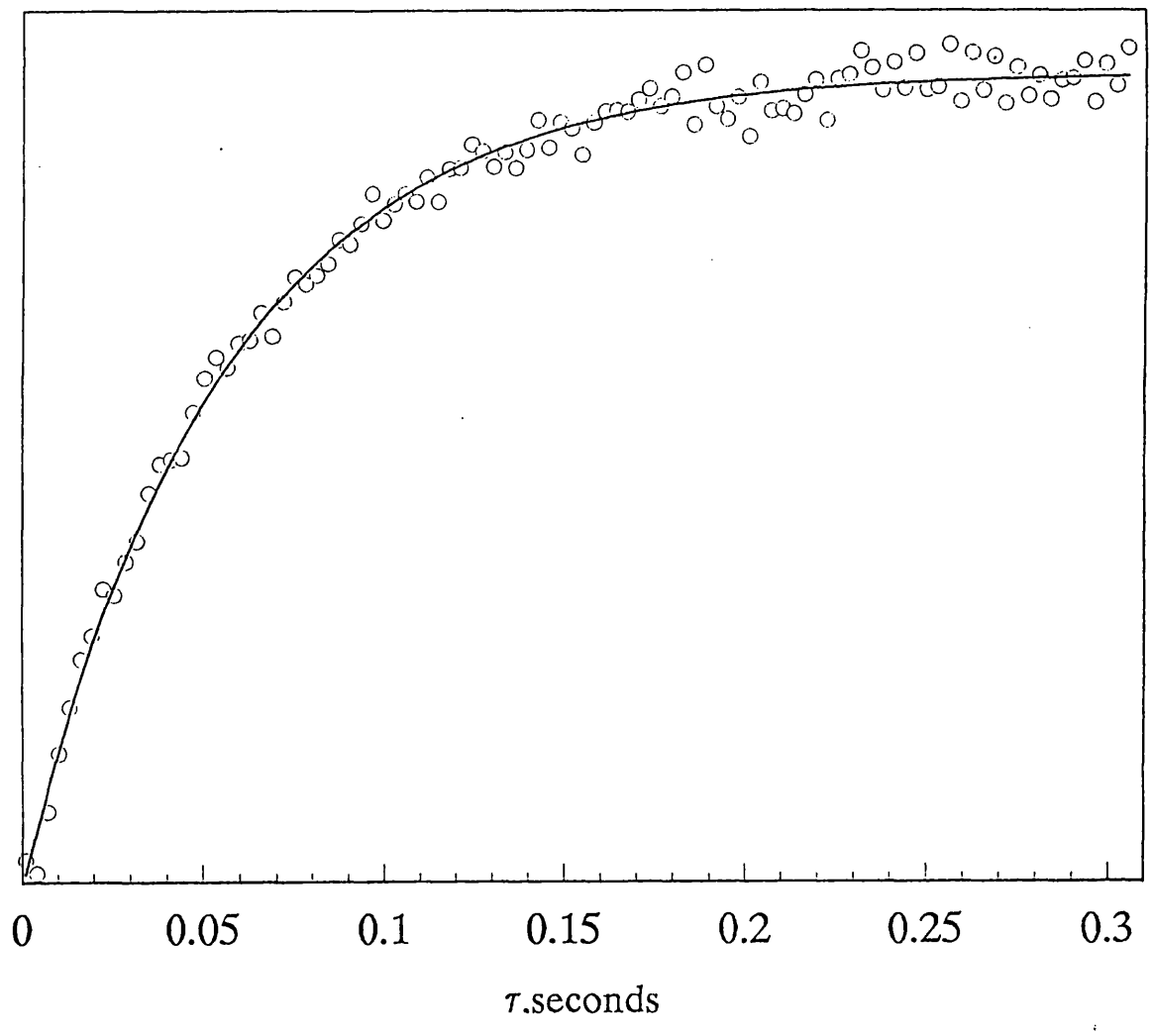

Figure 3.11(d) Saturation Recovery Curve of unenhanced A_1^- radical. 8 K. Fitted to single exponential. R1 estimate $= 18.092\ s^{-1}$. Standard deviation $0.367\ s^{-1}$

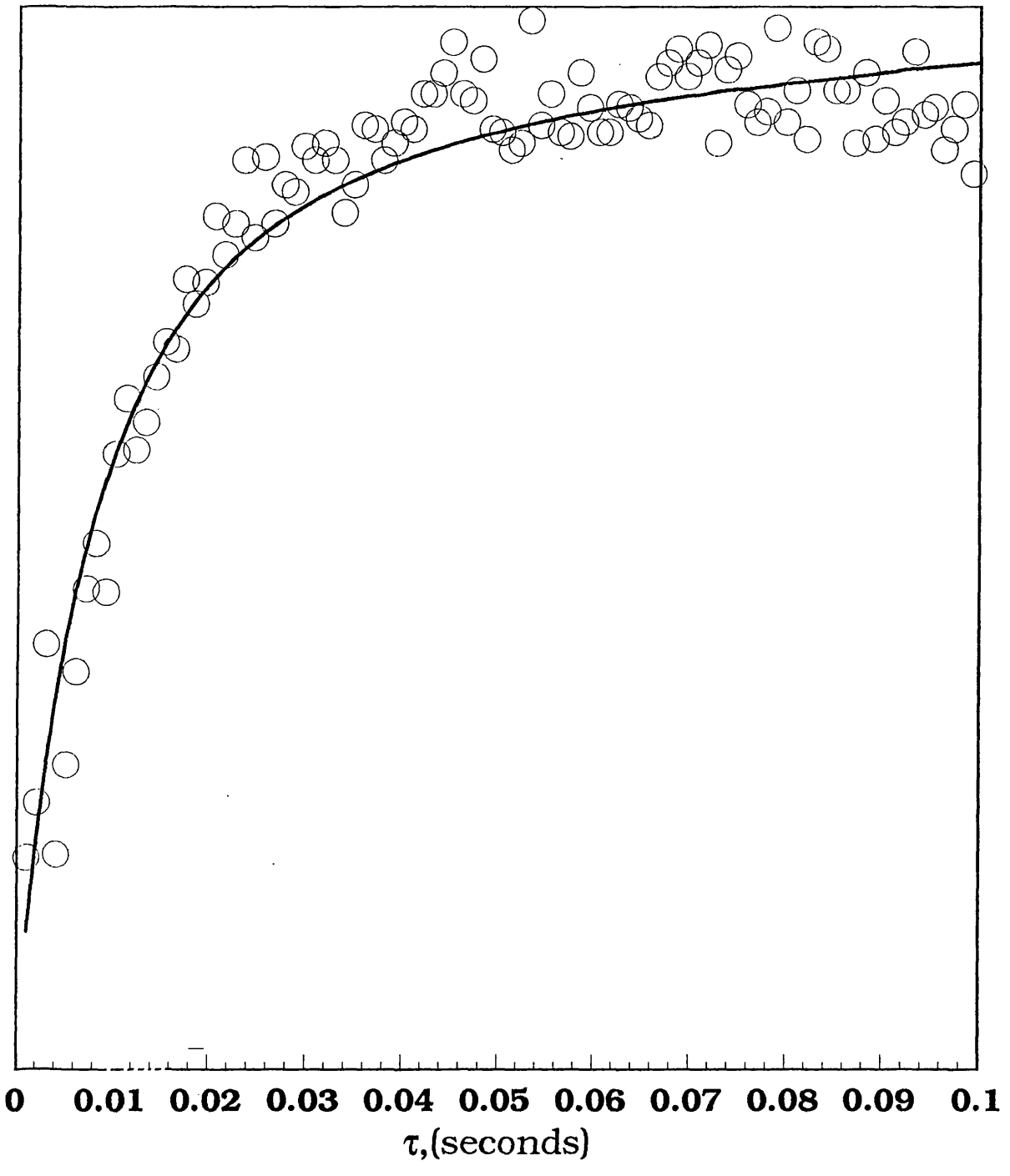

Figure 3.11(e) Saturation recovery curve of F_X- enhanced A_0^- radical. 8 K. Fitted to a multiexponential. $K_{1D}=143.73$. Standard deviation +/_ 18.98 s^{-1}

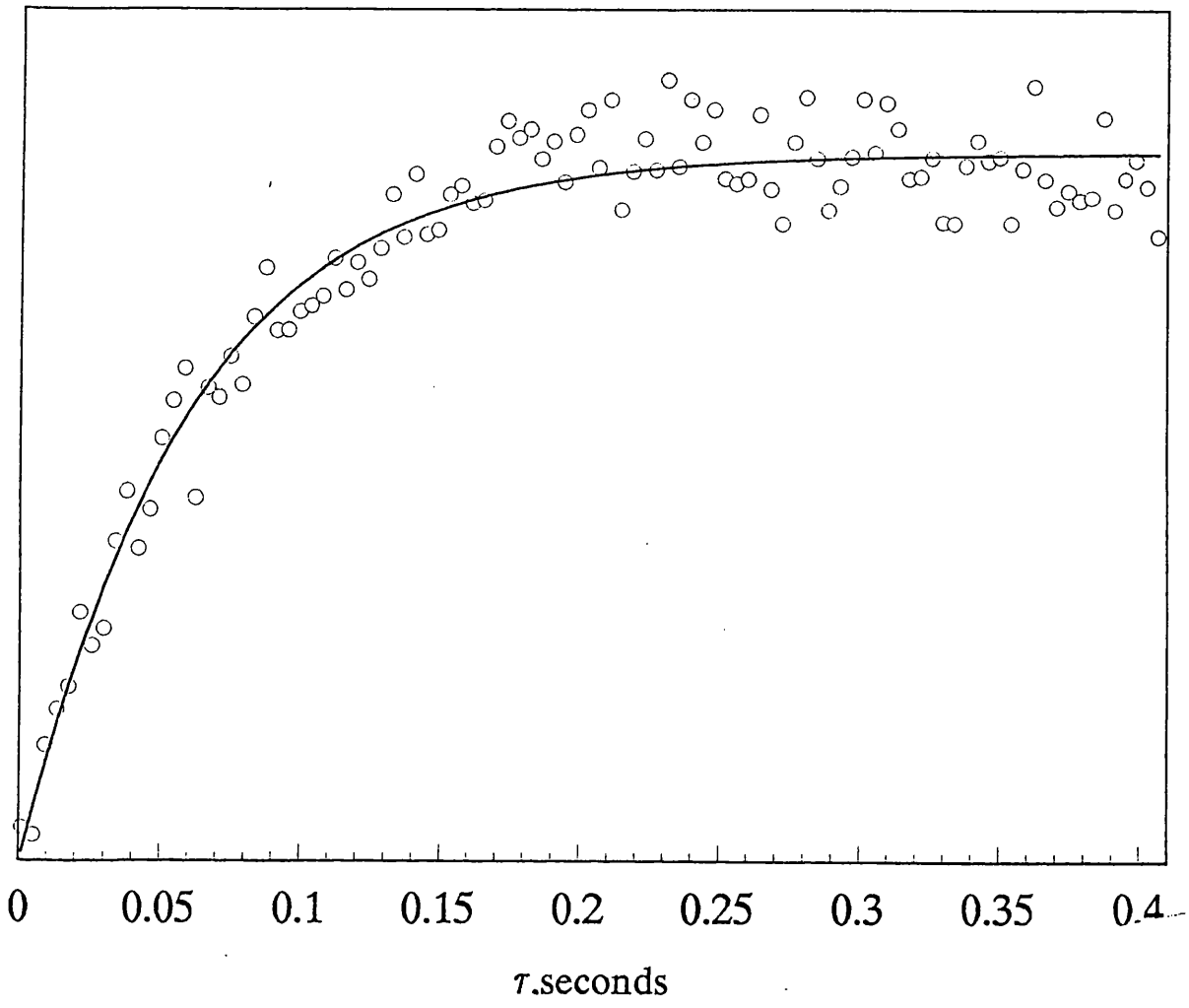

Figure 3.11(f) Saturation recovery curve of unenhanced A_0. 8 K. Fitted to a single exponential. R1=16.836. Standard deviation +/_ 0.367 s^{-1}

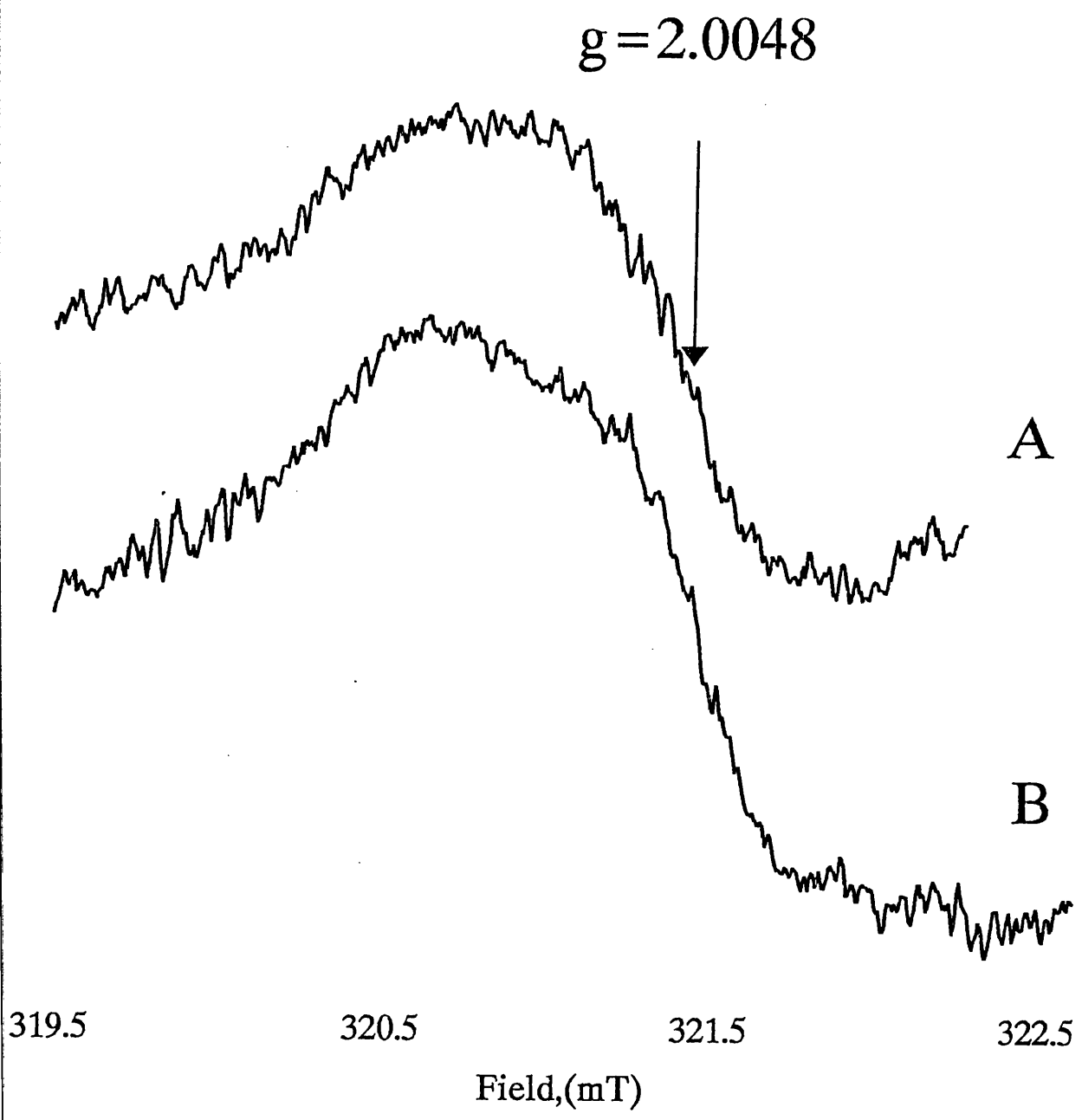

Figure 3.12 Cw ESR spectra of the (a) reduced A_1 and (b) reduced A_0 signals oserved in digitonin particles which have been depleted of all their iron - sulphur clusters. Sample concentration 1.0 mg / ml. Recording temperature : 77 K; microwave power : 5 μW; modulation width : 0.2 mT.

Table 3.3(i) Intrinsic and Enhanced Spin Lattice Relaxation Rates for Different g = 2.00 Radicals at 8 K.

RADICAL	T_1Enhanced/ms Triton particles (fitted to monoexpon.)	T_1 Intrinsic/ms Triton particles	T_1Enhanced/ms Digitonin (fitted to monoexp.)	T_1Intrinsic/ms Digitonin
A_0	12.9	64.0	14.6	63.0
A_1	19.1		16.3	64.3
P700	36.5	89.2		

Table 3.3(ii)

RADICAL	Enhanced T_1/ms Fitted to multiexponential	Intrinsic T_1/ms
A_0	7.0 ms +/_ 1ms	63 ms +/_ 3ms
A_1	9.4 ms +/_1ms	64 ms +/_ 2ms
P700	20ms+/_4ms	85 ms +/_2ms

3.4.6 Power Saturation Measurements on the Iron - Sulphur Cluster, FeS_X at 8 K.

Figure 3.13 shows a graph plotting the log of FeS_X signal intensity against the log of microwave power, based on power saturation measurements made at 8 K. The point of intersection gives the value of $P^{1/2}$, in this case 50 mW. The fact that at 8 K the FeS_X signal is saturated at a microwave power of 50 mW suggests that it is relaxing at an unusually fast rate, compared to other iron sulphur clusters.

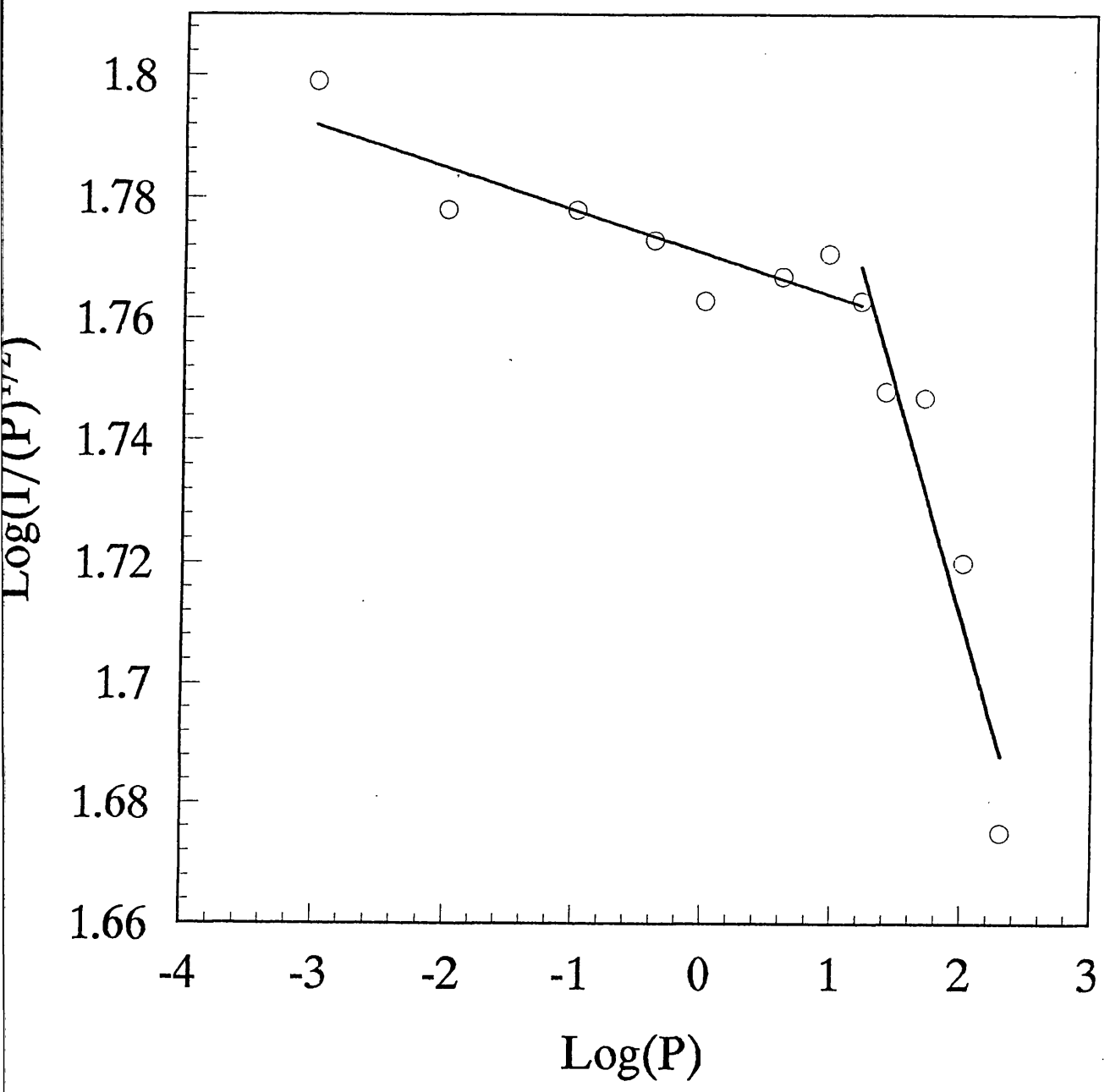

Figure 3.13

Plot of log of microwave powers against log of FeS_X intensity from power saturation measurements made at 8 K.

3.5 Discussion.

The cw ESR spectra of the radicals A_1 and A_0 both in the presence and absence of the fast relaxing iron - sulphur cluster radical, Fe-S_X^{-}, display linewidths of about 0.8 mT and 1.3 mT respectively. Extraction of the fast relaxing component from the centres has no significant effect on the linewidth of the g = 2 radical signal. This indicates that there is no exchange coupling mechanism operating between A_1 or A_0 and Fe-S_X, if there was, a significant broadening of the g = 2 radical signals would be expected in either or both cases and this is not observed. The possibility of exchange coupling was proposed on the strength of observations made by Mansfield and Evans[1988] that in digitonin but not Triton X-100 PSI particles, a decrease in the intensity of the Fe - S_X^{-} spectrum was observed when A_0, but not A_1,was reduced, indicating that there is an interaction A_0 and Fe-S_X but not between A_1 and Fe-S_X from which it was inferred that A_0 is closer to Fe-S_X than A_1. However we could not reproduce this result in digitonin PSI. The signal attributed to A_1 in that paper may have actually been a mixture of A_1 and A_0 if illuminations were carried out at pH 10.0. Secondly, it was not then known that there were two A_1s and two A_0s per P700, a detail which complicates the interpretation. In some digitonin preparations we observed a "cycling" effect in which the intensity of the Fe-S_X^{-} spectrum alternately increased and decreased with succesive short illuminations at 205K. However the effect could not be consistently reproduced and we were not able to provide a coherent explanation for it.

The T_1 measurements we have presented here show that Fe-S_X^{-} is interacting with A_1 and A_0 in both digitonin and Triton X-100 PSI particles. Assuming the major factor in determining the strength of interaction to be the distance between interacting radicals , and not say the chemical nature of the radical species, we can make qualitative deductions about

the relative distances separating Fe-S_X and the preceding redox components. With an estimated value for spin - lattice relaxation transient of the Fe-S_X and an appropriate value for the magnetic dipole constant, it is possible to calculate values for these distances in Å.

At temperatures below 8 K we were not able to obtain a reliable data for both enhanced and intrinsic g=2 radical T_1s, the intrinsic saturation recovery rates were too long to accurately determine. Secondly at lower temperatures, the spin - lattice relaxation rate of the iron sulphur cluster, FeS_X is in the μs time domain and we were not confident that this was fast enough to exert a full enhancement effect on the slower relaxing species. At 8 K we know the spin lattice relaxation rate of this cluster occurs on the ns time scale. At 8 K we could reproducibly obtain saturation recovery data sets for both enhanced and unenhanced g=2 radicals, which enabled us to determine enhanced and intrinsic spin lattice relaxation rates for the chlorin and quinone radicals. However by approximating the unenhanced T_1, it was found that the same relatavistic trend was preserved, with the acceptors arranged in order of decreasing enhancement by Fe-S_X^{--} : $A_0 > A_1 > P700$. Our saturation recovery data from Triton preparations supports the inference of Evans and Mansfield that A_0 is somewhat closer than A_1 to Fe-S_X but our measurements indicate that both interact with the fast relaxing paramagnet, the strength of interaction being about two - fold stronger in the case of A_0. Nor do we find that these interactions are disrupted in Triton X-100 PSI particles.

It could be argued that the relaxation enhancement of the quinone and chlorophyll radicals is due not only to the presence of Fe-S_X but also to the iron sulphur clusters, Fe-S_{AB}, which are reduced in all the samples examined. However it is unlikely that at 8 K (and below) that these clusters are contributing significantly to relaxation enhancement. Saturation recovery measurements made at temperatures between 3.7 K and 15 K show that at 8 K Fe-S_A is relaxing at the fast end of the ms time scale at 8 K the Fe-S_X cluster will be relaxing

very much faster (with a T_1 of ns). In the same preparation, at 8 K the $P700^+$ radical is relaxing far more slowly than the g =2 radical in a sample containing Fe-S_X^{--} . A T_1 at the fast end of the μs range for Fe-S_A^{--} is not reached until the cavity temperature is raised to around 14 K. At this temperature the $P700^+$radical T_1 is 38 ms, comparable to the $P700^+$ T_1 at 8K in the presence of Fe-S_X^{--} . With increasing temperatures the spin-lattice relaxation rates of the iron - sulphur clusters will become increasingly fast but not indefinitely so, at some point the T_1s of the three iron - sulphur clusters will plateau but in the temperature range relevant to this study Fe-S_X is relaxing very much faster than Fe-S_{AB}. This coupled with the fact that from the low resolution crystal structure it is known that the clusters, Fe-S_{AB} are about 12 to 15 Å further away from the other acceptors than is Fe-S_X considerably diminishes its effect as a relaxation enhancer. At 8 K it is almost certainly not relaxing rapidly enough to act as a significant enhancer.

Without carrying out any calculations a model of a PSI reaction centre can be constructed on the basis of a qualitative interpretation of the data. The intrinsic spin - lattice relaxation rates of the g=2 radicals were enhanced eight fold in the case of A_0, six fold in the case of A_1(the degree of enhancement of the quinone radical is lessened slightly if the Triton X-100 PSI data is taken) and four fold for P700. Given the error margin of a few milliseconds for the enhanced T_1 data the degree of enhancement for A_1 and A_0 could easily be of a very similar magnitude. This technique does not provide insights into the actual spatial location of acceptors but about the linear distances (relative or absolute) that separate two redox components. However saturation recovery data combined with information about the probable positions of transmembrane α-helices thought to contain ligands binding the molecules involved in light driven charge separation in PSI makes it possible for us to make certain inferences about the relative arrangement of the acceptors. A schematic of the structure

inferred by our measurements is given in figure 3.14 alongside the 6 Å crystal structure and structures derived from photovoltage and bioluminescence techniques.

Judging from relative differences in the degree of enhancement alone a model is

Figure 3.14

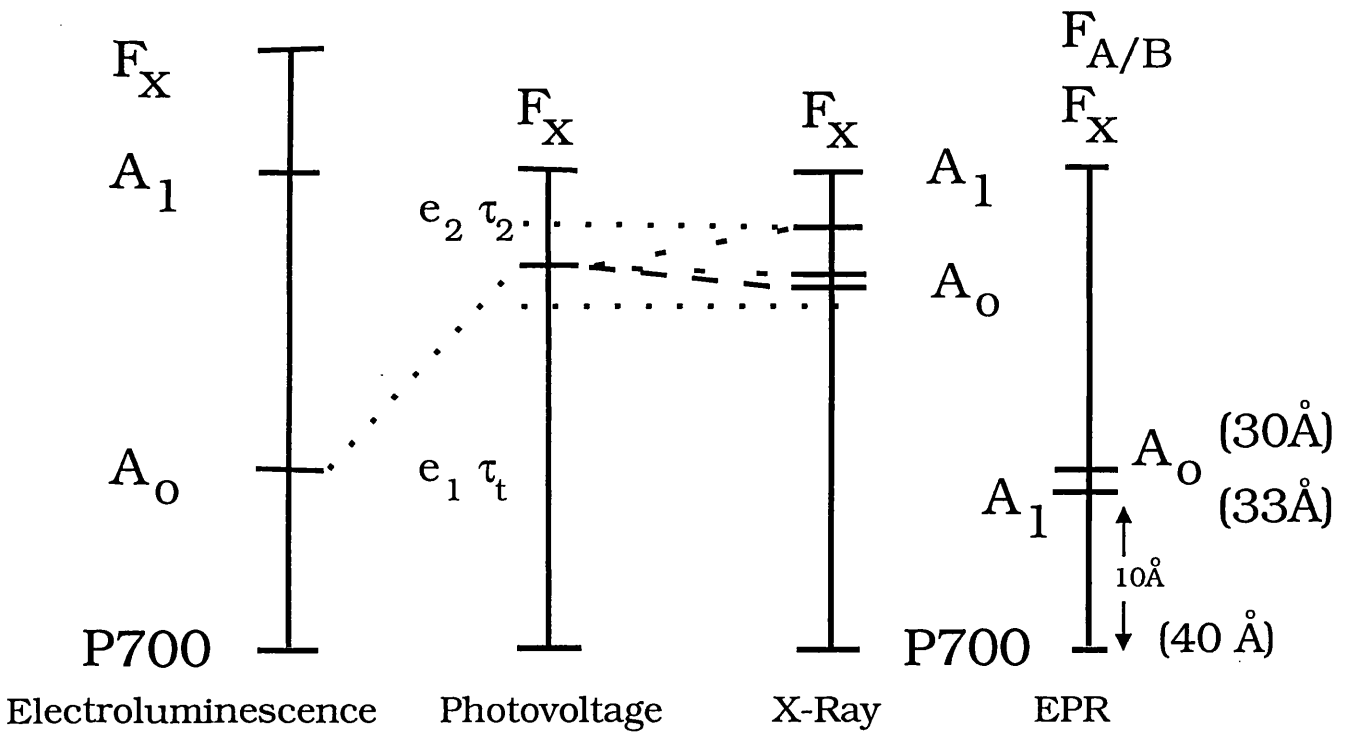

Figure 3.14 presents a schematic comparing the proportions of photosystem I as suggested by four different techniques used for probing structure, including the saturation recovery method. The redox components are arranged along straight lines so that the relative distances separating them can be clearly indicated, not because the techniques support a linear arrangement of the electron carriers *in vivo*. For the EPR (saturation recovery) model, the distances given in parentheses are those that were directly determined. The distance between P700 and A_1 and A_0 is inferred from these determinations.

suggested in which A_1 and A_0 are about equidistant from the iron - sulphur cluster, FeS_X, with if anything A_0 being slightly closer to this cluster, and the primary donor, P700, being further away from the cluster, FeS_X, than A_1. Of the non - crystalline structures the one which ours most resembles is the photovoltage model of Hecks *et al*, 1994, which in turn agrees reasonably well with the low resolution crystal structure. In this work they used picosecond photovoltage and fluorescence measurements to determine transfer rates and the relative dielectrically weighted transmembrane distances. Theirs resembles very closely the preliminary crystal structure. They find that the A_0 -- A_1 pair spans only about 20 % of the P700 -- A_1 distance. A qualitative interpretation of our data also suggests both A_0 and A_1 being separated from the iron - sulphur cluster, Fe-S_X, by a similar distance. However our data suggests that A_0 and A_1 are closer together than in either the emerging crystal structure or photovoltage model, with if anything A_1 somewhat further away from Fe-S_X than A_0 although within the error margin of the measurements these two acceptors could easily be equidistant from Fe-S_X.

Such a qualitative interpretation of the saturation recovery data does not take into account that the magnetic interaction between the slow and fast relaxing species has an r^6 dependency(r being the distance between two interacting paramagnets), as has been formulated by Hirsh *et al.* The saturation recovery method provides an opportunity to quantitate the distances between the acceptors. In order to calculate distances it is necessary to have a spin lattice relaxation rate for the fast relaxing paramagnetic species. As has already been discussed we were not able to directly measure the spin lattice relaxation rate of the iron - sulphur cluster at 8K when it relaxing rapidly enough to profoundly enhance the relaxation rate of the chlorin or quinone radical. This is due to an instrumental limitation. The instrument uses a T_2 (spin - spin coupled relaxation) detection system and spin - spin

relaxation rates are always considerably faster than spin-lattice relaxation rates at the same temperature. This means that at 8 K intensity corresponding to the iron - sulphur cluster, FeS_X^-, is no longer detectable in the field swept spectrum of the sample. As it is through the field sweep that the T_1 of a radical species is "accessed"it is no longer possible to carry out spin - lattice saturation recovery measurements on this iron - sulphur cluster. Nor does significantly increasing the sample concentration surmount this problem. The same measurements were carried out on a sample with a concentration of 5 mg chlorophyll / ml. Although the initial FeS_X signal was stronger in this sample, when the cavity temperature was raised to 8 K the FeS_X intensity had almost completely faded from the field sweep and saturation recovery measurements made at the FeS_X field position gave spurious results. Probably what was being measured in this instance was some slower relaxing underlying component. For this reason we have to use an estimated value for the T_1 of the iron - sulphur cluster based on the resolution limit of the instrument's detection system. Power saturation measurements can be used to obtain estimates of the relaxation rate of FeS_X but the resulting value is a mixture of T_1 and T_2 parameters. A tau value (interval between the first and second microwave pulses) of less than 112 ns was used in some of these saturation recovery experiments and so we know that the spin - spin coupled relaxation rate of FeS_X is considerably less than 112 ns and this provides a rough lower limit for the value of spin lattice relaxation transient (T_1). In the calculations a value for the T_1 of FeS_X of 50 ns has been used. This is similar to the estimated $T_1$of the non - haem iron atom used by Hirsh *et al* in their distance determination work.

The rearranged formula used in the calculation of distances is given below:

$$r^6 = \gamma s^2 \mu f^2 \,/\, \omega_s \, k_{1D} T_{1f}$$

γ_s is the magnetogyric ratio of the slow relaxing species which is identical to the γ_e , the

magnetogyric ratio of the unpaired electron which in SI units is : - 8.79 x 10^{-10} s.A.Kg^{-1}. μ_f is the magnetic dipole moment of iron (II), which is given by Hirsh as 5.35 Bohr magnetons which when converted into standard units is : -5.59 x 10^{-58} m^6 Kg / As^2. The top term of this equation when multiplied out gives 5.43 x 10^{-57} m^6. ω_s is the Larmour frequency of the slow relaxing species which expressed in SI units 9.05 x 10^9 s^{-1}. The value of k_{1D} is derived by fitting the spin lattice saturation recovery curve of the enhanced slow relaxing radical. T_{1f} is the spin lattice relaxation transient of the fast relaxing species.

Calculations using a 50 ns estimate (that used for the non haem iron by Hirsh *et al*) for the T_1 of FeS_X yield distances of 35Å between P700 and FeS_X, and from 29 to 31 Å between A_1/ A_0 and Fe-S_X. The first of these distances is in broad agreement with the 6 Å crystal structure. A distance of 35 Å between these two centres would mean that P700 and the intrinsically bound iron sulphur cluster are positioned about as far apart as is physically possible on opposing sides of the thylakoid membrane. These distances must be regarded as estimates. For greater accuracy a directly measured value for the spin lattice relaxation transient of the iron sulphur cluster would be required. If the distances that we have calculated are accurate they would indicate that the quinone and chlorin acceptors are about two times further away from the iron sulphur cluster, Fe-S_X than has so far been envisaged. It is quite possible that 50 ns is an underestimation of the spin lattice relaxation transient of the iron sulphur cluster and that its relaxation rate is an order of magnitude slower. The calculations were repeated using estimated values for the spin lattice relaxation transient of FeS_X of 100ns and 1000ns. The 100 ns rate is an approximate value of the spin - spin relaxation rate of FeS_X at 8 K and can be used as a lower limit for the value of this radical's spin lattice relaxation transient. Using a T_{1f} of 100 ns in the calcultions yield a P700 - FeS_X distance of 32 Å, and an A_1/ A_0 - FeS_X distance of 27 to 28 Å. Using a T_{1f} of 1000 ns gives the following

distances : P700 - FeS_X - 22 Å, A_1 / A_0 - FeS_X - 18 to 19 Å.

We have used another method of estimating the spin lattice relaxation of FeS_X. Bertrand *et al*, 1988, have measured changes in the half -height linewidth of the FeS_X signal at temperatures higher than 10 K. They make use of the relationship between the T_1 of the iron sulphur cluster and the linewidth of its ESR signal to estimate the spin lattice relaxation rates for this cluster at temperatures above 10 K. We have extrapolated this data to obtain a T_1 estimate for FeS_X at 8 K. This assumes that the mechanism of relaxation is the same at temperatures lower than 10 K. If this assumption is correct the spin lattice relaxation rate for FeS_X could be as fast as 5 - 10 ns. If the calculations are repeated using a fast T_1 of 10 ns a P700-FeS_X distance of 46 Å, and a A_1/A_0 - FeS_X distance of 38-41 Å are obtained. The most interesting feature of these calculated distances is the distance that they imply could separate P700 and the primary acceptor. They could be as little as 3 to 6 Å apart, which is some 5 to 10 Å shorter than the equivalent distance proposed by the other structures, with the possible exception of the bioluminescence model which places A_0 closer to P700 than do the photovoltage model and the preliminary crystal structure. It should be emphasised that the technique used here permits the calculation of vector distances separating FeS_X and the preceding acceptors and not actual distances between the preceding electron acceptors themselves. On the strength of these calculations P700 and A_0 could be greater than 6 Å apart, however our calculations would tend to favour a model in which P700 and A_0 are located close to one another.

We could not directly measure the spin - lattice relaxation rate of FeS_X at 8 K but from the saturation recovery measurements made of the T_1s and T_2s of FeS_X up to 8 K, we are confident that the spin lattice relaxation rate of FeS_X lies somewhere between 10 to 1000 ns. For this reason we cannot calculate definitive distances, but rather present a range within

which the actual distances lie.

The arrangement of the acceptors suggested by our data, i.e. in which the relative distance between the primary donor and A_0 / A_1 is 25 to 30 % of that between the primary donor and Fe-S_X , can be reconciled with kinetic data indicating that transfer between P700 and primary/secondary acceptors occurs in pico- or even femtoseconds and transfer from A_1 to Fe-S_X takes place in nanoseconds. However the distances obtained by this method are probably not directly comparable with those determined by X-ray crystallography. The distances determined in the latter case are centre to centre distances between regions of electron density. In the case of relaxation enhancement, the interaction is between the edges of electron clouds and so this technique results in edge to edge distances which are shorter than their crystallographic equivalents. Taking this into account, our distance estimates suggest the distance between the primary donor and A_0 / A_1 is significantly shorter than that between A_0 / A_1 and the iron - sulphur cluster, FeS_X. This arrangement is different to that presented in the 6 Å crystal stucture and the photovoltage model in which the spacing between the various acceptors is almost equal, with 12 to 15 Å separating P700, A_0 / A_1, FeS_X, and FeS_{AB}. In fact the crystal structure suggests that P700 could be as much as 20 Å away from the primary acceptor, which seems unlikely given the fast electron transfer rate that has been determined for the P700 ->A_0 reaction.

One other variable term of interest in the formula used for distance calculations is μ, the magnetic dipole moment. The value of this term will differ from one system to another. The magnetic dipole moment for the iron - sulphur cluster has not been determined to our knowledge and so in the calculations we have used the magnetic dipole moment of the non - haem iron which has a +2 oxidation state, whereas FeS_X is 4 Fe 4 S iron sulphur cluster consisting of both iron (II) and iron (III) ions. We would expect there to be a difference in

the value of this term between the two species but because of its weighting in the formula it is unlikely to have a significant effect on the result of the calculations.

Our distance measurements are most easily reconciled with the electron taking a zig - zag and not a linear path through the electron transport chain with A_1 positioned off the straight line. Figure 3.15 shows a schematic of a model whose proportions are inferred by saturation recovery measurements, a range of smallest possible distances between the acceptors (calculated using different fast T_1s) is quoted. In a branched arrangement it is possible for A_1 to be located a similar distance away from the primary donor, P700, and still act as the secondary acceptor. There is some kinetics data to support the existence of a zig zag electron pathway. Optical measurements made by Warden, 1990, determine that the iron - sulphur cluster radical, $Fe\text{-}S_X^{-}$, has a rise time of 5 ns. This could imply an alternative path from P700 to $Fe\text{-}S_X$ for the electron in which A_1 is by - passed. Our kinetics measurements made using a magnetic resonance technique clearly demonstrate that there is electron transfer between A_1 and FeS_X. However such measurements give no indication of what proportion of the electrons follow this path and the possibility of other pathways cannot be discounted. The low resolution crystal struture also presents a non - linear arrangement of acceptors, with A_0 and A_1 positioned on either side of the linear path between P700 and $Fe\text{-}S_X$. However this part of the structure must be treated with caution for while chlorophyll molecules, with ring diameter of about 10 Å can be visualised at this resolution, any proposed location for the considerably smaller phylloquine molecule must be regarded as very speculative.

A non - linear organisation of the acceptors would also be more compatible with the low - temperature by - pass of A_1 which is observed when the latter has been extracted or double reduced, suggesting that A_1 is not absolutely essential for photoreduction of the iron - sulphur clusters and that under certain conditions alternative routes are used by the electron.

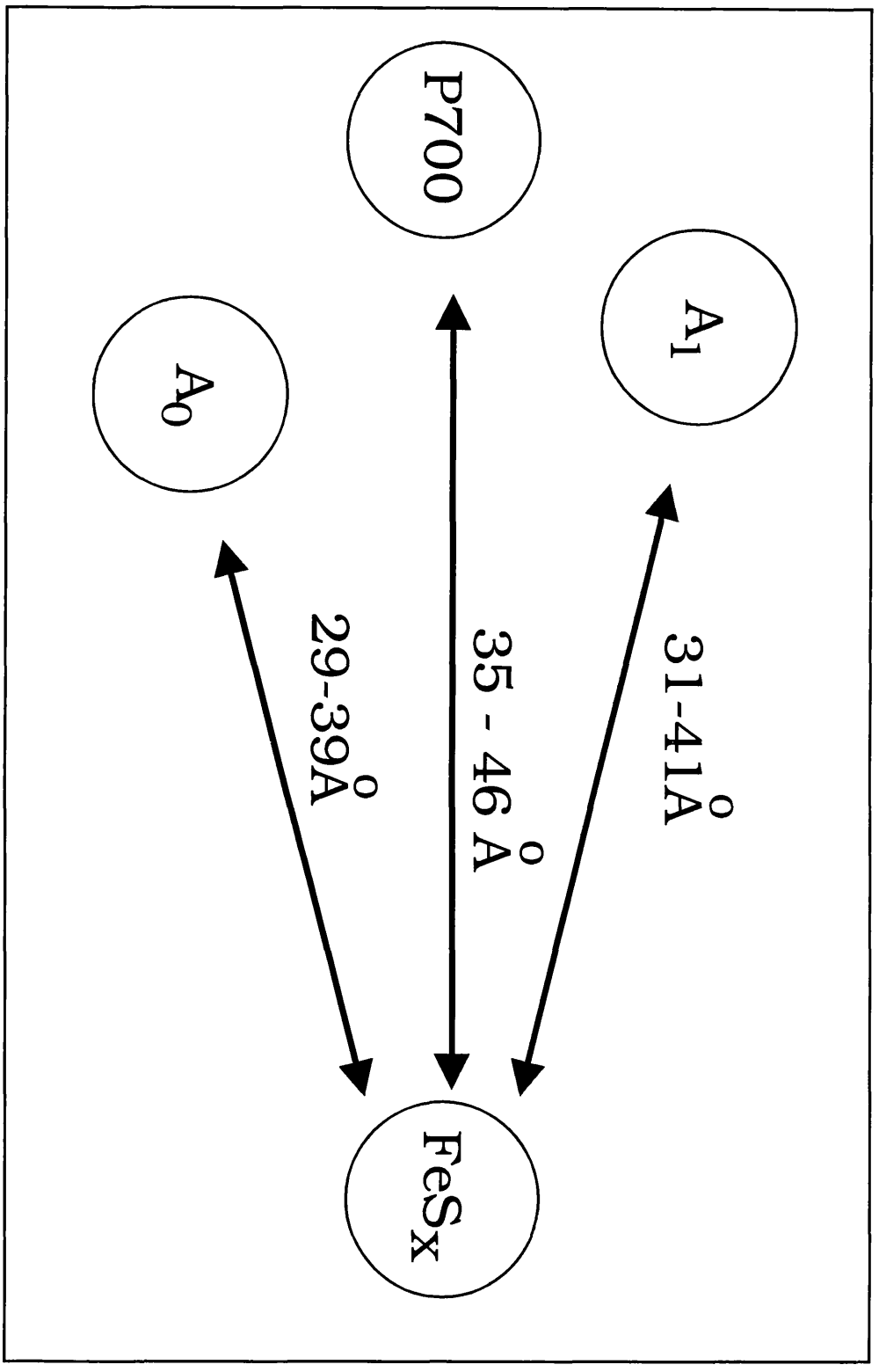

Figure 3.15

Range of distances calculated to separate the three g = 2.00 radicals from the iron - sulphur cluster, Fe - S_X.

Various functions have been proposed for A_1 in the event that it is not absolutely essential for forward electron transfer to the iron - sulphur clusters, such as roles in protection against photoinhibition by acting as an energy sink and in cyclic electron transport.

The pathways may have different activation energies with one path being favoured over the other under different conditions - this may permit some flexibility when the plant is exposed to more adverse conditions for example.

It has been argued that it is not A_0 but one of the accessory chlorophylls known to be bound to the Psa A and Psa B polypeptides that is reduced in photoaccumulation experiments. It is not possible to distinguish these two species spectroscopically, as both would be anionic chlorophyll monomers. However it is generally thought that if it is an accessory chlorophyll that is being reduced it is one which is located a similar distance from P700 as A_0 and therefore any distance information obtained about one would also apply to the other.

The model of PSI presented by Vos and Van Gorkom is based on a mathematical model of the effects of applying an electric field on the recombination rates of the charge pairs formed during the electrogenic steps of electron transfer in PSI. They compared the model to simulated results and to actual experimental results. Electroluminescence is the luminescence released by chlorophylls as a result of electric field induced charge recombination. By measuring the decay rates of the bioluminescence released it was possible for these workers to determine the relative contributions of each charge pair to the stabilisation process. They conclude that this process consists of at least three electrogenic steps : P700 to A_0, A_0 to A_1 and $A_1$to F_A. According to their measurements the first step takes up 30 % of the membrane, the second 50 % and the third 20 %. Given that the crystal structure indicates a distance of 12 - 15 Å between Fe-S_X and Fe-S_{AB} their model does not have sufficient room to accommodate Fe-S_X. These workers refer to kinetics data (Trisl *et al*,

1987) which found that there is no electrogenic step occurring within the time range 50 ps to 50 ns and that electrogenic transfer occrs within 50 ps. A rise time of $A_1$of about 50 ps has been determined and a rate of 200 ns has been determined for transfer from A_1 to Fe-S_X. However the relatively long distance (about 20Å) between A_0 and A_1 and the relatively short distance between A_1 and Fe-S_X that the electroluminescence model implies would fit better with the reverse of this kinetics data. These workers assume the $P700^+FeS_A^-$ spans the whole of the thylakoid membrane that would mean that according to their model there is about 12 Å between P700 and A_0 which is similar to the distance between these two acceptors in the model that we propose. This model from the bioluminescence work may arise from misassignment of the electrogenic steps or difficulties in relating luminescence decay rates to the structural properties of the system.

Our relaxation data suggests that A_1 in Triton PSI may be closer to the fast relaxer than A_1 in Digitonin PSI possibly because of some Triton - induced disruption of structure. Secondly we were unable to obtain an unenhanced T_1 for A_1 in Triton PSI particles - the "A_1"signal formed in Triton PSI depleted of all its iron - sulphur clusters gave a cw ESR spectrum that was broad and chlorophyll - like and an ESEEM spectrum containing a significant amount of nitrogen resonance. Because of this we are unable to establish the degree to which A_1 relaxation is enhanced in Triton PSI particles.

Using this method of studying structure it should be possible to obtain estimates of the distances that separate functional components. One difficulty is the exposure of the radical under study to other fast relaxing species which in the case of PSI are ferredoxin and plastocyanin. Ferredoxin is a two iron - two sulphur cluster which spectrally and in terms of relaxation properties resembles Fe-S_{AB}more than Fe-S_X, will be reduced by incubation with sodium dithionite but is located even further out on the stromal side of the thylakoid

membrane than is PsaC, the peptide binding the iron - sulphur clusters, Fe-S_{AB}. Thus its contribution to relaxation enhancement at 8K is likely to be insignificant. Also much of this peptide is removed on the hydroxyapatite column and so is present in reduced amounts in Triton PSI. Levels of plastocyanin are also reduced in Triton particles and in the presence of a powerful reductant like sodium dithionite the plastocyanin copper is reduced to a diamagnetic redox state. The other possible source of relaxation enhancement is the potassium ferricyanide used to oxidise the sulphide ions of the Fe-S_X. This could possibly have the effect of giving misleadingly fast intrinsic T_1 s. However the addition of the iron chelator, tiron, and the subsequent removal of the iron - chelator complex should eliminate this possible source of error.

In summary the results presented here suggest that in the PSI reaction centre the primary donor P700 is very close to the primary acceptor, A_0 . The range of estimated distances between these components that we propose (3 - 6 Å) agrees quite well with experimental work relating distance to rates of electron transfer (Moser *et al*, 1992). In this work, for an edge to edge distance of 6 Å , a transfer rate in the ps time domain or faster would be expected. Kinetics measurements carried out by Hastings *et al*, 1994, suggest a ps transfer rate for P700 ->A_0 reaction. Flash absorbance measurements (Heathcote *et al*, unpublished) yield a transfer rate of less than a picosecond.

Secondly our results suggest a relatively large distance separates the chlorin / quinone acceptors from FeS_X. This also agrees with kinetic data, indicating transfer rates betweeen these components to be in the ns time domain.

Because the paramagnetic species being studied in the saturation recovery experiments have been formed through photoaccumulation they are by definition competent in electron

transfer, the distance information yielded here should therefore apply to redox active species. Such information is complementary to crystallographic data which gives the precise locations of components but gives no indication as to whether or not such components participate in photochemistry.

Andersen, B., Koch, B., Scheller, H.V., Okkels, J.S. and Moller, B.L., 1990. Current Research in Photosynthesis, Volume 2, 671 - 674, Kluwer, Dordrecht.

Anderson, S.L., and M^{c}Intosh, L., 1991. J.Bacteriol. 173, 2761 - 2767.

Arnon, D.I., 1949. Plant Physiol. 24, 1 - 15.

Arnon, D.L., Whatley, F.R., and Allen, M.B., 1954. J. Amer. Chem. Soc. 76, 6324 - 25.

Arnon, D.L., Whatley, F.R., and Allen, M.B., 1955. Biochim. Biophys. Acta, 16, 607 - 8.

Astashkin, A.V., Kodera, Y., and Kwamon, A., 1994. Biochim. Biophys. Acta, 1187, 89 - 93.

Barber, J., 1988. Similarities and Differences Between PS2 and Purple Bacterial Reaction Centres. In "Light Energy", 178 - 96.

Barry, B.A., Bender, C.J., M^{c}Intosh, I., Ferguson - Miller, S., and Babcock, G.T., 1988. Israel J. Chem. 28, 129 - 32.

Bengis, C., Nelson, N., 1977. J. Biol. Chem., 252, 4564 - 69.

Berthold, D.A., Babcock, G.T., and Yocum, F., 1981. FEBS Lett., 134, 231 - 34.

Bertrand, P., Guigliarelli, B., Ganjda, J. - P., Setif, P., and Mathis, P., 1988. Biochim. Biophys. Acta, 933, 393 - 97.

Biggins, J., and Mathis, P., 1988. Biochemistry, 27, 1494 - 1500.

Biggins, J., Tanguay, N.A., and Frank, H.A., 1989. FEBS Lett.,250, 271 - 74.

Bittl, R., Van der Erst, A., Kamlowski, A., Lubitz, W., Stehlik, D., 1994. Chem. Phys. Lett. 226, 349 - 58.

Blankenship, R.E., Macguire, A., and Sauer, K., 1975. Proc. Natl. Acad. Sci. U.S.A., 72, 4943 - 47.

Blankenship, R.E., Trost, J.T., and Manchino, T. E., 1987. Properties of Reaction Centres from the Green Photosynthetic Bacterium, *Chloroflexus auranticus*, in "The Photosynthetic Reaction Centre - Structure and Dynamics" 119 - 127.

Bloembergen, N., Purcell, E.M., and Pound, R.V., 1948. Phys. Rev., 73, 679.

Blubaugh, D.J. and Govindjee, 1988. Photosynthesis Res., 19, 85 - 128.

Bock, C.H., Van der Est, V.J., Brettel, K., and Stehlik, D., 1989. FEBS Lett., 247, 91 - 96.

Bonnerjea, J., and Evans, M.C.W., 1982. FEBS Lett., 148, 313 - 316.

Bottin, H., Setif, P., 1991. Biochim. Biophys. Acta, 1057, 331 - 36.

Breton, J., and Ikegami, I., 1989. Photosynthesis Res., 21, 27 - 36.

Brettel, K., 1989. Biochim. Biophys. Acta, 976, 246 - 49.

Brettel, K., 1988. FEBS Lett., 239, 93 - 98.

Bruce, B.D., and Malkin, R., 1988. J. Biol. Chem., 263, 7302 - 8.

Bruce, B.D., and Malkin, R., 1988. Plant Physiol., 88, 1201 - 6.

Buttner, M., Xie, D. - L., Nelson, H., Pinther, W., Hauska, G., and Nelson, N., 1992. Biochim. Biophys. Acta, 1101, 154 - 56.

Buttner, M., Xie, D. - L., Nelson, N., Pinther, W., Hauska, G., and Nelson, N., 1992. Proc. Nat. Acad. Sci.,

Chitnis, P.R., Purvis, D., and Nelson, N., 1991. J. Biol. Chem., 25, 260.

Chitnis, P.R., Reilly, P.A., and Nelson, N., 1989. J. Biol. Chem., 264, 18381 - 85.

Crowder, M., and Bearden, A., 1983. Biochim. Biophys. Acta, 722, 23 - 35.

Diner, B.A., and Petrouleas, V., 1988. Biochim. biophys. Acta, 895, 107 - 25.

Evans, M.C.W., and Heathcote, P., 1980. Biochem. Biophys. Acta, 590, 89 - 96.

Evans, M.C.W., Sihra, C.K., Bolton, J.R., and Cammack, R., 1975. Nature, 256, 668 - 70.

Falzone, C.J., Kao, Y. - H., Zehao, J., MacLaughlin, L., Bryant, D.A., and Leconte, J.T.J., 1994. Biochemistry, 33, 6043 - 51, 6052 - 62.

Fish, L.E., Bogorad, L., 1986. Plant Biol., 2, 151 - 61.

Ford, R.C., and Evans, M.C.W., 1983. FEBS Lett., 160, 159 - 64.

Franzen, L.G., Frank, G., Zuber, H., Rochaix, J. - D., 1989. Plant Mol. Biol., 12, 463 - 74.

Furrer, R., and Thurnauer, M.C., 1983. FEBS Lett., 160 , 399 - 403.

Gast, P., 1982. Ph.D. Thesis, University of Leiden, Leiden, Netherlands.

Gerken, S., Brettel, K., Shlodder, E., and Witt, H. T., 1988. FEBS Lett., 237, 69 - 75.

Golbeck, J.H., and Bryant, D.A., 1991. Current Topics in Bioenergetics, 16, 83 - 177.

Golbeck, J.H., and Cornelius, J.M., 1986. Biochim. Biophys. Acta, 849, 16 - 24.

Golbeck, J.H., Mehari, T., Parrett, K., and Ikegami, I., 1988. FEBS Lett., 240, 9 - 14.

Golbeck, J.H., Parrett, K., McDermott, A.E., 1987. Biochim. Biophys. Acta, 893, 149 - 60.

Golbeck, J.H., and Warden, J.T., 1982. Biochim. Biophys. Acta, 681, 77 - 84.

Hanley, J.A., Kear, J., Bredenkamp, G., Li, G., Heathcote, P., and Evans, M.C.W., 1992. Biochim. Biophys. Acta, 1099, 152 - 56.

Hastings, G., Kleinherenbrink, F.A.M., Lin, S., McHugh, T.J., and Blankenship, R.E., 1994. Biochemistry,33, 3193 - 3200.

Hatanuka, H., Sonoike, K., Hirano, M., and Katoh, S., 1993. Biochim. Biophys. Acta, 1141, 45 - 51.

Heathcote, P., Hanley, J.A., and Evans, M.C.W., 1993. Biochim. Biophys. Acta, 144, 54 - 61.

Hecks, B., Wulf, K., Breton, J., Leibl, W., and Trissl, H. - W., 1994. Biochemistry, 33, No. 29, 8619.

Hervas, M., Ortega, J.M., Navarro, J.A., De la Rosa, M., Bottin, H., 1994. Biochim. Biophys. Acta, 1184, 235 - 41.

Hippler,M., Ratajczack, R., and Hachnel, W., 1989. FEBS Lett., 250, 280 -84.

Hirsh, D.J., Beck, W.F., Innes, J.B., and Brudvig, G.W., 1992. Biochemistry, 31, 532 - 41.

Hoganson, C.W., and Babcock, G.T., 1988. Biochemistry, 27, 5848 - 55.

Hoj, P., and Moller, B.L., 1986. J. Biol. Chem., 261, 14292 - 14300.

Hore, P.J., Hunter, D.A., McKie, C.D., and Hoff, A.J., 1987. J. Chem. Phys. Lett.,137, 495 - 500.

Ikegami, I., and Katoh, S., 1989. Plant Cell Physiol., 30, 175 - 182.

Ikeuchi, M., Hirano, A., Hiyama, T., and Inoue, Y., 1990. FEBS Lett., 263, 274 - 78.

Ikeuchi, M., Nyhus, K.J., Inoue, Y., and Pakrashi, H., 1991. FEBS Lett., 287, 5 - 9.

Iwaki, M., and Itoh, S., 1989. FEBS Lett., 256, 11 - 16.

Kim, D., Yoshihara, K., and Ikegami, I., 1989. Plant Cell Physiol., 30, 679 - 84.

Kjaer, B., Jung, Y.S., Yu, L., Golbeck, J.H., and Scheller, H.V., 1994. Phtosynthesis Res., 41, 105 - 14.

Kleinherenbrink, F.A.M., Chion, H.-C., Le Brutto, R., and Blankenship, R.E., 1994. Photosynthesis Res., 41, 115 - 23.

Koike, H., Ikeuchi, M., Hiyama, T., Inoue, Y., 1989. FEBS Lett., 253, 257 - 63.

Kuhlbrandt, W., and Wang, D.N., 1991. Nature, 350, 130 - 34.

Li, N., Warren, P., Golbeck, J.H., Frank, G., Zuber, H., and Bryant, D.A., 1991. Biochim. Biophys. Acta, 1059, 215 - 25.

Liebl, V., Mockensturm - Wilson, M., Trost, J.T., Brune, D., Blankenship, R.E., Vermaas,

W.F.J., 1993. Proc. Natl. Acad. Sci. U.S.A., 90, 7124.

Losche, M., Satoh, K., Feher, G., and Okamura, M.Y., 1988. Biophys. J, 53, 270.

Lunneberg, J., Fromme, P., Jekow, P., Schlodder, E., 1994. FEBS Lett., 338, 197 - 202.

Malkin, R., 1984. Biochim. Biophys. Acta, 4, 63 - 69.

Mansfield, R.W., and Evans, M.C.W., 1986. FEBS Lett., 203, 225 - 29.

Mansfield, R.W., and Evans, M.C.W., 1988. Isr. J. Chem., 28, 97 - 102.

Mathis, P., 1990. Biochim. Biophys. Acta, 1018, 163 - 67.

Mathis, P., and Setif, P., 1988. Photosynthesis Res., 16, 203 - 10.

M^{c}Dermott, A.E., Yachandra, V.K., Guiles, R.D., Sauer, K., Klein, M., Parrett, K., and Golbeck, J.H., 1989. Biochemistry, 28, 8056 - 59.

Mehari, T., Parrett, K.G., Warren, P.V., and Golbeck, J.H., 1991. Biochim. Biophys. Acta, 1056, 139 - 48.

Michel, H., and Deisenhofer, J., 1988. Biochemistry, 27, 1 - 7.

Moser,C.C., Keske, J.M., Warncke, K., Farid, R.S., and Dutton, P.L., 1992. Nature (London), 355, 796 - 802.

Nuijs, A.M., Van Dorssen, R.J., Duysen, N.B., and Amesz, J., 1985. Proc. Natl. Acad. Sci., 82, 6865 - 6868.

Obakata, J., Mikami, K., Hayashida, M., Sugiura, M., 1990. Nicotania, Plant Physiol., 92, 273 - 75.

Oh - oka, H., Takahashi, Y., Kuriyama, K., Saeki, K., and Matsubara, H., 1991. Plant Cell Physiol., 32, 11 - 17.

Oh - oka, H., Takahashi, Y., and Matsubara, H., 1989. Plant Cell Physiol., 30, 869 - 75.

Oh - oka, H., Takahashi, Y., Matsubara, H., and Itoh, S., 1988. FEBS Lett., 234, 291- 294.

Okkels, J.S., Scheller, H.V., Jepson, L.B., and Moller, B.L., 1989. FEBS Lett., 250, 575 - 79.

Okkels, J.S., Scheller, H.V., Svendson, I., and Moller, B.L., 1991. J. Biol. Chem., 266, 6767 - 73.

Palace, G.P., Franke, J.E., and Warden, J.T., 1987. FEBS Lett., 215, 58 - 62.

Parrett, K.G., Mehari, T., and Golbeck, J.H., 1990. Biochim. Biophys. Acta, 1015, 341 - 52.

Petrouleas, V., Brand, J.J., Parrett, K.V., and Golbeck, J.H., 1989. Biochemistry, 28, 2980 - 83.

Reilly, P., Hulmes, J.D., Pan, Y.C.E., Nelson, N., 1988. J. Biol. Chem., 263, 17658 - 62.

Rigby, S.E.J., Nugent, J.H.A., and O' Malley, P.J., 1994. Biochemistry, 33, 10043 - 49.

Rigby, S.E.J., Thapar, R., Evans, M.C.W., Heathcote, P., 1994. FEBS Lett., 350, 24 - 28.

Rogner, M., Muehlenhoff, U., Boekeama, E.J., Witt, H.T., 1990. Biochim. Biophys. Acta, 1015, 415 - 24.

Rogner, M., Nixon, P.J., Diner, B.A., 1990. J. Biol. Chem., 265, 6189 - 96.

Rousseau, F., Setif, P., and Lagoutte, B., 1993. The EMBO Journal, 12, no.5, 1755 - 65.

Ruffle, S.V., Donnelly, D., Blundell, T.L., and Nugent, J.H.A., 1992. Photosynthesis Res., 34, 287 - 300.

Rustandi, R.R., Snyder, S.W., Freezel, L.L., Michalski, T.J., Norris, J.R., Thurnauer, M.C., and Biggins, J., 1990. Biochemistry, 29, 8030 - 32.

Sakurai, H., Inoue, K., Fujii, T., Mathis, P., 1991. photosynthesis Res., 27, 65 - 71.

Schafheutle, M.E., Sethikona, E., Tummins, P.A., Johner, H., Gutgasell, P., 1990. Biochemistry, 29, 1216 - 25.

Scheller, H.V., Okkels, J.S., Hoj, P.B., Svendson, I., Roepstorff, P., and Moller, B.L., 1989. J. Biol. Chem., 264, 18402 - 18406.

Setif, P., and Bottin, H., 1989. Biochemistry, 28, 2689 - 97.

Setif, P., and Brettel, K., 1993, Biochemistry, 32, 7846 - 54.

Setif, P., Ikegami, I., and Biggins, J., 1987. Biochim. Biophys. Acta, 894, 146 - 56.

Setif, P., Mathis, P., and Vangaard, T., 1984. Biochim. Biophys. Acta, 767, 404 - 14.

Sieckman, I., Vanderest, A., Bottin, H., Setif,P., and Stehlik, D., 1991. FEBS Lett., 284, 98 - 102.

Smart, L.B., Warren, P.V., Golbeck, J.H., and M^{c}Intosh, L., 1993. Proc. Natl. Acad. Sci. U.S.A., 90, 1132 - 36.

Snyder, S.W., Rustandi, R.R., Biggins, J., Norris, J.R., and Thurnauer, M.C., 1991. Proc. Nat. Acad. Sci. U.S.A., 88, 9895 - 96.

Staffan, E.T., and Andersson, B., 1991. Photosynthesis Res., 27, 209 - 19.

Stehlik, D., Bock, C.H., Petersen, J., 1989. J. Phys. Chem., 93, 1612 - 19.

Steppuhn, J., Hermans, J., Nechustai, R., Herrman, G.S., Herrmann, R.G., 1989. Curr. Genet., 16, 99 - 108.

Steppuhn, J., Hermans, J., Nechustai, R., Ljungsberg, U., Thummler, G., Lottspiech, F., Herrmann, R.G., 1988. FEBS Lett., 237, 218 - 24.

Styring, S., Virgin, I., Ehrenberg, A., and Andersson, B., 1990. Biochim. Biophys. Acta, 1015, 269 - 78.

Tang, J., Thurnauer, M.C., and Norris, J.R., 1994. Chem. Phys. Lett., 189, 427 - 42.

Thurnauer, M.C., Bowman, M.K., and Norris, J.R., 1979. FEBS Lett., 100, 390 - 402.

Thurnauer, M.C., and Norris, J.R., 1980. Chem. Phys. Lett., 284, 98 - 102.

Thurnauer, M.C., and Rutherford, A.W., and Norris, J.R., 1982. Biochim. Biophys. Acta, 682, 332 - 38.

Trebst, A., 1986. Z. Naturforsch., 41c, 240 - 45.

Van den Meent, E.J., Kobyashi, M., Erkelens, C., Van Veelen, P.A., Amesz, J., and Watanabe, T., 1991. Biochim. Biophys. Acta, 1058, 356 - 62.

Van Kan, P.J.M., Otte, S.C.M., Kleinherenbrink, F.A.M., Nieveen, M.C., Aartsma, T.J., and Van Gorkum, H.J.C., 1990. Biochim. Biophys. Acta, 1020, 146 - 52.

Van Mieghm, F.J.E., Satoh, K., and Rutherford, A.W., 1991. Biochim. Biophys. Acta, 1058, 379 - 85.

Vos, M.H., Van Gorkom, H., 1988. Biophys. J., 58, 1547 - 55.

Warden, J.T., 1990. In "Current Research in Photosynthesis"(M.Baltscheffsky, ed.), 635 - 38, Kluwer, Dordrecht, The Netherlands.

Wasliewski, M.R., Johnson, D.G., Seibert, M., and Govinjee, 1987. Photosynthesis Res., 12, 181 - 90.

Webber, A.N., and Malkin, R., 1990. FEBS Lett., 264, 1 - 4

Wynn, R.M., Luong, C., Malkin, R., 1988. FEBS Lett., 229, 293 - 97.

Wynn, R.M., Omaha, J., and Malkin, R., 1989. Biochemistry, 28, 5554 - 60.

Zanetti, G., and Merati, G., 1987. Eur. J. Biochem., 169, 143 - 46.

Zhao, J.D., Li, N., Warren, P.V., Golbeck, J.H., and Bryant, D.A., 1992. Biochemistry, 31, 5093 - 99.

Zhao, J.D., Warren, P.V., Li, N., Bryant, D.A., Golbeck, J.H., 1990. FEBS Lett., 276, 175 - 80.

Ziegler, K., Lockau, W., and Nitschke, W., 1987. FEBS Lett., 217, 16 - 20.

Ziegler, K., Maldener, I., and Lockau, W., 1989. Z. Naturforsch., C:Biosci., 44, 468 - 72.

Zilber, A.L., Wynn, R.M., and Malkin, R., 1990. Current Research in Photosynthesis, ed. M. Baltscheffsky, 2 : 575 - 78.

Additional References.

Allen, J.P., Feher, G., Yeates, T.O., Komiyah, H., and Rees, D.C., 1987. Proc. Natl. Acad. Sci., U.S.A., 84, 6162 - 66.

Arnon, D.I., Whatley, and Allen, M.B., 1954. Science, 127, 1026 - 34.

Blackman, F.F., 1905. Ann. Botany, 19, 281.

Boardman, N.H., 1971. Methods in Enzymology, 23, 268 - 76.

Brettel, K., and Setif, P., 1987. Biochim. Biophys. Acta, 893, 109 - 114.

Chang, C.H., Tiede, D., Tang, J., Smith, U., Norris, J., and Schiffer, M., 1986. FEBS Lett., 205, 82.

Davis, I. H., Heathcote, P., Maclachlan, D.J., and Evans, M.C.W., 1993. Biochim. Biophys. Acta, 1143, 183 - 89.

Deisenhofer, J., Epp, O., Miki, K., Huber, R., and Michel, H., 1984. J. Mol. Biol., 180, 385 - 98.

de Saussure, N., 1804. Th. Recherches Chimiquessur la Vegetation, Nyon, Paris.

Duysens, L.N.M., Amesz, J., and Kump, B.M., 1961. Nature, 190, 510.

Emerson, R., and Arnold, W.J., 1932. J. Gen. Physiol., 16, 191.

Engelmann, T., 1884. Botan. Z., 42, 61, 97.

Evans, H., Dikson, D.P.E., Johnson, C.E., Rush, J.D., and Evans, M.C.W., 1981. Eur. J. Biochem., 118, 81 - 84.

Fischer, H., 1940. Naturmssenschaften, 28, 401.

Fish, L.E., and Bogorad, L., 1986. J. Biol. Chem., 261, 8134 - 39.

Fish, L.E., Kuck, U., and Bogorad, L., 1985.J. Biol. Chem., 260, 1413 - 21.

Guiliarelli, B., Guillaussier, J., Bertrand, P., Gayda, J.P., and Setif, P., 1989. J. Biol. Chem., 264, 6025 - 28.

Hill, R., 1937. Nature, 139, 881.

Hill, R., and Bendall, F., 1960. Nature, 186, 136 - 37.

Ikegami, I., and Itoh, S., 1987. Biochim. Biophys. Acta, 893, 517 - 23.

Ikegami, I., and Itoh, S., 1988. Biochim. Biophys. Acta, 934, 39 - 46.

Ingen - Housz, J., 1779. Experiments Upon Vegetables , Discovering their Great Power of Purifying the Common Air in Sunshine and Injuring it in the Shade and at Night, Elmsly and Payne, London.

Kok, B., Forbush, B., and McGloin, M., 1970. Photochem. Photobiol., 11, 457 - 75.

Krauss, N., Hinrichs, W., Witt, I., Fromme, P., Pritzkow, W., Zbiegniew, D., Betzel, C., Wilson, K.S., Witt, H.T., and Saenger, W., 1993. Nature, 361, 326 - 30.

Laemmli, U.K., 1970. Nature, 227, 680.

Malkin, R., 1986. FEBS Lett., 208, 343 - 46.

Mathis, P., and Setif, P.,1988. FEBS Lett., 237, 65 - 68.

Michel, H., 1982. J. Mol. Biol., 158, 562.

Moenne - Loccoz, P., Robert, B., Ikegami, I., and Lutz, M., 1990. Biochemistry, 29, 4740.

O' Malley, P., and Babcock, G.T., 1984. Proc. Natl. Acad. Sci. U.S.A., 81, 1098.

Pfister, K., Steinback, K.E., and Arntzen, E.J., 1981. Proc. Natl. Acad. Sci. U.S.A., 78, 981 - 85.

Ruben, S., Randall, M., Kamen, M., and Hyde, J.L., 1941. J. Am. Chem. Soc., 63, 877.

Rustandi, R.R., Snyder, S.W., Feezel, L.L., Michalski, Norris, J.R., and Thurnauer, M.C., 1990. Biochemistry, 29, 8030 - 32.

Rutherford, A.W., 1990. Biophys. Biochim. Acta, 1019, 128.

Tswett, M., 1906. Ber. Deut.Botan. Ges., 24, 316, 384.

Warden, J.T., and Golbeck, J.H., 1982. Biochim. Biophys. Acta, 681, 77 - 84.

Warden, J.T., and Golbeck, J.H., 1986. Biochim.Biophys. Acta, 849, 25 - 31.